


Review

Life-Related Hazards of Materials Applied to Mg–S Batteries

Krzysztof Siczek 

Department of Vehicles and Fundamentals of Machine Design, Lodz University of Technology,
90-924 Lodz, Poland; ks670907@p.lodz.pl

Abstract: Nowadays, rechargeable batteries utilizing an S cathode together with an Mg anode are under substantial interest and development. The review is made from the point of view of materials engaged during the development of the Mg–S batteries, their sulfur cathodes, magnesium anodes, electrolyte systems, current collectors, and separators. Simultaneously, various hazards related to the use of such materials are discussed. It was found that the most numerous groups of hazards are posed by the material groups of cathodes and electrolytes. Such hazards vary widely in type and degree of danger and are related to human bodies, aquatic life, flammability of materials, or the release of flammable or toxic gases by the latter.

Keywords: Mg–S battery; hazard; cathode material; anode material; electrolyte; separator



Citation: Siczek, K. Life-Related Hazards of Materials Applied to Mg–S Batteries. *Energies* **2022**, *15*, 1543. <https://doi.org/10.3390/en15041543>

Academic Editor: Carlos Miguel Costa

Received: 10 January 2022

Accepted: 17 February 2022

Published: 19 February 2022

Publisher's Note: MDPI stays neutral with regard to jurisdictional claims in published maps and institutional affiliations.



Copyright: © 2022 by the author. Licensee MDPI, Basel, Switzerland. This article is an open access article distributed under the terms and conditions of the Creative Commons Attribution (CC BY) license (<https://creativecommons.org/licenses/by/4.0/>).

1. Introduction

Nowadays, it is observed the strong development of various reversible electrical energy storages (batteries) based on Li electrodes, which are applied in commonly utilized electronic devices, automotive control and drive systems, and net applications [1–5]. The role of a safe charge and discharge processes for various batteries at high energy densities was emphasized in [6,7]. Such a high energy density in cells/batteries can be obtained using Li-metal anodes due to their specific capacities and low potentials [8,9]. The cycling process in cells utilizing lithium electrodes is accompanied by the formation of metallic lithium needle-like dendrites. The latter limited the electrochemical performance of cells over time and increased the fire hazard due to short circuits [10,11].

As an alternative to the Li–S batteries, Mg–S batteries are cheaper, exhibit a higher energy density, and are safer compared to the Li–S ones that have been developed [12–14]. The development of effective Mg–S batteries was bounded by a lack of inexpensive and non-nucleophilic electrolytes [15,16].

Parambath et al. [17] noticed that Mg–S cells have a high overpotential between charge/discharge cycles, rapid capacity fading, low cycling efficiency, and slow kinetics. Such problems are strongly affected by the dissolution of polysulfides (PSs) in the electrolyte and their subsequent shuttling to the Mg anode side.

Similarly, to the Li–S cell [18], the Mg–S one comprises an anode, a cathode with binder, an electrolyte, a separator, and a current collector [15,16,19], and sometimes a protective layer on the anode, as suggested in [17]. The scheme of the Mg–S cell is shown in Figure 1 (based on [20]).

Wang and Buchmeiser [16] reported that the number of studies on rechargeable Mg–S cells (Figure 2c) has recently significantly increased (Figure 2a). A timeline of various findings relating to the Mg–S cells in the time range from 2011 to 2019 is shown in Figure 2d. Figure 2b comprises an overview of the topics addressed in papers relating to Mg–S cells. From such a survey, it is clearly visible that studies on novel electrolyte systems, modifying sulfur cathode materials, and mechanistic studies were significantly preferred. By contrast, only a few studies concerned the other components of an Mg–S cell, such as the anode and the separator.

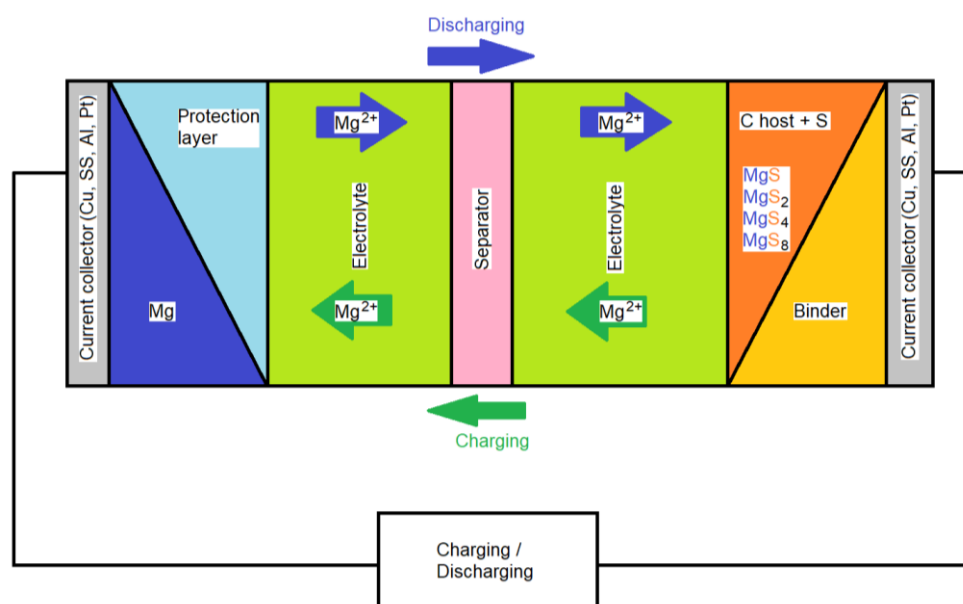


Figure 1. Scheme of an Mg–S cell. Based on [20].

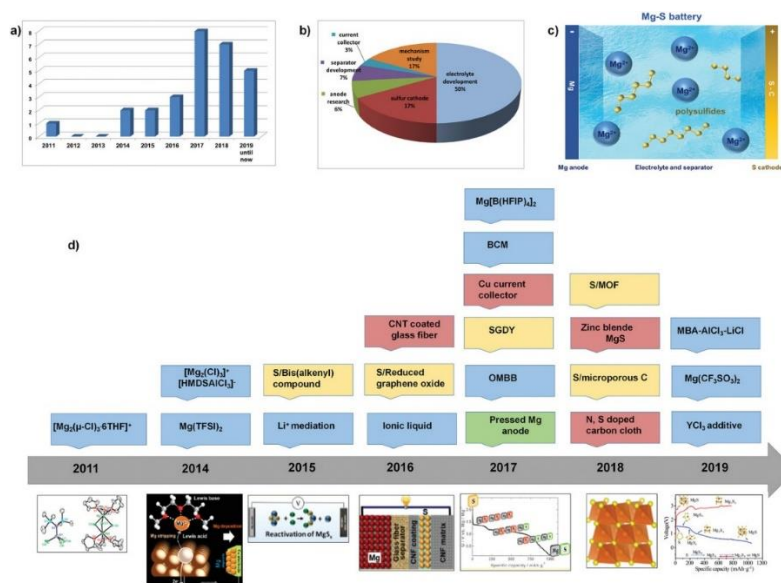


Figure 2. Development of Mg–S cells: (a) The increased trend of studies on Mg–S cells, number of papers on Mg–S cells since 2011; (b) a comparison of topics addressed in all papers related to Mg–S cells; (c) a scheme of an Mg–S battery with an S-based cathode and an Mg anode, separated by a separator and the electrolyte. Mg²⁺ ions are generated during electrochemical reaction of the Mg anode with the S cathode; (d) findings in the time range from 2011 to 2019 on Mg–S cells concerning electrolyte (blue), S-based cathode (yellow), anode (green), and current collector and separator (pink). Taken from [16] based on [21–27].

Wang and Buchmeiser [16] described how during discharging, oxidation of the Mg anode results in the generation of Mg²⁺ ions and a pair of electrons. Mg²⁺ ions travel to the S cathode via the electrolytes and separators, whereas the electron pair travels from the anode to the cathode via an electrical circuit loading the cell. In the cathode zone, S changes in a stepwise manner into long-chain polysulfides (PSs), short-chain ones, and, in the end, into Mg–S. During charging, Mg²⁺ ions are reduced and deposited onto the anode surface. The Mg–PSs re-react with some oxygen to form the initial sulfur state.

Although the design of the Mg–S cell was and is often modelled on that of the Li–S cell, the chemical reactions occurring in both types of cells differ from each other. The different reaction pathways affected by the preferential stabilization of S_2^{2-} and S_4^{2-} in the presence of Mg^{2+} and Li^+ are shown in Figure 3 [28].

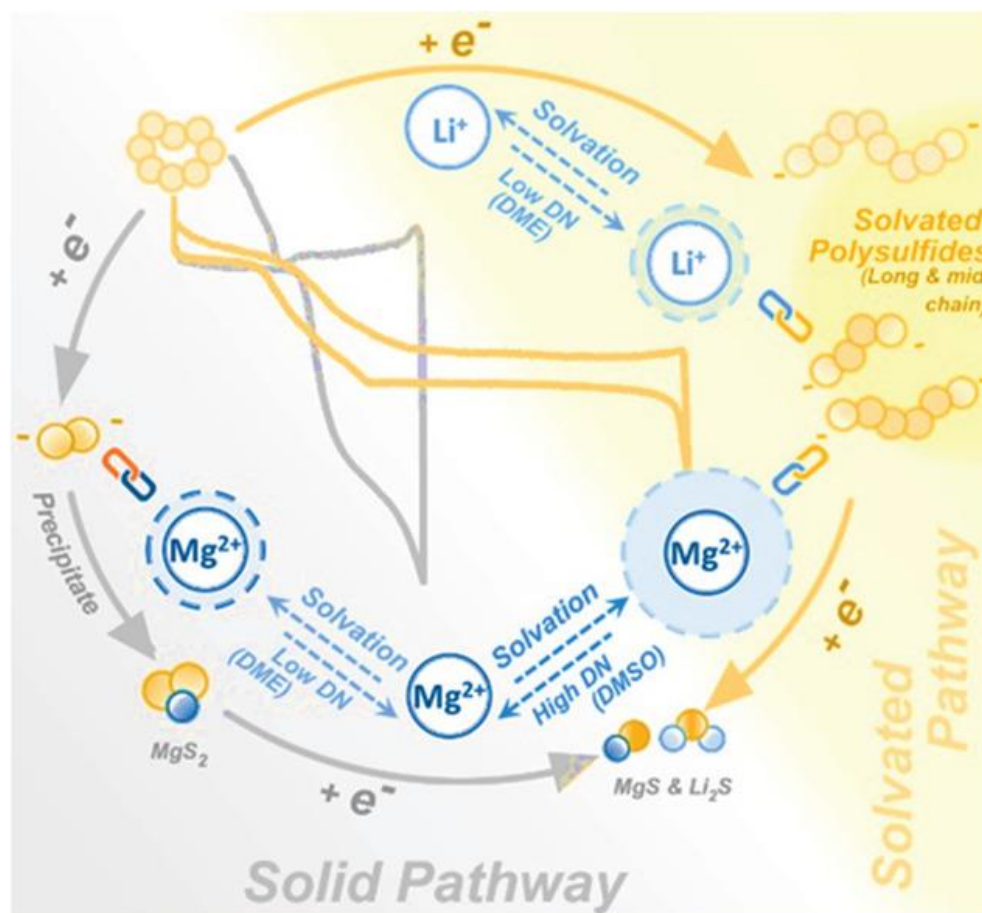


Figure 3. Schematic illustration of sulfur reduction reactions in the Li–S and Mg–S cells. Taken from [28].

Zou et al. [28] explained that the precipitation of S_8 and MgS_2 from PS solutions confirmed a low concentration of dissolved PSs in the Mg^{2+} -containing solutions. The lower PS concentration in the presence of Mg^{2+} than that of Li^+ resulted from the high electrostatic force between Mg^{2+} and S_x^{2-} , due to the greater charge density of Mg^{2+} than that of Li^+ , which supports the solid precipitation. The early MgS_2 precipitation and low PS concentration provided a sluggish “solid–solid” dominant reaction pathway and weakened the use of both solid S_8 and Mg–S.

The differences in the chemical reactions taking place in the Li–S cell and in the Mg–S cell have a great influence on the characteristics of such cells. Two subsequent galvanostatic discharge/charge profiles of Mg–S and Li–S two-electrode cells are shown in Figure 4. Such profiles point out that the Mg–S cell has limited discharge capacity, large polarizations, and rapid capacity decay [28].

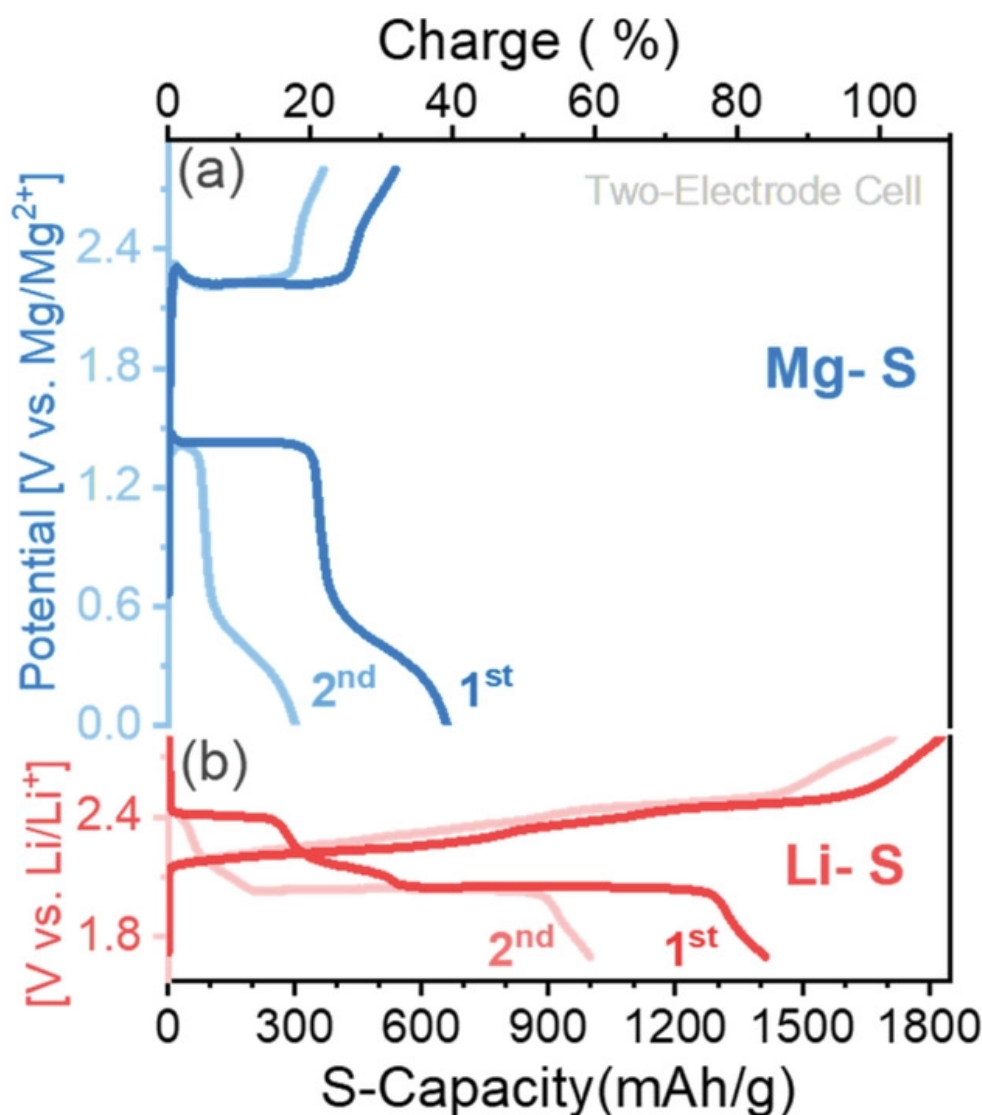


Figure 4. Galvanostatic discharge/charge profile of Mg-S and Li-S two-electrode cells with a respective electrolyte: (a) 0.5 m Mg(TFSI)₂ in DME; (b) LiTFSI in DME; operating under the load of 0.1 C. Taken from [28].

Wang et al. [29] also reported that the major practical problems of Mg-S cells related to the soluble Mg-PS intermediates and their inter-electrodes shuttling inducing high overpotentials, low S utilization, and poor Coulombic efficiency.

A separate problem related to the use of Li-ion and Li-S cells, and soon, also for the Mg-S ones, is their durability. This applies to situations when such cells are or will be used in nets powered by wind farms, photovoltaic devices, and others, where grids may experience large fluctuations in the available electric energy or electric voltage due to local overloads or environmental conditions such as weather conditions, accidents, and others. Then, such batteries become, periodically, the only sources of energy for the grid, or they are used to compensate for unfavorable temporary disturbances. The optimal selection of cells with a long life and good cyclability can determine not only the comfort, but sometimes also the health or even life of people, especially when it is associated with the need to provide power to medical devices operated in hard-to-reach areas.

Ford et al. [30] noticed that Li-S cells exhibited the well-known tendency to self-discharge. From a practical standpoint, the battery shelf-life is very important. Unfortunately, the Mg-S cells also suffer from severe self-discharge. For a common Mg-S electrolyte, they determined a multi-step self-discharge pathway. Covalent S₈ diffused to the metal

Mg anode and was transmuted into ionic Mg-PS in a non-faradaic reaction. Mg-PSs in solution were meta-stable, prone to prolonged reaction, and precipitated as solid Mg-PS species during both storage and operation.

The most often investigated form of Mg-S cell is the coin cell one (Table 1).

Although the coin Mg-S cell configuration is normally used in the laboratory for research, as has been presented further, commercial cells are commonly met in the form of cylinder cell or pouch cell configuration. The typical rechargeable battery configurations, including the coin one, the cylindrical one, the prismatic one, and the pouch one, are presented in Figure 5 [31].

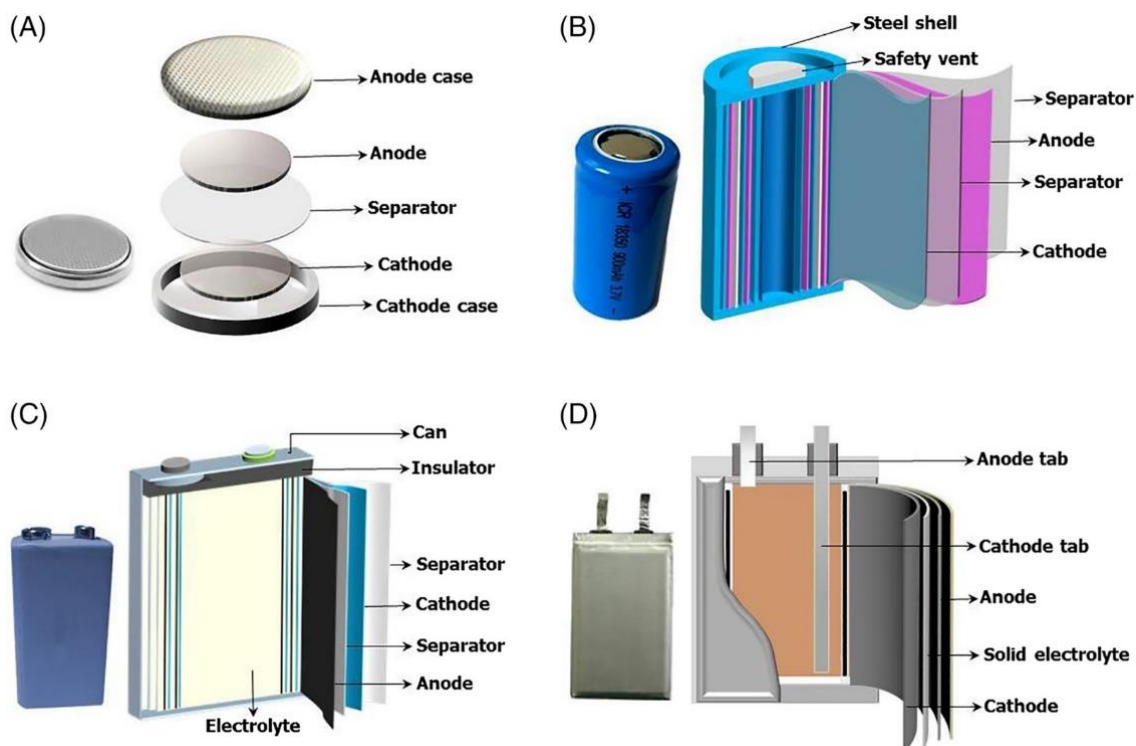


Figure 5. Schematic illustrations of typical rechargeable battery configurations: (A) coin; (B) cylindrical; (C) prismatic; (D) pouch shapes. Taken from [31].

Although the considerations presented in [32] particularly concern pros and cons of Li-ion cells, the features of the analyzed configurations may be very similar when such configurations are applied to Li-S cells and Mg-S cells.

The cylindrical cells exhibit high specific energy and mechanical stability and are adapted to automated manufacturing. Such a cell design allows added safety features impossible with other formats. It has high cyclability, long life, and low cost, but less than ideal packaging density. They are often applied to portable devices.

The prismatic cells are placed in an Al or SS case to enhance stability. Jelly-rolled or stacked, the cell is space-efficient but more expensive to manufacture than the cylindrical cell. Prismatic cells are utilized in electric powertrains and energy storage systems.

The pouch cell utilizes a laminated form placed in a bag. It is lightweight and relatively cheap, but under exposure to humidity and high temperatures exhibits a shorter life. There is a necessity to add a light stack pressure to prevent delamination and thus prolong the cell life. For Li-ion cells, a swelling of 8–10 percent over 500 cycles can occur. Large cells operate best with light loading and moderate charge times. The pouch cells are used for similar applications as the prismatic ones.

According to [33], Li-ion battery packs require a mandatory protection circuit to assure safety under all circumstances.

Governed by IEC 62133, the safety of a Li-ion cell or packs needs to be provided with the following safeguards:

- A Built-in PTC (positive temperature coefficient) for protecting against current surges;
- A CID (circuit interrupt device) for opening the circuit at a cell pressure of 1000 kPa;
- A safety vent for liberating gases on undue pressure buildup at 3000 kPa;
- A separator for inhibiting ion flow by a melting process when exceeding a certain temperature threshold.

The application of such safeguards for Mg–S cells also increases the safety of such cells, but in some cases can be an overprotective action and needs further research and optimization, particularly relating to the costs of their realization.

Wagner et al. [34] investigated the pouch cell prototype built within the framework of the Mag–S project, funded by the German Federal Ministry of Education and Research and in cooperation with Custom Cells Itzehoe (CCI) GmbH in Germany.

Montenegro et al. [35] described a prototype magnesium rechargeable battery (MRB) of the Mg–S-type comprising cells, each with an Mg foil anode, an S cathode, a magnesium tetrakis (hexafluoroisopropoxy) borate electrolyte, a plastic separator, and Al composite pouch cell packaging. They found that the pouch cell housing and electricity requirements for battery manufacture posed potential threats to the environment. The Al pouch cell packaging was found to strongly contribute to global warming, abiotic depletion, human toxicity, acidification, and photochemical oxidation.

According to Bautista et al. [36], the same authors proposed the following two modified pouch cell models: MgS-Evo1 and MgS-Evo2. The first configuration allowed a pouch cell mass share reduction from 45 wt.% to 3 wt.%. The second model allowed decreased separator thickness and, correspondingly, a mass share decrease from 10% to 2 wt.% and a much lower footprint.

Bieker et al. [37] reported that, unlike hard-case cell housings, pouch cells do not allow too much excess of liquid electrolyte without losing shape and stability.

Among the different cell formats (cylindrical, prismatic-hard case, and pouch), pouch cells best allow maximizing the specific energy because of the low weight of cell packaging. For the manufacturing of single prototype cells, stacking of electrodes and separators can be carried out with less effort than winding an electrode-separator stack for cylindrical cells [38]. Moreover, the cell volume changes can be evaluated and eventually better controlled or compensated [39–41]. In addition, several stages are feasible, starting from one-layered [42,43] versions with manageable active material amounts and going up to a few [40,44–46] and multilayered pouch cells [40,47–49]. The higher the stack, the more electrode area and, consequently, more sulfur-carbon composite is required [50].

The cylindrical type for Mg–S cells was proposed in [51].

According to [52], the Mg–S battery may be safer than the Li–S battery because Mg plating usually proceeds without dendrite formation.

The safety of the Mg–S battery is mainly related to the vapor pressure of the electrolyte. The over-pressure building up to 70–150 kPa during the heating of the cell up to 20–45 K over the electrolyte boiling point can trigger the battery explosion. The exothermic reaction between MgS and H₂O induced a sudden temperature jump in the battery.

The distinct performance, safety, and cost behaviors of various ether types of electrolytes resulted from the different CH₂CH₂O chain lengths.

A modified DME with a higher boiling point can be ideal for the Mg–S cell.

The Hazard Communication Standard (HCS) determines any chemical substance classified as a physical hazard, a health hazard, a simple asphyxiant, combustible dust, pyrophoric gas, or hazard not otherwise classified as a hazardous chemical. The HCS also defined the physical and health hazards, and the classes and categories of such hazards, Hazard Communication. The evolution of Mg–S batteries is accompanied by various hazards related to the use or manufacturing of the components of these batteries. The aim of the study was to identify such hazards and battery components that cause the most of these hazards. It turns out that such hazards belong to three groups. The first one comprises

the possible occurrence of fire, flammable gas or explosion, and corrosion in contact with the atmosphere or water. The second one relates to the toxic or allergic effects on skin, eyes, the gastrointestinal and respiratory tracts, to the generation of genetic defects, damage to fertility or unborn children, organs, and carcinogenicity. The last one relates to aquatic life.

2. Anode Materials

2.1. Metallic Mg Anodes

Various Mg–S batteries use Mg metallic anodes, which have a strong effect on their electrochemical performance due to its interactions with an electrolyte [10,53–61].

The phenomenon of the blocking deposits (in layer form) on the Mg anode resulting from electrolyte disintegration or reaction with traces of H₂O and O₂ averts the diffusion of Mg²⁺ ions. Thanks to this, reversible Mg deposition and dissolution are limited [54,60,61]. Among others, polar aprotic solvents such as carbonates and nitriles often form an impenetrable film on the metallic surface. This decreases the available types of the electrolyte [11,61,62].

An anode made of metallic Mg in the form of discs [21,63], plates [22], ribbons [64], or foils [21,23,24,65,66] has a low surface area [16]. Table 1 presents some Mg–S batteries using Mg anodes in the form of foil [22,25,28,52,67–72], disc [13,21,30,73], foil disc [24,74], ribbons [64], and others. The largest group is those using Mg foil anodes.

Table 2 contains some information related to the hazards of metallic Mg [75]. According to [75,76], Mg in contact with water releases flammable gas. It may cause skin and temporary eye irritation. When ingested, it may cause irritation of the gastrointestinal tract. When inhaled, it may cause irritation to the respiratory system. According to [76,77], it is also self-heating and may catch fire.

2.2. Alternative Anodes

Carbonate-based solvents are much more resistant to corrosion and anodic oxidation compared to ether-based ones [78]. On the other hand, when the Mg metal reacts with carbonate solvents an impermeable film on top of the Mg anode is usually generated, strongly limiting Mg deposition during charging [60,79,80]. To compensate for this unwanted tendency, the use of a conductive and preventive auxiliary layer on Mg anodes is necessary [79,81–83]. Such a layer, usually the PVD (physical vapor deposited) one, may block the corrosion process of the metal surface caused by tracers of O₂ or H₂O, S, and the electrolyte [84]. Such a protective layer should be uniform and of a thickness below 10 nanometers to provide high ionic conductivity with no increase in cell impedance [84]. Therefore, an atomic Al₂O₃ layer deposited on Mg can be suitable for Mg anodes [84–86].

Table 2 shows information about the hazards related to the use of Al₂O₃ [87]. It seriously irritates eyes and damages organs via prolonged or repeated exposure. It is able to irritate the respiratory tract.

Various hazards related to the use of materials for anodes in Mg–S cells are presented in Figure 6. The largest number of the hazards identified belonged to the hazard group related to the possible occurrence of fire, flammable gas, or an explosion. Three single hazards were identified that referred to the hazard groups related to the toxic or allergic effects on eyes, the respiratory tracts, and the generation of damages to organs, respectively.

Only a few materials are used for the anodes in Mg–S batteries, which pose only a few hazards associated with their use.

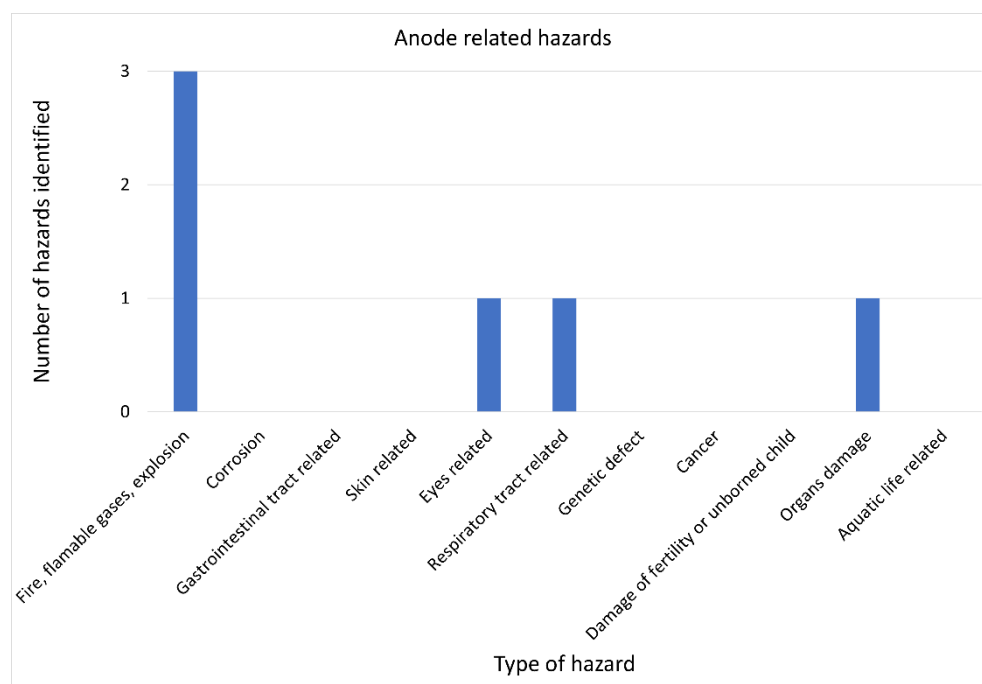


Figure 6. The number of the hazards identified versus type of hazard for anode materials in Mg–S cells.

3. Separators

Various separators usually isolate a cathode and an anode in the liquid electrolyte cells, allowing a free ion transport [88,89]. The Mg–S batteries mainly utilized separators based on glass fiber sheets [12,22,23,65–68,73,90–92] and microporous polymer membranes [13,64,93–97]. Glass fiber separators possess better thermal dimensional stability, porosity, permeability, and ionic conductivity than the other ones, but they are more expensive and need more electrolyte [88,89].

Table 1 presents some Mg–S batteries utilizing separator materials such as PTFE [25], PE film [21], borosilicate glass fiber sheet [71,90], glass fiber [22,26,28,30,52,67,68,72,74], Celgard microporous membrane [13,30,93], CNF-coated glass fiber [24], glass microfiber filter [70,73], ENTEK PE membrane [94], glass wool [98], and others. It is seen that the glass fiber separator is the most often used in Mg–S batteries.

There has been no information found about hazards related directly to the glass fiber separators. However, some of these related to the use of glass fibers have been available.

According to [99], glass fiber, when ingested, is able to cause disturbances in the gastrointestinal tract. Breathing in glass fiber dust or particulates is able to irritate the nose, throat, and respiratory tract. The contact of the skin or eyes with glass fiber dust or particulates can temporarily irritate skin or eyes. Long-term exposure to a glass fiber environment may cause temporary negative effects.

According to [100], woven fiberglass fabric exhibits a mechanically irritating ability. Breathing such dust and fibers can temporarily irritate the mouth, nose, and throat. Their contact with skin can result in itching and transitory irritation. Their contact with eyes can initiate a temporary mechanical irritation. Ingestion of them can initiate a temporary mechanical irritation of the stomach and intestines. Prolonged breathing or skin conditions that are mechanically irritated can increase the probability of worsening health from contact with this material.

Due to the low solubility and irreversibility of MgS and Mg₃S₈, the surface of separators can be modified to increase the Mg–S cell performance [24,27].

Yu and Arumugam [24] reported an activated carbon nanofiber (CNF)-coated glass fiber separator, prepared using vacuum filtration.

There has been no information found about hazards related directly to the activated carbon nanofiber (CNF)-coated glass fiber separators. However, some information related to the use of carbon nanofibers has been available.

According to [101], carbon nanofibers are found as a non-hazardous substance or mixture. Moreover, according to [102], carbon (graphite) nanofibers are found as a non-hazardous substance or mixture. However, according to [103], graphitized carbon nanofibers are flammable as both liquid and vapor. They are detrimental in contact with skin or if inhaled. They can seriously irritate the eyes and are able to damage fertility or an unborn child (Table 2).

The use of a catalyst to reactivate neutral MgS and Mg₃S₈ also allows for improving the cyclability. For example, TiS₂ has a catalytic effect on the activation of low-order Mg-PSs [104–106]. Moreover, Xu et al. [27] reported a TiS₂-coated separator obtained via vacuum filtration.

According to [107], TiS₂ releases flammable gas when in contact with water. It irritates the skin and seriously irritates the eyes. It can also irritate the respiratory tract (Table 2).

Wang et al. [29] utilized a functional Mo₆S₈ modified separator with a high adsorption capability of PSs and acted simultaneously as a mediator, accelerating the PS conversion kinetics.

Various hazards related to the use of materials for separators in Mg-S cells are presented in Figure 7. The four pairs of the identified hazards belonged to the hazard group related to the possible occurrence of fire, flammable gas, or an explosion, and the hazard group related to toxic or allergic effects on skin, eyes, and the respiratory tracts, respectively. A single hazard was identified and referred to the hazard group related to the generation of damages to fertility or an unborn child.

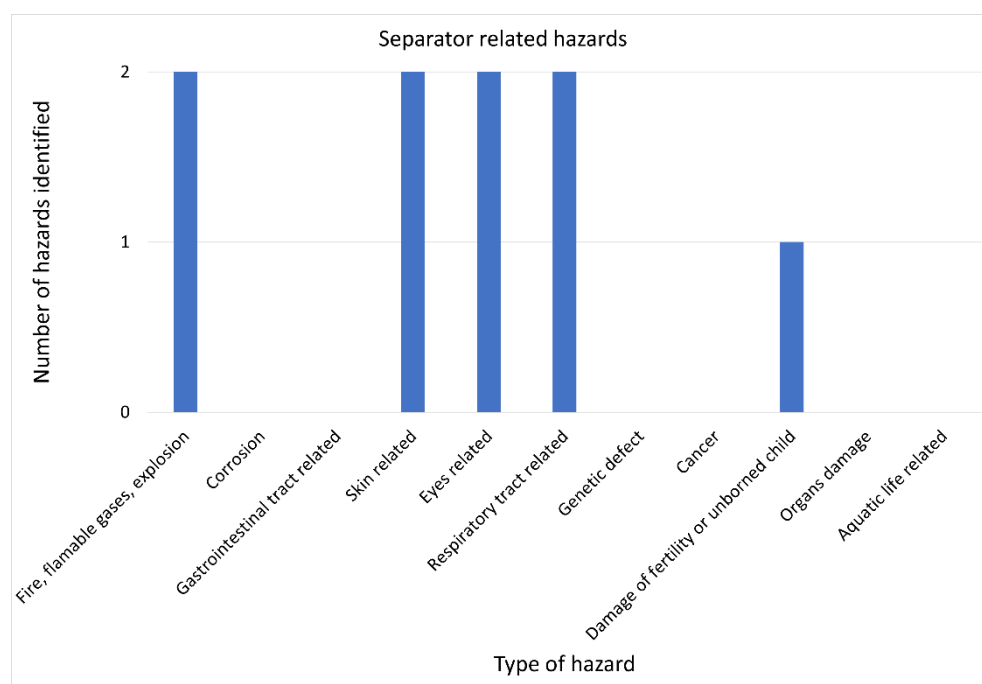


Figure 7. The number of the hazards identified versus the type of hazard for separator materials in Mg-S cells.

Similarly, in the case of anode materials, only a few materials are utilized as separators in batteries, which pose only a few hazards related to their use. However, such hazards are more numerous and much more varied compared with the case of the anode materials.

4. Cathodes

Mg–S batteries utilized intercalation cathodes [108–112], e.g., transition metal sulfides such as TiS_2 and Mo_6S_8 , [14,63,113,114], as well as transition metal oxides such as V_2O_5 [115,116] or MnO_2 [117,118], MoO_3 [119] conversion cathodes such as sulfur and oxygen, organic cathodes such as 2,5-dimethoxy-1,4-benzoquinone [120–124] and carbon-based cathodes such as fullerenes [125] have been investigated and discussed so far [54,111,120,126–128]. Wang and Buchmeiser [16] reviewed mainly sulfur-based conversion cathodes. The other types of cathode materials have been discussed in other reviews [53,55,112,116,120,128–130].

Table 1 presents some Mg–S batteries used as cathodes of the S/C type [15,25,26,67], S/CMK type [21,52,71,72,90], S/ACC type [22,30,70,74], S/CNTS type [15,24,73], S/MOFs type [68], MgPS/G-CNTs type [131], S/NG type [13], S/rGO type [93], S/MC type [64,94], S/CB type [98] and S/KB/PTFE type [28]. It is clearly seen that the S/C type, the S/CMK one, and the S/ACC one are the most often reported types of cathodes applied in Mg–S batteries.

There was no information found about hazards relative to the use of the Mo_6S_8 .

Some clusters with an Mo_6S_8 unit have been reported to decompose to MoS_2 , molybdenum metal, or both, by thermal treatment under various atmospheres [132–134].

Chen et al. [135] notified the low toxicity of MoS_2 -very-thin-film.

However, according to [136], MoS_2 powder causes serious eye irritation and may cause respiratory irritation.

Manganese oxides (MnO_2) as pseudocapacitive electrode materials showed environmental friendliness [137–139].

Some hazard expressions related to MnO_2 are shown in Table 2.

Ji et al. [140] notified the non-toxicity of MnO_x (i.e., MnO , MnO_2 , Mn_2O_3 , and Mn_3O_4).

According to [141], MnO_2 is detrimental when swallowed or inhaled. Despite its incombustibility, it intensifies the combustion of other substances.

Table 2 presents some hazard expressions related to V_2O_5 [142]. It is detrimental when swallowed or inhaled. It can irritate respiratory tract. It probably elicits genetic defects and damage to an unborn child. It also induces damage to organs via long-term or repeated endangering. It is poisonous to aquatic life.

Whittingham [143] suggested a low toxicity of a cathode made of V_2O_5 .

According to [144], MoO_3 is toxic if swallowed. It seriously irritates the eyes and can irritate the respiratory tract. It probably, causes cancer and is detrimental to aquatic life, with long-lasting effects.

Table 2 presents some hazards related to the use of 2,5-dimethoxy-(1,4) benzoquinone [145]. According to [146], it is irritating to the eyes and skin on contact. Inhalation causes irritation of the lungs and respiratory system.

Fullerenes can also cause hazards [147] as presented in Table 2. According to [148], they cause serious eye irritation and may cause respiratory irritation. Moreover, [149] reported that fullerenes may cause eye irritation and dermal irritation. Their inhalation may lead to lung irritation and may irritate the gastrointestinal tract. High concentrations of dust may be irritating to the eyes and skin.

Active Cathodes Materials

Contrary to intercalation cathodes, in the S-based one belonging to the conversion cathode groups (O_2^- , CuF_2^- , AgCl^- , and S-based), the cyclability of battery results in the reduction and oxidation of elemental sulfur [7]. The unwanted phenomenon of O_2 -based cathode materials is the irreversible formation of the electrochemically inactive discharge product MgO [150]. The discharge products of CuF_2^- and AgCl^- -based cathodes also exhibit low solubility [150].

According to [151,152], oxygen may cause or intensify fire and is a known oxidizer. Usually transported under pressure, it may explode if heated (Table 2).

Hazards related to the use of CuF_2 [153] are shown in Table 2. It causes severe skin burns and eye damage and may cause respiratory irritation [154]. According to [153], contact with acids liberates very toxic gases containing hydrogen fluoride and copper oxides.

Table 2 contains also some hazards related to the use of AgCl [155]. According to [156], it causes respiratory tract irritation. It can irritate the eyes, skin, and digestive tract. It also can induce cyanosis. According to [157], it can induce corrosion in contact with metals, and exhibits a high level of toxicity to the aquatic life with long-lasting effects.

Yoo et al. [54] stated that sulfur is appreciated due its non-toxicity and a high theoretical energy density (1675 mAh g^{-1}). Table 2 presents sample information about hazards related to the use of sulfur. According to [158], it exhibits flammable features and can irritate the skin. As reported in [159], it is able to be detrimental when swallowed or inhaled.

Du et al. [65] reported that the cathode materials in Mg–S batteries utilize carbonaceous materials with elemental sulfur (α - or β - S_8). The use of various porous carbon additives for the accommodation of S_8 in the cathode allows enhancing the loading of active materials and limiting the diffusion of PPs [93]. The utilized carbon materials comprise carbon black [25,160], activated carbon clothes (ACC) [22,66,74,85,92], and metal organic frameworks (MOFs) [68].

Two reports about the toxicity of Super P carbon were found in the literature.

Chaudhuri et al. [161] found a carbon black (Super P) as a particle of low toxicity (PSLT). However, carbon black can reveal its direct genotoxicity or even reproductive toxicity. High concentrations of carbon black results in the inflammation and oxidative stress in the lungs, sometimes followed by mutations.

As reported in [162], Super P carbon may induce irritation of the eyes and skin.

As reported in [163], elemental C exhibited a very low toxicity. A health hazard can occur when humans are exposed to carbon black, not elemental C. Chronic inhalation endangering to carbon black can temporarily or permanently damage lungs and heart. Pneumoconiosis was observed in employees producing carbon black. Inflammation of the hair follicles and oral mucosal lesions occurred during skin endangering. Carbon black was not found as carcinogenic to humans. The high toxicity can be exhibited by some simple C compounds such as carbon monoxide (CO) or cyanide (CN). The environmental effect of C was found to be neutral.

Tamames-Tabar et al. [164] studied the toxic effects of the porous metal-organic frameworks (MOFs) comprising Fe, Zn, Zr carboxylates or imidazolates. The MOF NPs exhibited low cytotoxicity. The lower toxicity was observed in the Fe carboxylate NPs and the higher toxicity in the Zn imidazolate ones.

Ruyra et al. [165] studied the toxic effect of uncovered MOFs on zebrafish embryos. They found that such an effect was affected by the material setup and the leaching manner of metal ions.

During studies on rat pheochromocytoma cells, Ren et al. [166] found that the toxic effect of IRMOF-3, a rigid cubic zinc-based MOF, was affected by time exposure and strength.

Studying the behavior of hepatic cells (HepG2 and Hep3B) and lung cells (A549 and Calu-3), Grall et al. [167] found a weak toxic effect of mesoporous MOFs based on Fe, Al, or Cr.

Wagner et al. [168] evaluated the toxic effects of MIL-160, a microporous hydrophilic Al-based MOF comprising a five-membered ring and an oxygen heteroatom, and ZIF-8, a hydrophobic framework of zeolitic imidazolate, on human bronchial epithelial (BEAS-2B) cells.

There was no information found about the hazards related directly to the use of activated carbon clothes (ACC). However, Table 2 contains some information about the hazards related to activated carbon. According to [169], activated carbon may cause eye irritation. Its dust may also cause respiratory irritation. According to [170], its powder is self-heating in large quantities and may catch fire. In the latter case CO and CO_2 may be liberated.

The application of elemental S in cathodes can induce the unwanted so-called “shuttle effect” [73,74,171]. This phenomenon can be avoided when sulfur is encapsulated in carbon-

based materials, such as microporous [95,172], mesoporous [173], or hollow carbonaceous materials [174–176]. Mg–S batteries cathodes utilize porous carbon materials, such as CMK-3 [12,21,177], nitrogen-doped graphene [13], carbon nanotubes (CNTs) [65], carbon nanofibers [24,178], and reduced graphene oxide (rGO) [93].

Table 2 contains some hazards related to the use of CMK-3. According to [179], ordered mesoporous carbon CMK-3 is suspected of causing cancer. Under fire conditions, carbon oxides are formed. Similarly, mesoporous carbon [180] is suspected to cause cancer.

There was no information found in the literature about hazards related to the use of nitrogen-doped graphene.

However, Wang and Jiang [181] studied the toxic effects of graphene oxide (GO) and N-doped graphene quantum dots (N-GQDs) on red blood cells (RBCs). The adsorption of GO extracted the lipid bilayer, causing hemolysis and aberrant forms of cells. By contrast, N-GQDs violate the structure and conformation of lipid, inducing only aberrant cells.

According to [182], graphene nanoplatelets can create a combustible dust-air mixture. They can irritate eyes, skin, and respiratory tract irritation.

As reported in [183], conductive graphene sheets can irritate skin, mucous membranes, and eyes.

According to [184], the toxic effects of the graphene-family nanomaterials (GFNs) in animals or cell models was affected by the lateral size, surfacial structure, functionalization, charge, purity, formation of aggregates, and corona effect. The GFN toxic effect took the form of physical destruction, oxidative stress, unwanted DNA changes, inflammation, apoptosis, autophagy, and necrosis. In the mentioned mechanisms, (toll-like receptors-) TLR-, transforming growth factor β - (TGF- β -), and tumor necrosis factor-alpha (TNF- α) dependent-pathways formed the signaling pathway network that was highly dependent on the oxidative stress.

Table 2 presents some hazards related to the use of carbon nanotubes and carbon nanofibers. According to [185], CNTs cause serious eye irritation and may induce respiratory irritation.

According to [186], carbon nanofibers seriously irritate the eyes and can irritate the respiratory tract. However, according to [101], they exhibit no known hazards.

As reported in [187], reduced graphene oxide (rGO) may cause irritation to the respiratory tract, skin irritation, and eye irritation. However, according to [188], and [189], it exhibits no known hazards.

Using the CMK-3 as cathode material facilitates preparation of strongly organized interwoven composites [177]. The formation of MgS, MgS₄, and various Mg_xS₈ (x = 1, 2, 3, 8) structures in the cathode have been reported during Mg–S battery cyclability [26,27,177].

There was no information found about hazards related to the use of Mg₃S₈, MgS₄, or MgS₈.

According to [190], a high amount of MgS is self-heating and potentially fire-catching. It causes severe skin burns and damages the eyes. It is detrimental if swallowed, poisonous in contact with skin, and very poisonous to aquatic life.

Besides the mesoporous CMK-3/S cathode, a porous graphdiyne can be applied as a cathode material.

Du et al. [73] obtained an S-comprising cathode based on S graphdiyne (SGDY). Graphdiyne (GDY) was a carbon allotrope with layers of benzene rings and butadiyne linkages.

There was no information found about hazards related to the use of sulfur-doped graphdiyne.

Zheng et al. [191] compared some properties of graphene oxide (GO) and GDY oxide (GDYO). Contacts of GO NPs with a human hepatocyte membrane led to its ruffle, methuosis, and apoptosis. Adhesion of GO to cells results in their stress and the creation of reactive oxygen species. In contrast, GDYO did not adhere to the cell membrane. Both GDYO and GO were able to induce vivo mutagenesis but no erythrocyte-killing effect. Additionally,

both of them proved to be antioxidants and bioequivalent in binding to single-stranded DNA and doxorubicin.

Wang et al. [94] used a microporous carbon as the carbon host for the adsorption of small S_{2-4} inside its structure and of S_8 molecules on the outside wall of the carbon and prepared a sulfur at microporous carbon composite (S@MC) as the electrochemical active material for cathode. Cui et al. [192] proposed the positive electrode utilizing S, a metal sulfide, and a ternary Cu composite. The metal sulfides included FeS_2 , SnS_2 , MoS_2 , Co_3S_4 , and Ni_2S_3 . Such materials can effectively block the shuttle effect on the Mg–S battery.

According to [193], microporous carbon exhibits no known hazards.

Table 2 presents some hazards related to the use of FeS_2 , SnS_2 , MoS_2 , CoS_2 and Ni_2S_3 . There was no information found about hazards relative to Co_3S_4 .

According to [194], FeS_2 can induce an allergic skin reaction, and allergic or asthmatic symptoms, or breathing problems after inhalation. It is also very poisonous to aquatic life, with prolonged effects.

As reported in [195], SnS_2 irritates skin and seriously irritates eyes. It can also irritate the respiratory tract.

According to [196], MoS_2 causes skin irritation, serious eye irritation, and may cause respiratory irritation. Similarly, as reported in [136], MoS_2 powder seriously irritates the eyes and can irritate the respiratory tract.

As reported in [197], CoS_2 can induce an allergic skin reaction, and is very poisonous to aquatic life with prolonged effects.

According to [198], Ni_2S_3 can induce an allergic skin reaction and genetic defects. It also can induce cancer when inhaled. It damages organs via prolonged or repeated exposure and is very poisonous to aquatic life with prolonged effects.

Most Mg–S batteries possess cathode materials utilizing elemental S or S hosted by microporous or mesoporous carbon materials. The shuttle effect, similarly to Li–S batteries, strongly affects the efficiency of Mg–S batteries. To weaken this effect, sulfur can be covalently bound to a conductive carbon matrix, as applied in various Li–S batteries [199–205]. Moreover, preventive layers on the active material in the cathodes can also block the dissolution and loss of S from the cathode material [206].

Various hazards related to the use of materials for cathodes in Mg–S cells are shown in Figure 8. The highest number of the hazards identified belonged to the hazard group related to the toxic or allergic effects on the eyes. Only a single hazard was identified and referred to the hazard group related to the generation of damages to fertility or an unborn child. Moreover, only two pairs of the hazards identified belonged to the hazard groups related to the generation of genetic defects and organ damage, respectively. No hazard was identified related to the corrosion.

It is clearly visible that the materials of cathodes in Mg–S batteries belong to the group posing a lot of hazards related to the use of such materials, much more than those related to materials for anodes or separators in Mg batteries. Such hazards vary widely in type and degree of danger.

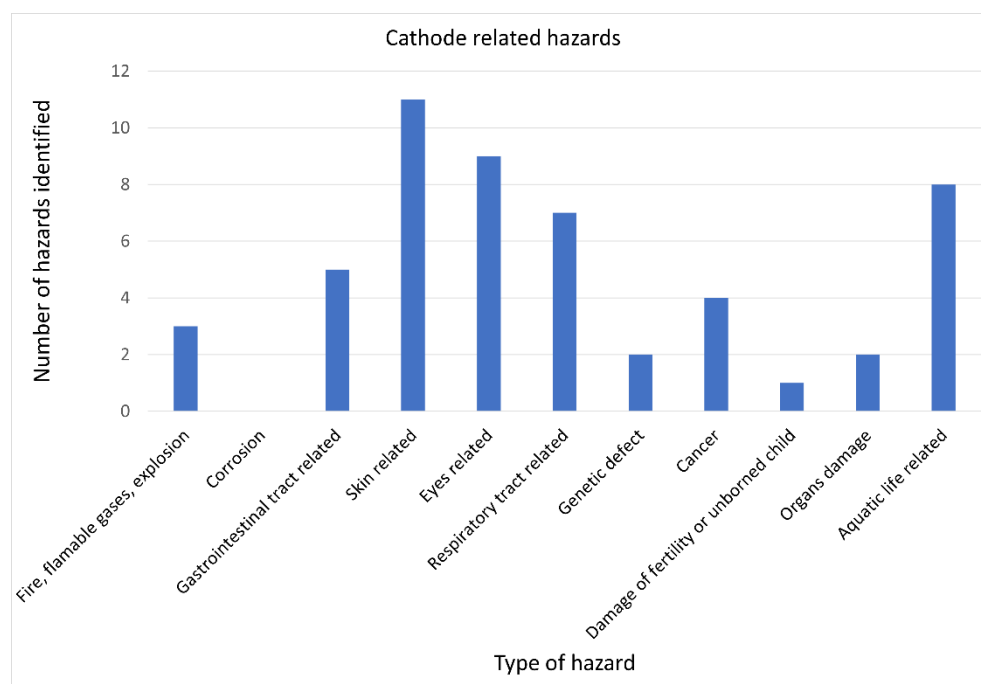


Figure 8. The number of the hazards identified versus the type of hazard for cathode materials in Mg–S cells.

5. Current Collectors

In Mg–S cells, the current collector material strongly affects their electrochemical behavior, especially when they use halogen-comprising corrosive electrolytes [207]. The available metal-based current collectors are in the form of the following: Al foil [13,21,23,65], stainless-steel (SS) foil [12,66,92,95,96], carbon-coated aluminum foil [91], copper [64,65,94,95,97], and the anticorrosion alloy Inconel 625 [90,93,95].

Table 1 presents Mg–S batteries using Inconel 625 [22,74,90,93], stainless steel (SS) [28,30,67–69,71], Cu [15,64,67,73,94,98], and the others as a material for the current collector. The above-mentioned materials are most commonly used for current collectors, while the Al, Ni, Mo, and CNF are more seldom reported.

Table 2 presents some hazards related to the use of Al foil, stainless steel, graphite, copper, and Inconel 625 alloy.

According to [208], Al foil has a low hazard for trained personnel and in solid form is not hazardous. Moreover, as reported in [209], it is not a hazardous material. However, according [210], it is a flammable solid and causes acute aquatic toxicity.

Suspensions of Al dust in air may pose a severe explosion hazard [208,210]. Explosion or fire hazards may be present when the above-mentioned dust and fines or molten Al are in contact with water or certain metal oxides including rust and copper oxide [211]. Al dust or fumes are nuisance particulates [208].

As reported in [211], Al dust and/or fumes may pose a physiological hazard after inhalation or ingestion. They can induce an influenza-like illness and lung cancer when chronically overexposed.

According to [212], Al metal foil is toxic to lungs. If it is heated or in a dust form, it can irritate respiratory tract. Heating it can emit Al₂O₃ fumes and induce fume metal fever after inhalation. Chronic exposure to Al dust may cause dyspnea, cough, asthma, chronic obstructive lung disease, pulmonary fibrosis, pneumothorax, pneumoconiosis, encephalopathy, weakness, incoordination and epileptiform seizures, and other neurological symptoms.

Contact with the Al dust may cause mechanical irritation of the skin or eyes [211]. Moreover, according to [212], Al metal foil is a slight irritant in contact with skin.

As reported in [213], stainless steel foil containing Fe, Cr, and Ni was subjected to processes generating particulates can cause hazards to health or environmental effects presented in Table 2. Similarly, according to [214], stainless steel foil containing Mn, Ni, Cr, Mo, Cu, Al, W, Co, and Sn can also cause hazards to health or environmental effects presented in Table 2.

According to [215], stainless steel in the powdered form is poisonous to aquatic life and reactive in contact with water, and also exhibits pyrophoricity, flammability, self-heating capabilities, carcinogenicity, and acute toxicity. During the production of stainless steel, dust, fumes, or particulates are generated. Exposure to such dust or fumes can irritate the eyes, skin, and respiratory tract. Fine particulates dispersed in the air may present an explosion hazard. Inhalation of such dust and fumes can induce metal fume fever.

There was no information found about the hazards related to C-coated Al foil; however, they are akin to those related to aluminum and graphite, as presented in Table 2. According to [216], Al is very poisonous to aquatic life, also with prolonged effects.

According to [217], graphite powder causes serious eye irritation and may also cause respiratory irritation and cancer by inhalation. It can also damage organs via long-term or repeated exposure.

As reported in [218,219], Cu foil is not considered a hazardous material. However, according to [220], Cu dusts, mists or fumes can occur when Cu foil is cut or laminated. They can irritate eyes and respiratory tract. If they comprise arsenic, they are carcinogenic to humans. Sharp edges of Cu foil can induce cuts during its production.

Moreover, as reported in [221], Cu foil is fatal if swallowed or inhaled, and is very poisonous to aquatic life. It causes serious eye irritation, and may cause allergic skin reactions, genetic defects, and damage to the digestive system, hematopoietic system, kidneys, nose, respiratory tract, and/or skin, via long-term or repeated exposure if inhaled. Additionally, it can produce combustible dust.

According to [222], Inconel in the solid form can be allergic to people sensitive to the metals contained in it. User-generated dust or fumes can irritate the skin and eyes. Chronic exposure can induce dermatitis or conjunctivitis. Excessive inhalation of fumes released during welding may pose prolonged health effects. According to [223], Inconel 625 dust clouds may be explosive and can irritate the eyes. High dust levels may irritate the respiratory system.

Additionally, edges of Inconel 625 strips [224] may be sharp and can cause cuts. Hot metal and UV radiation produced can cause burns. Metal (Al, Mn, Mo, Cr, Ni, Co, Nb, Cu, Ti, Fe, W, and V) ingestion can cause toxic effects. The inhalation of welding or spraying fumes may cause damage to the lungs and respiratory tract. Co and Ni are animal carcinogens and inhalation of their fumes and dusts should be avoided. The prolonged inhalation of Mn fumes and dust may cause irreversible damage to the nervous system, resulting in Parkinson's disease-like symptoms.

While Cu is usually unstable when mated with chloride-containing electrolytes [225], the application of Cu current collectors below 1.7 V versus Mg/Mg²⁺ allows the use of an S cathode with the Grignard-based nucleophilic all-phenyl complex (APC) electrolyte [95]. The electrochemical behavior of such cells is better than the ones with SS current collectors. The copper sulfides can form at the interface between S and Cu, partially protecting the free S in the cathode from reactions with APC electrolytes (vide supra). No such copper sulfides occurred on cathodes based on SS current collectors dried at 50 °C [95].

Muthuraj et al. [226] developed a 3D porous current collector, made of a N-, S-dually doped carbon cloth (DCC), that is stable if mated with corrosive electrolytes and capable of catching PSs. It was and possessed a 3D interconnected porous structure that ensures high cycle stability and conductivity.

There was no information found about hazards directly related to a N-, S-dually doped carbon cloth; however, some information is available related to the N-doped porous carbon, the N/S co-doped graphene presented in Table 2 and the N/S co-doped carbon nanodots.

According to [227], N-doped graphitic porous carbon can be cancerogenic. Additionally, hazardous decomposition products such as carbon oxides are formed under fire conditions.

As reported in [228], N/S co-doped graphene powder causes serious eye irritation, and may cause respiratory irritation.

Ji et al. [229] reported that the N, S-doped C nanodots (N,S-CNDs), usually exhibited a high antioxidative ability in free radical scavenging in physicochemical conditions. During studies conducted using two cell lines, the uptake of the N,S-CNDs initiated the formation of intracellular reactive oxygen species (ROS), thus inducing oxidative stress and deleteriousness to both cell lines. The mitochondrial membrane potential enhanced with the concentration of the CNDs. The N,S-CNDs supports ROS generation via interactions with the electron transport chain in the mitochondrial membrane because of the S composite in the CNDs.

Various hazards related to the use of materials for current collectors in Mg–S cells are presented in Figure 9. It is visible that the highest number of the hazards identified belonged to the hazard group related to the toxic effects on aquatic life. Two sets of seven hazards identified belonged to the hazard groups related to the toxic or allergic effects on the respiratory tract and to the generation of damage to organs, respectively. Additionally, only three pairs of the identified hazards belonged to the hazard groups related to the toxic or allergic effects on the gastrointestinal tract, the generation of genetic defects, and damages to fertility or an unborn child, respectively. No hazard was identified related to the corrosion.

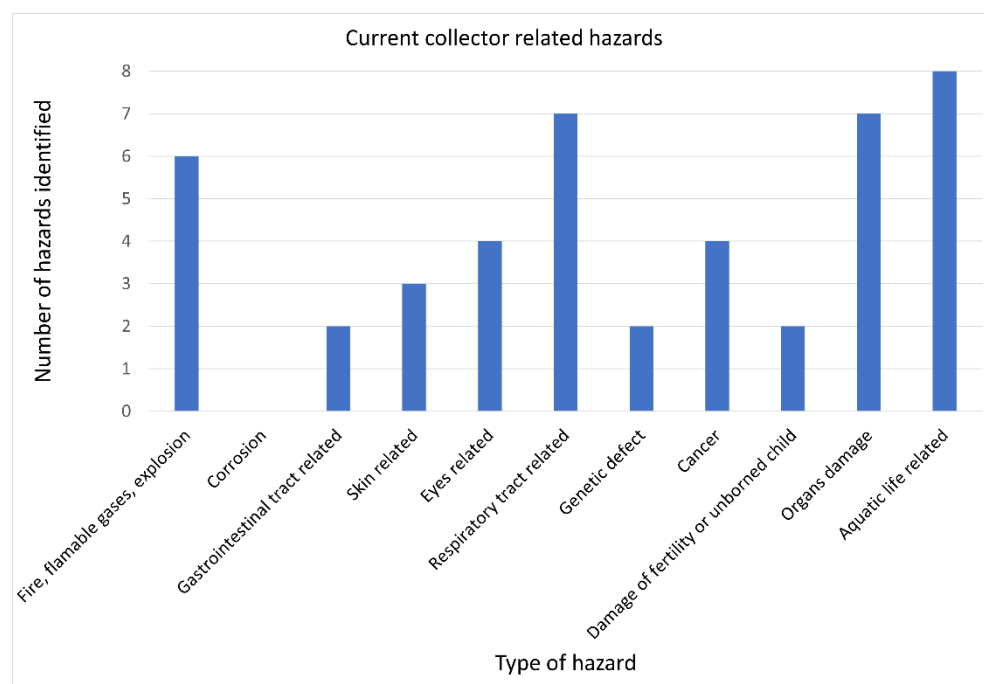


Figure 9. The number of the hazards identified versus the type of hazard for current collector materials in Mg–S cells.

Materials for current collectors belong to the group posing much more hazards related to their use compared to the case of anode materials and separator materials. However, hazards related to the materials of current collectors are less numerous and less varied compared to the case of the cathode materials.

6. Binders

Various binders are used in the cathodes of Mg–S batteries. The most commonly used is 10%wt. [12,15,21,64–68,90,93,94,98] or about 10%wt. [131] of polyvinylidene fluoride

(PVdF) as a binder. Table 1 also shows that the most commonly used binder (bind) is the PVdF one.

Li et al. [13] also utilized a PVdF binder during their studies on Mg–S batteries.

According to [230], poly(vinylidene fluoride) irritates the skin and seriously irritates the eyes. It can also irritate the respiratory tract.

Kim et al. [25] utilized a 4%wt. poly(tetrafluoroethylene) (PTFE) as a binder in Mg–S batteries.

Zou et al. [28] applied a 5%wt. PTFE binder into the cathode of an Mg–S battery.

There were three pieces of information found about the toxicity of PTFE.

Sajid and Ilyas [231] found that PTFE-coated cookware emits different gases and chemicals of mild to severe toxicity. Further studies are need into the toxicity and fate of ingested PTFE coatings. The poisonous perfluorinated carboxylic acid (PFOA) is also utilized during the production of PTFE. The PFOA can exist in the gas phase emitted from the cooking utensils under normal cooking temperatures. Therefore, PFOA is replaced with GenXs, although the latter can also have a similar level of toxicity. Therefore, more research is necessary on the human exposure and poisonous effects of PTFE, PFOA, GenX, and other alternatives.

Shimizu et al. [232] stated that PTFE can induce polymer fume fever in humans.

According to [233], polytetrafluoroethylene is of low oral toxicity but can irritate gastrointestinal tract. Dust and vapors, or fumes, evolved during thermal processing can irritate the respiratory system. It can irritate the skin and eyes. It is also low-level poisonous to aquatic organisms.

Sheng et al. [52] utilized a mixture of 5% sodium carboxyl methyl cellulose (NaCMC) and 5% styrene butadiene rubber (SBR) as a binder in an Mg–S battery.

According to [234], sodium carboxymethyl cellulose is detrimental to aquatic life, also with long-lasting effects (Table 2).

As reported in [235], the SBR binder is flammable under high heat and flame and can generate toxic and combustible fumes, such as carbon monoxide, chlorinated and hydrocarbon compounds, and soot. It may cause skin and eye irritation. An excessive inhalation of it can cause headache, nausea, and irritation.

Various hazards related to the use of materials for binders in Mg–S cells are shown in Figure 10. It is visible that the highest number of the hazards identified belonged to the hazard group related to the toxic effects on aquatic life. Only three single hazards were identified and referred to the hazard groups related to the toxic or allergic effects on the skin, eyes, and respiratory tract, respectively.

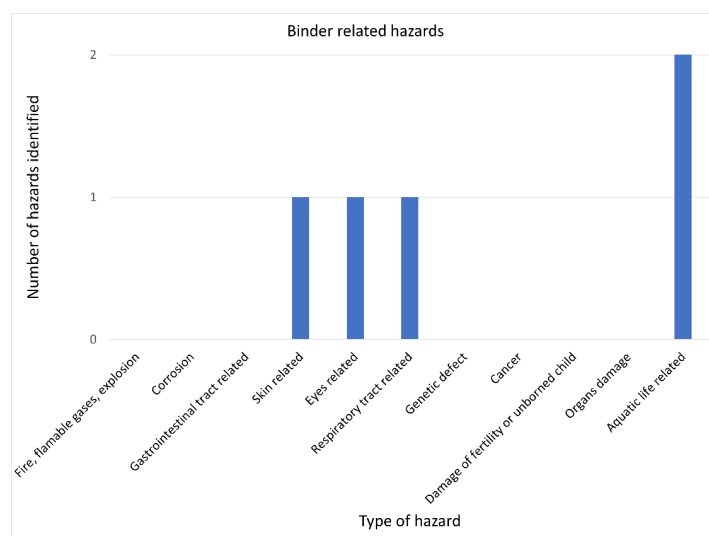


Figure 10. The number of the hazards identified versus the type of hazard for current collector materials in Mg–S cells.

Similarly, in the case of the anode materials, it can be noticed that only a few materials are used for the binders accompanied with cathode materials in Mg–S batteries. Such binder materials pose only a few hazards associated with their use.

7. Electrolyte Systems

There are some limitations to the electrolyte systems usable for Mg–S batteries [11,119–122]. Many kinds of electrolytes in Mg batteries are of a nucleophilic nature and therefore are incompatible with S cathodes. Therefore, the transformation of the cathode material is needed for compatibility with the nucleophilic electrolytes [73,94,95]. Moreover, new non-nucleophilic electrolytes compatible with S cathodes have been developed. Various hazards related to the use of nucleophilic electrolytes were discussed in subchapter 7.1. Such hazards related to the non-nucleophilic ones were described in subchapter 7.2. Subchapter 7.3. comprises a summary of electrolyte systems for Mg–S battery electrolytes, and hazards associated with them.

7.1. Nucleophilic Electrolytes

Initially, the APC electrolyte obtained from the reaction between PhMgCl and AlCl_3 has been found to be incompatible with S-based conversion cathodes, because of the nucleophilicity of the organomagnesium compounds [12,150]. Therefore, at the beginning, the APC electrolyte seemed to be not predestined for use in Mg–S cells. Since an appropriate current collector [95] and cathode materials [73] have been developed, the APC electrolyte has come back for use in Mg–S batteries.

There was no information found about hazards relative to APC electrolyte.

Table 2 presents some information about hazards related to the use of AlCl_3 , PhMgCl , and LiCl .

According to [236], AlCl_3 causes severe skin burns and eye damage. Additionally, it may cause respiratory irritation [237].

As reported in [238], chlorophenylmagnesium causes severe skin burns and serious eye damage.

The use of a Cu-based current collector instead of an SS one allows effective cycling of a cell based on an S_8 cathode and an APC electrolyte [95]. Moreover, the addition of LiCl into the nucleophilic electrolyte improves cycle performance of such a cell [95].

The electrochemical effectiveness of an Mg–S battery can be increased by using micro-porous carbon as the cathode material, Cu as a current collector, and a nucleophilic APC electrolyte containing LiCl as an additive ([94] Table 1).

The SGDY cathode is also compatible with the nucleophilic APC electrolyte, even though the current collector in the Mg–S battery is made of Al instead of Cu [73].

According to [239], LiCl is detrimental if swallowed it causes skin irritation and serious eye irritation.

7.2. Non-Nucleophilic Electrolytes

The high electrophilicity of the S cathode allows the use of non-nucleophilic electrolytes in many Mg–S cells [56,240]. The less/non-nucleophilic electrolytes in Mg–S cells can be qualified into two groups, including chloride-comprising ones and chloride-free, noncorrosive ones. Various hazards related to the use of chloride containing non/less nucleophilic electrolytes were discussed in subchapter 7.2.1. The hazards related to the utilization of non/less corrosive, non-nucleophilic electrolytes for Mg–S batteries were presented in subchapter 7.2.2.

7.2.1. Chloride-Containing, Non/Less Nucleophilic Electrolytes

Electrolytes in Mg–S batteries are obtained using Mg salts combining an Mg complex comprising a non-nucleophilic base, including $[\text{HMDS}]_2\text{Mg}$ ([14,15] Table 1), HMDSMgCl [241], magnesium bis(diisopropyl)amide [98] with a B- or Al-containing Lewis acid ([13] Table 1).

Liebenow et al. [241] found that the Hauser base-derived magnesium hexamethyldisilazide chloride (HMDSMgCl) electrolyte facilitated the Mg stripping and plating in Mg cells.

There was no information found about hazards related to the use of HMDSMgCl.

Table 2 presents some information of hazards related to the use of BF_3 , hexamethyldisilazane, and magnesium bis(hexamethyldisilazide).

According to [242], boron trifluoride (BF_3) contains gas under pressure and may explode if heated. It induces severe skin burns and damage of eyes and even serious one. It can irritate the respiratory tract and damage organs via long-term or repeated exposure. It is also detrimental to aquatic life.

As reported in [243], hexamethyldisilazane is a highly flammable liquid and vapor. It is detrimental if swallowed or inhaled and poisonous if in contact with the skin. It is also detrimental to aquatic life, with prolonged effects.

According to [244], magnesium bis(hexamethyldisilazide) induces severe skin burns and damage to the eyes, even serious ones.

As reported in [245], magnesium bis(diisopropyl)amide is a highly flammable liquid and vapor and, in contact with water, releases flammable gas. It may be fatal after swallowing and entering the airways; it is poisonous after inhalation. It induces severe skin burns and damage to the eyes. It may cause respiratory irritation and genetic defects, and probably induce cancer. It is also detrimental to aquatic life, with prolonged effects.

Kim et al. [25] increased the performance of the HMDSMgCl electrolyte by creating molecular species with a $[\text{Mg}_2(\mu\text{-Cl})_3][\text{HMDSAICl}_3]$ species after adding AlCl_3 .

Kim et al. [25] also obtained cell with a purified $[\text{Mg}_2(\mu\text{-Cl})_3][\text{HMDSAICl}_3]$ within tetrahydrofuran (THF) as an electrolyte, an elemental S/carbon black composite as the cathode, and Mg foil as the anode (Table 1). In addition, the active compound $[\text{Mg}_2(\mu\text{-Cl})_3 \cdot 6\text{THF}] + [\text{HMDSAICl}_3]^-$ could only be received from THF [12].

There was no information found about the hazards relative to $[\text{Mg}_2(\mu\text{-Cl})_3][\text{HMDSAICl}_3]$ and $\text{Mg}_2(\mu\text{-Cl})_3$.

Table 2 presents some information about hazards related to the use of tetrahydrofuran. According to [246], it is a highly flammable liquid and vapor. It is detrimental if it is swallowed and suspected of causing cancer. It causes serious eye irritation and may cause respiratory irritation.

Zhao-Karger et al. [90] obtained the electrolytes by a one-step reaction between magnesium bis(hexamethyldisilazide) $[(\text{HMDS})_2\text{Mg}]$, AlCl_3 in diglyme, and tetraglyme (Table 1). Such a reaction results in an electrochemically active combination, $[\text{Mg}_2\text{Cl}_3][\text{HMDSAICl}_3]$, dissolvable both in diglyme and tetraglyme. Additionally, the desirable Mg plating and stripping also occurs when the ionic liquid (IL) N-methyl-N-butyl-piperidinium TFSI (PP14TFSI) is added to the above-mentioned electrolyte.

Such an electrolyte was also studied by ([24,93] Table 1, [91,227]) but with the other sets of cathodes, anodes, and current collectors.

Ford et al. [30] also utilized an electrolyte comprising a mixture of $(\text{HMDS})_2\text{Mg}$ and AlCl_3 within THF as a solvent.

There was no information found about hazards relative to N-methyl-N-butyl-piperidinium TFSI, and $[\text{Mg}_2\text{Cl}_3][\text{HMDSAICl}_3]$.

Table 2 presents some information on hazards related to the use of diglyme and tetraglyme.

According to [247], 2-methoxyethyl ether is a flammable liquid and vapor. It may form explosive peroxides and may damage fertility or an unborn child.

As reported in [248], tetraethylene glycol dimethyl ether can damage an unborn child and probably fertility as well.

Sheng et al. [52] utilized a mixture of $\text{Mg}(\text{HMDS})_2$, AlCl_3 , and MgCl_2 (1:2:1) within DEG or TEG as an electrolyte for the Mg–S batteries studied (Table 1).

Zou et al. [28] utilized an Mg–HMDS (mixture of 49 wt.% $\text{Mg}(\text{HMDS})_2$, 38 wt.% AlCl_3 , and 13 wt.% MgCl_2) within a tetraethylene glycol dimethyl ether TEGDME as an electrolyte for the Mg–S batteries investigated (Table 1).

Table 2 contains one hazard related to the use of TEGDME that may damage fertility or an unborn child [249]. As reported in [250], tetraethylene glycol dimethyl ether (TEGDME) causes eye irritation and may cause skin and respiratory tract irritation. It is air-sensitive and hygroscopic.

Gao et al. [22] investigated a cell comprising an electrolyte of 0.1 m (HMDS)₂Mg–2AlCl₃–MgCl₂ with the addition of lithium bis(trifluoromethanesulfonyl)imide (LiTFSI), active carbon cloth/elemental S as the cathode and Mg foil as the anode (Table 1).

Zhou et al. [68] also found LiTFSI as an effective additive for Mg–S cells (Table 1).

By adding an excess of metallic Li into the [HMDS]₂Mg-based electrolyte, Zuo et al. [251] obtained an increase in the electrochemical performance of the Mg–S cells (Table 1).

Table 2 presents some information of the hazards related to the use of LiTFSI and Li.

As reported in [252], bis(trifluoromethane)sulfonimide lithium is poisonous when swallowed or in contact with the skin. It induces severe skin burns and damage to the eyes. It can also damage organs via long-term or repeated exposure. It is detrimental to aquatic life, with prolonged effects.

According to [253], contact of Li with water results in the release of flammable gases capable to spontaneous ignition. It also induces severe skin burns and damage to the eyes.

Nuli et al. [97,254] investigated an electrolyte for Mg–S cells comprised of magnesium bis(diisopropylamide) MBA and AlCl₃ dissolved in THF. The electron-rich amide in MBA weakens the anodic stability of the salt, but the addition of AlCl₃ improves the stabilization of the Mg–N bonds in MBA. The molar ratio of MBA and AlCl₃ varied from 2:1 to 1:2 [97].

Zhao et al. [97] also compared the oxidation stability of the 0.25 m MBA–AlCl₃/THF electrolyte with the nucleophilic 0.4 m APC electrolyte, (PhMgCl)₂–AlCl₃/THF, obtaining the better stability of the MBA–2AlCl₃/THF electrolyte than that of the APC electrolyte mating with an Al or SS working electrode.

The electrochemical performance was further increased when it was also dissolved with 1 mol L^{−1} of LiCl into 0.25 mol L^{−1} MBA/0.5 mol L^{−1} of AlCl₃ in THF, effectively limiting the amount of Mg–PSs in the electrolyte [97].

Du et al. [65] developed an organic Mg–B-based (OMBB) electrolyte via a reaction between tris(hexafluoroisopropyl) borate B[HFP]₃, MgCl₂, and excessive Mg powder in DME. The optimal MgCl₂: B[HFP]₃ ratio was equal to 1:2 (Table 1).

There was no information found about hazards relative to organic Mg B-based OMBB electrolyte. Table 2 presents some information about hazards related to the use of B[HFP]₃.

According to [255], tris(2H-hexafluoroisopropyl) borate causes skin irritation, serious eye irritation, and may also cause respiratory irritation.

Ha et al. [21] studied the compatibility of 0.3 m Mg(TFSI)₂ in glyme/diglyme with an S-based cathode in the Mg–CMK/S cell (Table 1).

Similarly, Itaoka et al. [96] investigated Mg–S cells utilizing elemental S and a bis(alkenyl) compound with a crown ether (18-Crown 6-Ether) unit (S-BUMB₁₈C₆) and a linear ether unit (S-UOEE) as cathode materials jointly with an electrolyte comprising Mg(TFSI)₂.

There was no information found about hazards relative to the use of S-BUMB₁₈C₆ and S-UOEE [96]. Table 2 presents some information about hazards related to the use of 18-Crown 6-Ether.

The incompatibility between a glyme-based solvent and Mg(TFSI)₂ induced the development of dendrites on the Mg anode as reported in [256,257]. Mixtures of diglyme and Mg(TFSI)₂ are chemically unstable because of water impurities found in commercial salts [258]. To improve the chemical purity of Mg(TFSI)₂, it can be added to C₈H₁₈Mg [92,257,259].

Li et al. [70] used a small concentration (below 50 × 10^{−3} m) of iodine (I₂) as an additive into an electrolyte comprising Mg(TFSI)₂ within DME as a solvent.

There was no information found about the hazards related to the use of Mg(TFSI)₂:I₂/DME electrolyte.

According to [259], iodine is detrimental after swallowing, inhalation, or contact with skin. It causes skin irritation and serious eye irritation and may cause respiratory irritation.

It also damages organs (thyroid gland) via long-term or repeated exposure by swallowing. It is very poisonous to aquatic life.

Table 2 presents some information about hazards related to the use of $C_8H_{18}Mg$, trifluoromethanesulfonic acid, $Mg(TFSI)_2$, butane, and $Mg(OH)_2$.

According to [260], magnesium bis(trifluoromethanesulfonimide) causes severe skin burns and eye damage.

As reported in [261], contact of dibutylmagnesium with air results in a spontaneous fire. Its contact with water results in the release of flammable gases capable of spontaneous ignition. It also induces severe skin burns and damage to the eyes.

According to [262], trifluoromethanesulfonic acid may induce corrosion in contact with metals and is detrimental if swallowed. It induces severe skin burns and damage to the eyes and may cause respiratory irritation.

As reported in [263], butane is a gas of very high flammability. Under pressure, it may explode if heated.

According to [264], magnesium oxide may be detrimental if inhaled, swallowed, or absorbed through the skin. It may cause respiratory tract irritation, skin irritation, and eye irritation.

As reported in [265], magnesium hydroxide causes skin irritation and serious eye irritation. It may also cause respiratory irritation.

According to [266], 18-crown 6-ether is detrimental if swallowed and causes serious eye irritation.

Gao et al. [74] studied the Mg-S/ACC cell with a 1 M $Mg(TFSI)_2/MgCl_2/DME$ electrolyte comprising the $MgCl_2$ addition (Table 1).

Ford et al. [30] utilized an electrolyte comprising a mixture of $MgTFSI_2$ and $MgCl_2$ within DME as a solvent (Table 1).

Sheng et al. [52] reported the use of two mixtures as the electrolytes for the Mg-S batteries studied. The first one comprised $Mg(TFSI)_2$, $MgCl_2$ (1:0.8) within DME, DEG, or TEG solvent; the second one comprised $Mg(TFSI)_2$ and $MgCl_2$ (1:0.8) within pure DOL and DOL/DME mix (1:3; 1:1; 3:1) solvent (Table 1).

As reported in [267], $MgCl_2$ releases flammable gases when in contact with water.

According to [268], magnesium chloride hexahydrate causes skin irritation and serious eye irritation, and also may cause respiratory irritation.

As reported in [269], magnesium chloride can irritate the eyes, skin, and respiratory tract, it can damage kidneys and it irritates the gastrointestinal tract. Inhalation of its fumes can induce metal fume fever.

Yang et al. [64] developed a new electrolyte containing magnesium trifluoromethanesulfonate ($Mg(CF_3SO_3)_2$)– $AlCl_3$ – $MgCl_2$ –anthracene– $LiCl$ dissolved in THF and tetraglyme (Table 1). An Mg-S microporous carbon cell comprising 0.125 m $Mg(CF_3SO_3)_2$ + 0.25 m $AlCl_3$ + 0.25 m $MgCl_2$ + 0.025 m anthracene/THF and tetraglyme (1:1, v:v) electrolyte was studied.

Gao et al. [22] added $LiCl$ and 0.5 M $LiCF_3SO_3$, respectively, to a 0.125 m $Mg(CF_3SO_3)_2$ + 0.25 m $AlCl_3$ + 0.25 m $MgCl_2$ + 0.025 m anthracene/THF and tetraglyme (1:1, v:v) solution.

Table 2 contains some information about hazards related to the use of anthracene, $Mg(CF_3SO_3)_2$, and $LiCF_3SO_3$.

According to [270], magnesium trifluoromethanesulfonate induces severe skin burns and eye damage.

As reported in [271], anthracene is detrimental if swallowed. It causes serious eye irritation and may cause respiratory irritation. It exhibits acute aquatic toxicity, and is very poisonous to aquatic life with prolonged effects.

According to [272], lithium trifluoromethanesulfonate causes skin irritation and serious eye irritation, and may also cause respiratory irritation.

Nakayama et al. [26] utilized an Mg electrolyte composed of magnesium chloride ($MgCl_2$) and ethyl n-propyl sulfone (EnPS), which was the simplest, non-Grignard, Lewis acid-free electrolyte.

There was no information found about hazards related to the use of EnPS; however, according to [273], propyl sulfone can irritate the eyes, skin, respiratory tract, and digestive tract. As reported in [274], dipropyl sulfone may decompose upon combustion, or in high temperatures, to generate poisonous fume.

7.2.2. Non/Less Corrosive, Nonnucleophilic Electrolytes

Muldoon et al. [225] found that corrosion caused by chlorides in the electroactive species $[\text{Mg}_2(\mu\text{-Cl})_3 \cdot 6\text{THF}]$ and the unwanted bulky nature of the cations, such as the two octahedrally coordinated Mg atoms linked by three chlorides, forced the use of chloride-free salts for Mg–S cells.

Li et al. ([13] Table 1) obtained a chloride-free electroactive salt, $[\text{Mg}(\text{THF})_6][\text{AlCl}_4]_2$, from the reaction of MgCl_2 with two analogues of AlCl_3 in THF and an IL, i.e., N-methyl-N-butyl pyrrolidinium bis(trifluoromethanesulfonyl)imide (PYR14TFSI).

Bi et al. [72] combined $\text{MgCl}_2/\text{AlCl}_3/\text{Mg}$ (ratio of 1:1:1) within a DME (MMAC) electrolyte with IL, such as 1-butyl-1-methylpyrrolidinium bis(trifluoromethanesulfonyl)imide (Pyr14TFSI), obtaining, as result, an MMAC-IL electrolyte of much better performance compared to the MMAC one.

There was no information found about the hazards relative to $[\text{Mg}(\text{THF})_6][\text{AlCl}_4]_2$.

According to [275], 1-Butyl-1-methylpyrrolidinium bis(trifluoromethylsulfonyl)imide exhibits no known hazards. However, as reported in [276], it causes skin irritation and serious eye irritation, and may cause respiratory irritation (Table 2).

The other Lewis acid for the electrolyte of Mg–S cells is also a subject of investigation.

Xu et al. [131] developed a Y-based electrolyte by changing AlCl_3 with YCl_3 . This was obtained from the reaction of MgCl_2 and two analogues of YCl_3 with the IL PYR14TFSI and diglyme (Table 1).

According to [277], yttrium trichloride causes skin irritation and serious eye irritation and may cause respiratory irritation (Table 2).

Zuo et al. [278] developed the other two electrolytes, dissolving 0.2–0.8 mol L^{−1} of AlCl_3 and 0.006–0.024 mol L^{−1} of TiCl_4 in an ether-based solvent. Moreover, an excess of Mg was introduced with a weight ratio between Mg and the solution equal to 3:10 and 12:10, respectively.

According to [279], titanium tetrachloride is detrimental if swallowed and fatal if inhaled. It induces severe skin burns and potentially severe eye damage. It can also irritate the respiratory tract (Table 2).

One group of noncorrosive electrolytes utilizes weakly coordinating anions (WCAs), which can be applied to the production of novel salts for electrolytes utilized in Mg–S cells [280–282].

Zhao-Karger et al. [71] developed a fluorinated magnesium alkoxyborate-based electrolyte. They obtained the conductive salts from the reaction of $\text{Mg}[\text{BH}_4]_2$ with fluorinated alcohols (RF-OH) in ethereal solvents (such as DME). By using hexafluoro-2-propanol (hfip), the conductive salt, $\text{Mg}[\text{B}(\text{hfip})_4]_2 \cdot 3 \text{DME}$ was received when solvent has been removed. This type of Mg salt was insensitive to water and air.

Zhao-Karger et al. examined a 0.6 m $\text{Mg}[\text{B}(\text{hfip})_4]_2 \cdot 3 \text{DME}/\text{DME}$ electrolyte [71].

The same group of researchers also used 0.8 m of $\text{Mg}[\text{B}(\text{hfip})_4]_2$ in diglyme/tetraglyme as an electrolyte for Mg–S cells with an S/CMK-3 cathode, and an Mg plate anode [71].

These authors also studied the effect of the concentration of conductive salt in the electrolyte, $\text{Mg}[\text{B}(\text{hfip})_4]_2 \cdot 3 \text{DME}$, on battery cyclability by using ACC-based S composites as cathode materials [66].

According to [283], 1,1,1,3,3,3-hexafluoro-2-propanol causes severe skin burns and potentially serious eye damage, and it probably can damage an unborn child. It can also damage organs via long-term or repeated exposure.

Xiu et al. [284] reported that magnesium tetrakis(hexafluoroisopropoxy) borate is non-corrosive.

According to [285], $\text{Mg}[\text{B}(\text{hfip})_4]_2$ is a non-corrosive electrolyte.

Zhang et al. [67] obtained a so-called B-centered base Mg (BCM) electrolyte from the reaction of tris(2H-hexafluoroisopropyl) borate (THFPB) with MgF_2 within a DME solvent (Table 1). Such an electrolyte was also utilized during studies conducted by ([98] Table 1).

Xu et al. [69] utilized a mixture of $Mg(BH_4)_2$ and THFPB within a DGM solvent as an electrolyte for the Mg–S battery studied (Table 1).

According to [286], contact of $Mg(BH_4)_2$ with water results in the release of flammable gases. It is toxic if swallowed, inhaled, or comes into contact with the skin. It also induces severe skin burns and damage to the eyes (Table 2).

There was no information found about hazards relative to boron-centered base magnesium (BCM) electrolyte.

According to [255], the tris(2H-hexafluoroisopropyl) borate causes skin irritation and serious eye irritation and may cause respiratory irritation (Table 2).

Similarly, as reported in [287], magnesium fluoride also causes skin irritation and serious eye irritation and may cause respiratory irritation (Table 2).

According to [288], 1,2-dimethoxyethane is a highly flammable liquid and vapor. It is detrimental if swallowed or inhaled and may also damage fertility or an unborn child (Table 2). It may also form explosive peroxides.

Hintennach [289] modified this electrolyte by the addition of a mixture of two thiobarbituric acid derivatives, including thiobarbital and 2-thiobarbituric acid, with a concentration in the range of 0.01–1.9 wt.%.

There was no information found about the hazards related to the use of such a modified electrolyte. However, according to [290], thiobarbituric acid causes skin, serious eye irritation, and may cause respiratory irritation (Table 2). Additionally, as reported in [291], 2-thiobarbituric acid exhibits no known hazards.

7.3. Summary of Electrolyte Systems for Mg–S Batteries

Various hazards related to the use of materials for electrolytes in Mg–S cells are shown in Figure 11. The highest number of the hazards identified and referred to the hazard group related to the toxic effects on skin. Two sets of twenty hazards identified belonged to the hazard groups related to the toxic or allergic effects on the eyes and respiratory tract, respectively. Only two single hazards identified belonged to the hazard groups related to the generation of genetic defects and cancers, respectively. Only a pair of the hazards identified and referred to the hazard group related to corrosion. Moreover, only three hazards identified belonged to the hazard group related to the generation of damages to organs.

Various electrolyte systems applicable to Mg–S batteries are still being investigated. Their development is limited by their need for compatibility with an S cathode and are strongly affected by the effective syntheses of noncorrosive Mg salts and the use of various solvents and additives. The promising Mg salts include B- or Al-centered weakly coordinating anions. Moreover, polymer-based electrolytes should also be under consideration. However, their incompatibility with the Mg anode and a low Mg ion transfer number is still not resolved. Electrolytes are also the group causing the majority of the hazards related to the Mg–S cells, both due to the number of new types of electrolytes and substances used to produce them. Such hazards vary widely in type and degree of danger, much more so than in the case of the mentioned earlier cathode materials.

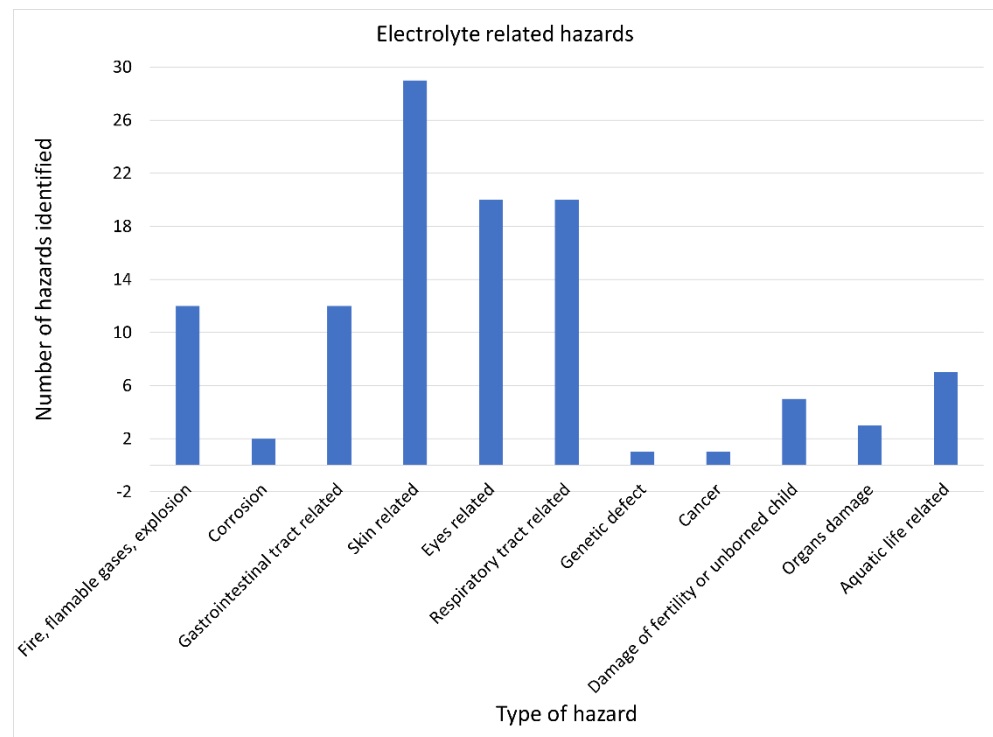


Figure 11. The number of the hazards identified versus the type of hazard for electrolyte materials in Mg–S cells.

Table 1. Materials for components of Mg–S batteries.

| Electrolyte | Cell Type | Anode | Separator | Cathode | Current Collector | Ref. |
|---|-------------------|--------------|--------------------------|--|---|------|
| HMDSMgCl:AlCl ₃ /THF | CR2032 coin cell | Mg foil | PTFE | S/C (S/C (61% S, 35% CB, 4% PTFE (bind)) on C substrate) | n.a. | [25] |
| (HMDS) ₂ Mg:AlCl ₃ /TEG | Swagelok cell | Mg:CB | borosilicate glass fiber | S/CMK (75% S/CMK, 15% Super P, 10% PVdF (bind) NMP or CMC (bind) water) | Inconel 625 | [90] |
| (HMDS) ₂ Mg:AlCl ₃ :LiTFSI/TEG | Swagelok cell | Mg foil | Whatman glass fiber | S/ACC (impregnation of activated carbon cloth with sulfur) | Inconel | [22] |
| [Mg(THF) ₆][AlCl ₄] ₂ PYR ₁₄ TFSI/THF | CR2016 coin cells | Mg disk | Celgard 2400 | S/NG (S, N-doped GO, Super P, PVDF (bind)) | Al | [13] |
| (HMDS) ₂ Mg:AlCl ₃ /TEG | Swagelok cell | Mg/C pellets | Celgard 2500 | S/rGO (75% S/rGO, 15% Super P, 10% PVdF (bind) NPM) | Inconel 625 | [93] |
| (HMDS) ₂ Mg:AlCl ₃ /TEG | coin cell | Mg foil disc | CNF-coated glass fiber | S/CNF (preactivated CNF matrix filled with S) | CNF | [24] |
| MgTFSI ₂ -MgCl ₂ -DME | coin-cell | Mg foil disk | glass fiber | S/ACC (impregnation of active carbon cloth with S). | Inconel, Mo, or W laminate layer | [74] |
| THFPB-MgF ₂ -DME | CR2032 coin cell | Mg foil | glass fiber | S/C (80% S/C, 10% acetylene black, 10% PVdF (bind) NPM) | SS foil, Ni foil, Cu foil, pyrolytic graphitic film | [67] |
| B(HFP) ₃ -MgCl ₂ -Mg/DME | CR2032 coin cell | Mg disc | glass microfiber | S/CNTs (80% S-C (S-AMC, S-CNT or S-CMK), 10% Super P, 10% PVdF (bind) NMP) | Cu foil | [73] |

Table 1. Cont.

| Electrolyte | Cell Type | Anode | Separator | Cathode | Current Collector | Ref. |
|--|------------------|-------------|---|---|-------------------------------|-------|
| $[\text{Mg}(\text{DG})_2]$ $[\text{HMDSAlCl}_3]_2/\text{DG}$ | coin cell | Mg | n.a. | S/CNT (80% S/C (8:2), 10% GO/CNT, 10% PVdF (bind) NMP) | n.a. | [15] |
| PhMgCl:AlCl ₃ /THF | CR2016 coin cell | Mg | ENTEK PE membrane | S/MC (70% S@MC, 20% Super P, 10% PVdF (bind) NMP) | Cu foil | [94] |
| PhMgCl:AlCl ₃ :LiCl/THF | CR2016 coin cell | Mg | ENTEK PE membrane | S/MC (70% S@MC, 20% Super P, 10% PVdF (bind)-NMP) | Cu foil | [94] |
| (HMDS) ₂ Mg-AlCl ₃ - LiTFSI-DG | CR2032 coin cell | Mg foil | Whatman glass fiber with/without RGO layer | S/MOFs (70% ZIF (NPs with Zn)-C-S (various S loading), 20% Super P, 10% PVdF (bind) NMP) | SS or Mo | [68] |
| Mg(BH ₄) ₂ :THFPB/DGM | coin cell | Mg foil | n.a. | S/C (80% S/C, 10% acetylene black, 10% PVdF (bind) NPM) | Al, GF, SS, Ni, Cu, and Ag | [69] |
| Mg(TFSI) ₂ :I ₂ /DME | Swagelok cell | Mg foil | glass microfiber | S/ACC | n.a. | [70] |
| MgCl ₂ :YCl ₃ - PYR ₁₄ TFSI/DG | CR2032 coin cell | Mg | n.a. | MgPS/G-CNTs (30% MgS ₈ , 60% G-CNT, 10% PVdF (bind)-NMP) | n.a. | [131] |
| Mg(CF ₃ SO ₃) ₂ :MgCl ₂ : AlCl ₃ - AT/THF/TG | CR2016 coin cell | Mg ribbon | ENTEK PE | S/MC (80% S@MC, 10% Super P, 10% PVdF (bind)-NPM) | Cu foil | [64] |
| Mg(CF ₃ SO ₃) ₂ :MgCl ₂ :AlCl ₃ : LiCl- AT/THF/TG | CR2016 coin cell | Mg ribbon | ENTEK PE | S/MC (80% S@MC, 10% Super P, 10% PVdF (bind)-NPM) | Cu foil | [64] |
| Mg(CF ₃ SO ₃) ₂ :MgCl ₂ :AlCl ₃ : LiCF ₃ SO ₃ - AT/THF/TG | CR2016 coin cell | Mg ribbon | ENTEK PE | S/MC (80% S@MC, 10% Super P, 10% PVdF (bind)-NPM) | Cu foil | [64] |
| THFPB-MgF ₂ -DME | CR2032 coin cell | Mg metallic | glass-wool | S/CB (60% (S ₈ , Cu ₂ S, or CuS), 30% Super P, 10% PVdF (bind)-NMP {- THF for S ₈ }) | Cu foil | [98] |
| MgCl ₂ /EnPS | CR2016 coin cell | Mg | glass fiber | S/C Pellet type (S or MgS, conductive carbon, PTFE (bind)-acetone Sheet type (S or MgS, conductive carbon, SBR, CMC (bind)-water:ethanol) | Ni | [26] |
| Mg(TFSI) ₂ /glyme/diglyme | CR2032 coin cell | Mg disc | microporous PE film | CMK/S (70 % CMK/S, 20% Super P, 10% PVdF (bind)-NMP) | Al | [21] |
| Mg[B(hfip) ₄] ₂ ; MgBOR(hfip)/DEG-TEG | Swagelok cell | Mg foil | borosilicate glass fiber | CMK/S (75 wt.% S/CMK, 15 wt.% CB, 10 wt.% CMC (bind)-NMP) | SS | [12] |
| (Mg/MgCl ₂ /AlCl ₃ {1:1 ratio}-DME (MMAC)/Pyr14TFSI | coin cell | Mg foil | Whatman glass fiber | CMK/S (80% CMK/S, 10% CB, 10 wt.% PVdF (bind)-NMP) | Mo foil | [72] |
| Mg(TFSI) ₂ :MgCl ₂ {1:0.8}-DME, DEG or TEG Mg(TFSI) ₂ :MgCl ₂ {1:0.8}-pure DOL or DOL:DME {1:3; 1:1 or 3:1} Mg(HMDS) ₂ :AlCl ₃ :MgCl ₂ {1:2:1}-DEG or TEG | CR2032 coin cell | Mg foil | Whatman glass fiber | CMK/S (80% CMK/S, 10% Super P, 5% NaCMC, 5% SBR (bind)-deionized water) | C-Al foil | [52] |
| MgTFSI ₂ /MgCl ₂ -DME; MgHMDS ₂ /AlCl ₃ -THF | CR2032 coin cell | Mg disc | glass fiber or Celgard 2325 | ACC/S | SS | [30] |

Table 1. Cont.

| Electrolyte | Cell Type | Anode | Separator | Cathode | Current Collector | Ref. |
|--|------------|---------|--|---|-------------------|------|
| Mg-HMDS (Mg(HMDS) ₂ :AlCl ₃ :MgCl ₂ {49:38:13}-TEGDME | n.a. | Mg foil | Whatman glass fiber | S/KB/PTFE (95 wt.% S/KB (8:2), 5 wt.% PTFE (bind)-IPA) | SS | [28] |
| Mg[B(hfip) ₄] ₂ -3DME | pouch cell | Mg disc | Mix (60 wt.% Mo ₆ S ₈ , 30 wt.% SuperP, 10 wt.% PVDF) on Celgard 2340 or 90 wt.% SuperP and 10 wt.% PVDF | S/C (80 wt.% S/C, 10 wt.% Super P, 10 wt.% PVdF (bind)-NMP); also a variant of mix (90 wt.% S/C, 10 wt.% Mo ₆ S ₈) instead of pure S/C | Al foil | [29] |

Table 2. Hazard statements related to materials utilized in Mg–S batteries.

| Element of Mg–S Battery | Material | Class of EC 1272/2008 | References |
|--------------------------------|---|---|-------------------------|
| Anode | Mg | H228, H261 H228, H252, H261 | [75] [77] |
| | Al ₂ O ₃ | H319, H335, H372 | [87] |
| | CNF TiS ₂ | H226, H312 + H332, H319, H360D. H261, H315, H319, H335 | [103] [107] |
| Current collector | Al foil | H228, H400 H400, H410 | [210] [216] |
| | Al Sheet and Foil (mixture) | H228, H251, H252, H261, H400, H410, H411 | [211] |
| | Graphite | H319, H335, H350i, H373 | [217] |
| | Stainless steel | H242, H300, H310, H317, H331, H332, H351, H410 | [213] |
| | Cu | H316, H320, H334, H317, H341, H351, H360/H361, H370, H371, H335, H372, H373, H413 | [214] |
| | Inconel 625 powder | H300, H330, H317, H319, H340, H373, H400 | [221] |
| | N-doped Graphitic Porous Carbon N/S co-doped Graphene powder | H317, H334, H351, H372 H351 H319, H335 | [223] [227] [228] |
| Cathode | MoS ₂ Powder | H319, H335 | [136] |
| | MoS ₂ | H315, H319, H335 | [196] |
| | MnO ₂ | H302, H332 | [141] |
| | MoO ₃ | H301, H319, H335, H351, H412 | [144] |
| | V ₂ O ₅ | H302, H332, H335, H341, H361d, H372, H411 | [142] |
| | C ₈ H ₈ O ₄ | H302, H315, H319, H335 | [145] |
| | Fullerenes | H315, H319, H351, H335 | [147] |
| | CuF ₂ | H314, H318 | [153] |
| | AgCl | H400, H410 | [155] |
| | Sulfur | H315, H228 | [158] |
| | Activated carbon | H303, H313, H315, H333 H252 | [159] [170] |
| | Mesoporous Carbon CMK-3 | H320, H335 | [169] |
| | Mesoporous Carbon | H351 | [179] |
| | Carbon Nanofiber | H351 | [180] |
| | Carbon Nanotube | H319, H335 | [186] |
| | MgS | H319, H335 | [185] |
| FeS ₂ | H302, H311, H314, H400 | [190] | |
| SnS ₂ | H334, H410 | [194] | |
| Ni ₂ S ₃ | H315, H319, H335 | [195] | |
| CoS ₂ | H317, H341, H350i, H372, H410 H317, H410 | [188] [197] | |

Table 2. Cont.

| Element of Mg-S Battery | Material | Class of EC 1272/2008 | References |
|-----------------------------------|---|--|------------|
| | O ₂ (compressed) | H270, H280 | [152] |
| Binder | polyvinylidene fluoride | H315, H319, H335 | [230] |
| | Na carboxymethyl cellulose | H402, H412 | [234] |
| Electrolyte | Tetrahydrofuran | H225, H302, H319, H335, H351 | [246] |
| | AlCl ₃ | H314 | [236] |
| | PhMgCl | H314, H318 | [238] |
| | LiCl | H302, H315, H319 | [239] |
| | BF ₃ | H280, H330, H314, H318, H335, H373, H402 | [242] |
| | Hexamethyldisilazane | H225, H302 + H332, H311, H412 | [243] |
| | Mg bis(hexamethyldisilazide) | H314, H318 | [244] |
| | Mg bis(diisopropyl)amide | H225, H261, H304, H314, H331, H335, H341, H351, H412 | [245] |
| | 2-Methoxyethyl ether | H226, H360FD | [247] |
| | Tetraethylene glycol dimethyl ether | H360Df | [248] |
| | C ₂ F ₆ LiNO ₄ S | H301, H311, H314, H373, H412 | [252] |
| | Li | H260, H314 | [253] |
| | Anthracene | H302, H319, H335, H400, H410 | [271] |
| | B[HFP] ₃ | H315, H319, H335 | [255] |
| | C ₈ H ₁₈ Mg | H250, H260, H314 | [261] |
| | Trifluoromethanesulfonic acid | H290, H302, H314, H335 | [262] |
| | Mg(TFSI) ₂ | H314 | [260] |
| | Butane | H220, H280 | [263] |
| | Mg(OH) ₂ | H315, H319, H335 | [265] |
| | 18-Crown 6-Ether | H302, H319 | [266] |
| | LiCF ₃ SO ₃ | H315, H319, H335 | [272] |
| | C ₁₂ H ₁₂ MgO ₆ | H315, H319, H335 | [268] |
| | Mg(CF ₃ SO ₃) ₂ | H314, H318 | [270] |
| | C ₁₁ H ₂₀ F ₆ N ₂ O ₄ S ₂ | H315, H319, H335 | [276] |
| | MgCl ₂ | H261 | [267] |
| | YCl ₃ | H315, H319, H335 | [277] |
| | TiCl ₄ | H302, H314, H318, H330, H335 | [279] |
| | (CF ₃) ₂ CHOH | H314, H318, H361, H373 | [283] |
| | tris(2H-hexafluoroisopropyl) borate | H315, H319, H335 | [255] |
| | MgF ₂ | H315, H319, H335 | [287] |
| | 1,2-dimethoxyethane | H225, H303, H332, H360 | [288] |
| | Thiobarbituric Acid | H315, H319, H335 | [290] |
| Mg(BH ₄) ₂ | H261, H301, H311, H331, H314 | [286] | |
| TEGDME | H360 | [249] | |
| | Iodine | H302, H312, H315, H319, H332, H335, H372, H400 | [259] |

Note: H225-Highly flammable liquid and vapor; H226-Flammable liquid and vapor; H228-Flammable solid; H242-Heating may cause a fire; H251-Self-heating, may catch fire; H252-Self-heating substances/mixtures, in large quantities may catch fire; H260-In contact with water releases flammable gases that may ignite spontaneously; H261-Substance and mixture that, in contact with water, emits flammable gas; H270: May cause or intensify fire, oxidizer; H280 Contains gas under pressure, may explode if heated; H290-May be corrosive to metals; H300-Fatal if swallowed; H301-Toxic if swallowed; H302-Harmful if swallowed; H303-May be harmful if swallowed; H304-May be fatal if swallowed and enters airways; H310-Fatal in contact with skin; H311-Toxic in contact with skin; H312 + H332-Harmful in contact with skin or if inhaled; H313-May be harmful in contact with skin; H314-Causes severe skin burns and eye damage; H315-Causes skin irritation; H316-Mild skin irritation; H317-May cause an allergic skin reaction; H-318-Causes serious eye damage; H319-Causes serious eye irritation; H320-Causes eye irritation; H330-Fatal if inhaled; H331-Toxic if inhaled; H332-Harmful if inhaled; H333-May be harmful if inhaled; H334-May cause allergy or asthma symptoms or breathing difficulties if inhaled; H335-May cause respiratory irritation; H340-May cause genetic defects; H341-May cause genetic defects; H350i-May cause cancer by inhalation; H351-Suspected of causing cancer; H360F/D-May damage fertility or an unborn child; H360/H361-May damage fertility or an unborn child; H361d-Suspected of damaging an unborn child; H370-Causes damage to organs; H371-May cause damage to organs; H372-Causes damage to organs through prolonged or repeated exposure; H373-May cause damage to organs through prolonged or repeated exposure; H400-Acute aquatic toxicity; H402-Harmful to aquatic life; H410-Very toxic to aquatic life with long-lasting effects; H411-Toxic to aquatic life with long-lasting effects; H412-Harmful to aquatic life with long lasting effects; H413-May cause long lasting harmful effects to aquatic life.

8. Handling of Mg–S Battery Materials with Hazards Related to Their Use

In addition to the rather natural tendency to avoid (what is sometimes impossible) and minimize direct contact with hazardous substances, a few general recommendations can be made, as have been discussed in the many reference safety data sheets also presented in this review.

- In contact with flammable substances, it can be necessary to wear a self-contained breathing apparatus in pressure-demand, Mine Safety and Health Administration/National Institute for Occupational Safety & Health (MSHA/NIOSH) approved, or the equivalent one, and full protective gear;
- In the case of fire occurrence, it is needed to use the appropriate extinguishing media, including water, dry chemicals, chemical foam, or alcohol-resistant foam;
- If the substance causes, or may cause, irritation or allergy to the eyes, it is required to wear appropriate protective eyeglasses or chemical safety goggles as described by the Occupational Safety and Health Administration (OSHA's) eye and face protection regulations in 29 Code of Federal Regulations (CFR) 1910.133 or European Standard EN166;
- If the substance causes or may cause irritation or allergy to the skin, it is needed to wear appropriate protective gloves to prevent skin exposure. Moreover, it is necessary to wear appropriate protective clothing to prevent skin exposure;
- If the substance causes, or may cause, irritation or allergy of the respiratory tract, and particularly if the exposure limit can be exceeded, it is required to use a NIOSH/MSHA or European Standard EN 149 approved respirator;
- If the substance causes, or may cause, irritation or allergy of the gastrointestinal tract, it is necessary to use good personal hygiene practices, including washing hands before eating, drinking, smoking, or using the toilet;
- If spills or leaks of a dangerous substance may occur, it is needed to absorb the spill with an inert material (e.g., vermiculite, sand, or earth), then place it in a suitable container. It is also necessary to clean up spills immediately, following precautions in the Protective Equipment section, and provide an adequate intensity of ventilation;
- When in contact with a hazardous substance, it is necessary to wash thoroughly after handling. Before the planned reuse, it is needed to remove contaminated or soiled clothing and wash them.

Usually, hazardous substances should be stored in a cool, dry, well-ventilated area away from incompatible substances. The containers used for the storage of such substances should be kept tightly closed.

The use of various materials, particularly in the case of the Mg–S cells, is always associated with identified, partly identified, or non-identified hazards. This aspect can be significant in relation to the further recycling of such materials [292].

To complete the hazard identification, it is needed to collect, up to reaching completeness, information in the following three categories:

- Chemical identity;
- Physical and chemical properties;
- Health effects.

The main sources of information related to chemical identification comprise the following:

- Company records;
- SDSs and product safety bulletins from manufacturers or suppliers;
- OSHA chemical sampling information pages;
- The Merck Index [293];
- ChemID;
- Trade associations' documents.

The main sources of information related to the physical and chemical properties comprise the following:

- Fire Protection Guide to Hazardous Materials [294];
- USA Department of Transportation Emergency Response Guidebook [295];
- OSHA Occupational Chemical Database [296];
- Hazardous Substances Data Bank (HSDB) [297];
- Product safety bulletins from manufacturers or suppliers;
- National Institute for Occupational Safety and Health (NIOSH) documents [298],
- NIOSH Pocket Guide to Chemical Hazards [299],
- International Chemical Safety Cards [300],
- OECD eChemPortal [301],
- The Merck Index [293],
- CRC Handbook of Chemistry and Physics [302],
- Sax's Dangerous Properties of Industrial Materials [303],
- Bretherick's Handbook of Reactive Chemicals Hazards [304],
- Trade associations' documents.

Some recommended reference sources for health effects include:

- Frank R. Lautenberg Chemical Safety for the 21st Century Act [305];
- Company-sponsored research reports;
- SDSs and product safety bulletins from manufacturers and suppliers;
- OSHA Occupational Chemical Database [296];
- Hazardous Substances Data Bank (HSDB) [297];
- National Institute of Occupational Safety and Health (NIOSH) documents [298];
- NIOSH Pocket Guide to Chemical Hazards [299];
- Centers for Disease Control and Prevention (CDC) documents [306];
- Agency for Toxic Substances and Disease Registry (ATSDR) documents [307];
- International Chemical Safety Cards [300];
- NIOSH Registry of Toxic Effects of Chemical Substances (RTECS) [308];
- OSHA chemical sampling information pages;
- IARC Monographs on the Identification of Carcinogenic Hazards to Humans [309];
- NTP Annual Report on Carcinogens [310];
- ACGIH Threshold Limit Values (TLVs) and Biological Exposure Indices (BEIs) [311];
- OECD eChemPortal [301];
- Hawley's Condensed Chemical Dictionary [312];
- Sax's Dangerous Properties of Industrial Materials [303];
- Trade associations' documents.

From the point of view of the further development of the materials used to produce Mg–S batteries, it is important to deal with material mixtures (materials of cathodes, separators, and electrolytes) because each material included in the mixture creates different hazards separately or together with other components of the mixture. The procedure for dealing with such mixtures, and for determining their resultant hazards, is described in [313].

Particularly important and useful for the determination of hazards of mixtures are those determined for several hazard classes for the classified ingredients of the mixtures.

It can be expected that further types of materials will be successively involved in the production of new Mg–S batteries, bringing new or already identified hazards related to their use of these materials. Therefore, it is important to subject each new, or existing, material for which such hazards have not been identified, so far, to a certain group of identification tests. Such identification tests include experimental studies of chemical reactions with various active substances, in particular substances modeling aggressive environmental impacts (oxidation and corrosion), and simulation tests in models based on the mixture rule. In addition, identification studies include *in vitro* studies on mammalian cell lines [314,315], and *in vivo* studies in mouse, rat, and rabbit models [316,317] for the toxic and allergic effects on skin, eyes, digestive and respiratory systems, pregnancy, cancer generation, and the selection of appropriate therapies. Using software [318], these results can be extrapolated to different groups of people and their organs. However, clinical trials will be required over a longer period. Having the results of these studies for individual

component materials, it will be possible to estimate their impact on humans and animals if they are used as components of mixtures in accordance with the methodology described in [313]. Furthermore, the cut-off values and the concentration limits can also be determined using these tests, especially in vivo tests.

9. Methods

Using ‘logical’ database searches, the set of publications (literature) from electronic databases including ‘ISI Web of Science’, ‘Scopus’, and ‘Google Scholar’ was obtained. The period studied in the literature on Mg–S cells ranged from 1974 to 2022. Mostly, articles published in English are comprised, as they are widely accessible to readers around the world. Only a few were published in Germany.

10. Summary

Various hazards related to the use of materials in Mg–S cells are presented in Figure 12. It is visible that the highest number of the hazards identified belonged to the hazard group related to the toxic effects on skin. Two other hazard groups are also characterized by many hazards identified, namely, those related to toxic or allergic effects on the eyes and respiratory tract, respectively. The lowest number of the hazards identified belonged to the hazard group related to corrosion. Additionally, only five of the hazards identified referred to in the hazard group related to the generation of genetic defects. Two other groups are also characterized by a relatively small number of identified hazards, equal to nine—the first one related to the generation of cancers and the second one related to the generation of damages to fertility, or an unborn child, respectively.

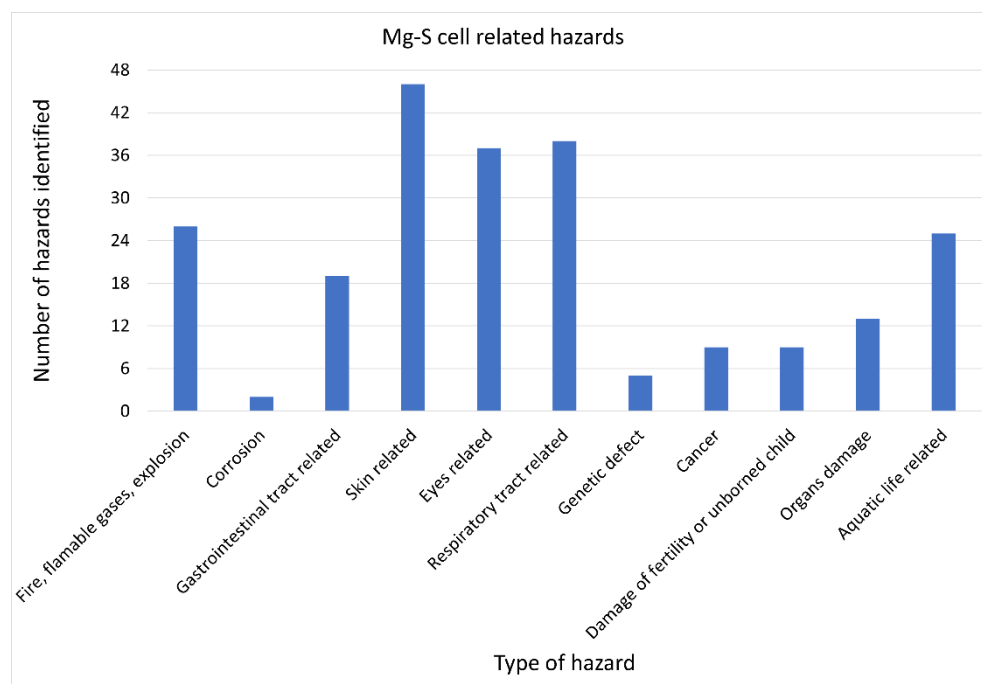


Figure 12. The number of the hazards identified versus the type of hazard for materials in Mg–S cells.

The ratio of the number of the hazards identified related to the single component of the Mg–S cell and the total number of the hazards identified related to the Mg–S cell versus the Mg–S related group of hazards is shown in Figure 13. The highest value of such a ratio characterizes the electrolyte-related group of the hazards identified. Additionally, the relatively high values of such a ratio were obtained for the cathode-related and current collector-related groups of the hazards identified.

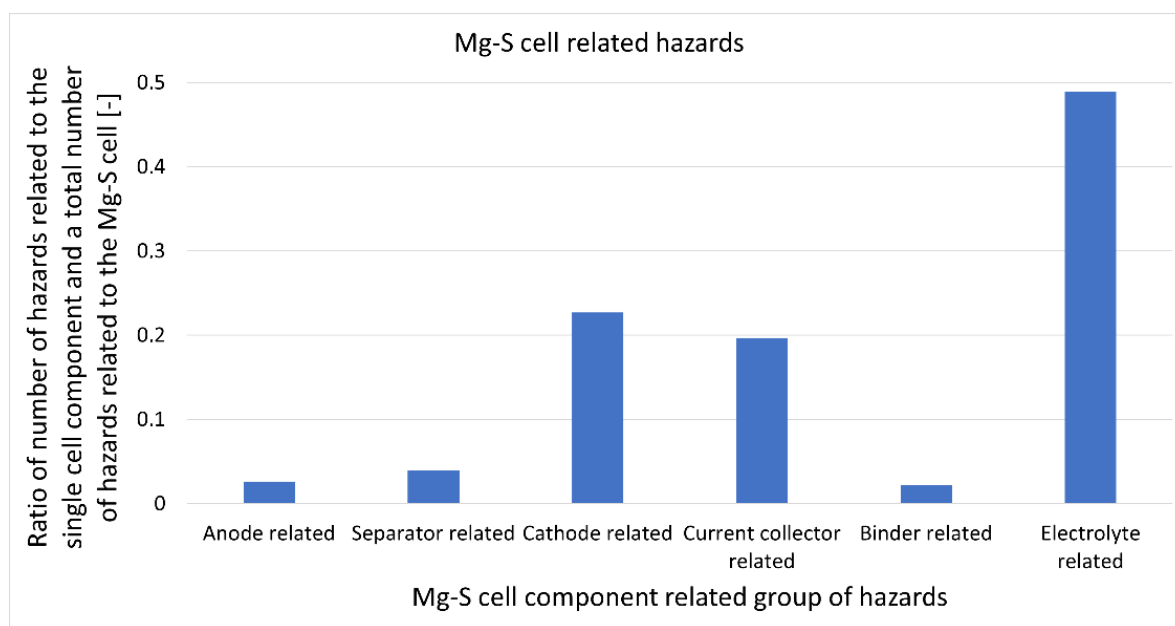


Figure 13. The ratio of the number of the hazards identified related to the single-cell component, and the total number of the hazards identified related to the Mg–S cell versus the Mg–S related group of hazards.

Therefore, when developing a new Mg–S cell configuration, it can be carefully assumed that the group of the life-related hazards characterized by a whole Mg–S cell is well determined by those related to the electrolyte, cathode, and current collector of such a cell.

The Mg–S batteries utilized a lot of materials for their anodes, separators, current collectors, binders, cathodes, and electrolytes. These materials pose various hazards related to their use. The most numerous groups of hazards are posed by the material groups of cathodes and electrolytes. Even for the two latter groups, such hazards vary widely in type and degree of danger. One group of the mentioned hazards is related directly to the human body, involving the eyes, skin, respiratory and digestive tract, and also fertility or an unborn child. The other group of such hazards is related to aquatic life. Yet another group is related to the flammability of materials or the release of flammable or toxic gases by them. Interestingly, some of the described hazards are similar to those found in the case of Li–S batteries’ cathodes, separators, or binders, but some are clearly different, as in the case of anodes [319]. Additionally, the popular Celgard separators are applicable also for Li-ion batteries [320], which environmental and human health impacts were discussed in [321]. Moreover, it should be postulated that pregnant women should not be involved in the production or recycling processes related to Mg–S cells.

Funding: This research received no external funding.

Data Availability Statement: Not applicable.

Conflicts of Interest: The author declares no conflict of interest.

References

- Dunn, B.; Kamath, H.; Tarascon, J.M. Electrical energy storage for the grid: A battery of choices. *Science* **2011**, *334*, 928–935. [[CrossRef](#)] [[PubMed](#)]
- Tarascon, J.M.; Armand, M. Issues and challenges facing rechargeable lithium batteries. *Nature* **2001**, *414*, 359–367. [[CrossRef](#)] [[PubMed](#)]
- Goodenough, J.B.; Kim, Y. Challenges for rechargeable Li batteries. *Chem. Mater.* **2010**, *22*, 587–603. [[CrossRef](#)]
- Liu, C.; Li, F.; Lai-Peng, M.; Cheng, H.M. Advanced materials for energy storage. *Adv. Mater.* **2010**, *22*, E28–E62. [[CrossRef](#)] [[PubMed](#)]

5. Yoo, H.D.; Markevich, E.; Salitra, G.; Sharon, D.; Aurbach, D. On the challenge of developing advanced technologies for electrochemical energy storage and conversion. *Mater. Today* **2014**, *17*, 110–121. [[CrossRef](#)]
6. Wang, Y.; Chen, R.; Chen, T.; Lv, H.; Zhu, G.; Ma, L.; Wang, C.; Jin, Z.; Liu, J. Emerging non-lithium ion batteries. *Energy Storage Mater.* **2016**, *4*, 103–129. [[CrossRef](#)]
7. Wu, F.; Yushin, G. Conversion cathodes for rechargeable lithium and lithium-ion batteries. *Energy Environ. Sci.* **2017**, *10*, 435–459. [[CrossRef](#)]
8. Choi, N.S.; Chen, Z.; Freunberger, S.A.; Ji, X.; Sun, Y.K.; Amine, K.; Yushin, G.; Nazar, L.F.; Cho, J.; Bruce, P.G. Challenges facing lithium batteries and electrical double-layer capacitors. *Angew. Chem. Int. Ed.* **2012**, *51*, 9994–10024. [[CrossRef](#)]
9. Manthiram, A. Materials challenges and opportunities of lithium ion batteries. *J. Phys. Chem. Lett.* **2011**, *2*, 176–184. [[CrossRef](#)]
10. Hong, X.; Mei, J.; Wen, L.; Tong, Y.; Vasileff, A.J.; Wang, L.; Liang, J.; Sun, Z.; Dou, S.X. Nonlithium metal–sulfur batteries: Steps toward a leap. *Adv. Mater.* **2019**, *31*, 1802822. [[CrossRef](#)]
11. Mohtadi, R.; Mizuno, F. Magnesium batteries: Current state of the art, issues and future perspectives. *Beilstein J. Nanotechnol.* **2014**, *5*, 1291–1311. [[CrossRef](#)] [[PubMed](#)]
12. Zhirong, Z.K.; Maximilian, F. Magnesium-sulfur battery: Its beginning and recent progress. *MRS Commun.* **2017**, *7*, 770–784. [[CrossRef](#)]
13. Li, W.; Cheng, S.; Wang, J.; Qiu, Y.; Zheng, Z.; Lin, H.; Nanda, S.; Ma, Q.; Xu, Y.; Ye, F.; et al. Synthesis, Crystal Structure, and Electrochemical Properties of a Simple Magnesium Electrolyte for Magnesium/Sulfur Batteries. *Angew. Chem. Int. Ed.* **2016**, *55*, 6406–6410. [[CrossRef](#)]
14. Zhao-Karger, Z.; Zhao, X.; Fuhr, O.; Fichtner, M. Bisamide based non-nucleophilic electrolytes for rechargeable magnesium batteries. *RSC Adv.* **2013**, *3*, 16330–16335. [[CrossRef](#)]
15. Xu, Y.; Li, W.; Zhou, G.; Pan, Z.; Zhang, Y. A non-nucleophilic mono-Mg²⁺ electrolyte for rechargeable Mg/S battery. *Energy Storage Mater.* **2018**, *14*, 253–257. [[CrossRef](#)]
16. Wang, P.; Buchmeiser, M.R. Rechargeable Magnesium–Sulfur Battery Technology: State of the Art and Key Challenges. *Adv. Funct. Mater.* **2019**, *29*, 1905248. [[CrossRef](#)]
17. Parambath, V.B.; Zhao-Karger, Z.; Diemant, T.; Jäckle, M.; Li, Z.; Scherer, T.; Gross, A.; Behm, R.J.; Fichtner, M. Investigation on the formation of Mg metal anode/electrolyte interfaces in Mg/S batteries with electrolyte additives. *J. Mater. Chem. A* **2020**, *8*, 22998. [[CrossRef](#)]
18. Han, W.; Li, Q.; Zhu, H.; Luo, D.; Qin, X.; Li, B. Hierarchical Porous Graphene Bubbles as Host Materials for Advanced Lithium Sulfur Battery Cathode. *Front. Chem.* **2021**, *9*, 653476. [[CrossRef](#)]
19. Huang, D.; Tan, S.; Li, M.; Wang, D.; Han, C.; An, Q.; Mai, L. Highly Efficient Non-Nucleophilic Mg(CF₃SO₃)₂-Based Electrolyte for High-Power Mg/S Battery. *ACS Appl. Mater. Interfaces* **2020**, *12*, 17474–17480. [[CrossRef](#)]
20. Utkarsh, C.; Preetam, B.; Sanjeevikumar, P.; Dikshita, K.; Garima, P.; Samriddhi, N.; Mahika, S.; Murali, B.; Prashant, S.; Shalu, S.; et al. Review—Carbon Electrodes in Magnesium Sulphur Batteries: Performance Comparison of Electrodes and Future Directions. *J. Electrochem. Soc.* **2021**, *168*, 120555. [[CrossRef](#)]
21. Ha, S.Y.; Lee, Y.W.; Woo, S.W.; Koo, B.; Kim, J.S.; Cho, J.; Lee, K.T.; Choi, N.S. Magnesium(II) Bis(trifluoromethane sulfonyl) Imide-Based Electrolytes with Wide Electrochemical Windows for Rechargeable Magnesium Batteries. *ACS Appl. Mater. Interfaces* **2014**, *6*, 4063–4073. [[CrossRef](#)]
22. Gao, T.; Noked, M.; Pearse, A.J.; Gillette, E.; Fan, X.; Zhu, Y.; Luo, C.; Suo, L.; Schroeder, M.A.; Xu, K.; et al. Enhancing the Reversibility of Mg/S Battery Chemistry through Li⁺ Mediation. *J. Am. Chem. Soc.* **2015**, *137*, 12388–12393. [[CrossRef](#)] [[PubMed](#)]
23. Robba, A.; Vizintin, A.; Bitenc, J.; Mali, G.; Arçon, I.; Kavčič, M.; Žitnik, M.; Bučar, K.; Aquilanti, G.; Martineau-Corcos, C.; et al. Mechanistic Study of Magnesium–Sulfur Batteries. *Chem. Mater.* **2017**, *29*, 9555–9564. [[CrossRef](#)]
24. Yu, X.; Arumugam, M. Performance Enhancement and Mechanistic Studies of Magnesium-Sulfur Cells with an Advanced Cathode Structure. *ACS Energy Lett.* **2016**, *1*, 431–437. [[CrossRef](#)]
25. Kim, H.S.; Arthur, T.S.; Allred, G.D.; Zajicek, J.; Newman, J.G.; Rodnyansky, A.E.; Oliver, A.G.; Boggess, W.C.; Muldoon, J. Structure and compatibility of a magnesium electrolyte with a sulphur cathode. *Nat. Commun.* **2011**, *2*, 427. [[CrossRef](#)] [[PubMed](#)]
26. Nakayama, Y.; Matsumoto, R.; Kumagae, K.; Mori, D.; Mizuno, Y.; Hosoi, S.; Kamiguchi, K.; Koshitani, N.; Inaba, Y.; Kudo, Y.; et al. Zinc Blende Magnesium Sulfide in Rechargeable Magnesium-Sulfur Batteries. *Chem. Mater.* **2018**, *30*, 6318–6324. [[CrossRef](#)]
27. Xu, Y.; Ye, Y.; Zhao, S.; Feng, J.; Li, J.; Chen, H.; Yang, A.; Shi, F.; Jia, L.; Wu, Y.; et al. In Situ X-ray Absorption Spectroscopic Investigation of the Capacity Degradation Mechanism in Mg/S Batteries. *Nano Lett.* **2019**, *19*, 2928–2934. [[CrossRef](#)]
28. Zou, Q.; Sun, Y.; Liang, Z.; Wang, W.; Lu, Y.C. Achieving Efficient Magnesium-Sulfur Battery Chemistry via Polysulfide Mediation. *Adv. Energy Mater.* **2021**, *11*, 2101552. [[CrossRef](#)]
29. Wang, L.; Jankowski, P.; Njel, C.; Bauer, W.; Li, Z.; Meng, Z.; Dasari, B.; Vegge, T.; Gar-cía-Lastra, J.M.; Zhao-Karger, Z.; et al. Dual Role of Mo₆S₈ in Polysulfide Conversion and Shuttle for Mg–S Batteries. *Adv. Sci.* **2022**, 2104605. [[CrossRef](#)]
30. Ford, H.O.; Doyle, E.S.; He, P.; Boggess, W.C.; Oliver, A.G.; Wu, T.; Sterbinsky, G.E.; Schaefer, J.L. Self-discharge of magnesium–sulfur batteries leads to active material loss and poor shelf life. *Energy Environ. Sci.* **2021**, *14*, 890–899. [[CrossRef](#)]
31. Liang, Y.; Zhao, C.Z.; Yuan, H.; Yuan, C.; Zhang, W.; Huang, J.Q.; Yu, D.; Liu, Y.; Titirici, M.; Chueh, Y.L.; et al. A review of rechargeable batteries for portable electronic devices. *InfoMat* **2019**, *1*, 6–32. [[CrossRef](#)]
32. BU-301a: Types of Battery Cells. 2022. Available online: <https://batteryuniversity.com/article/bu-301a-types-of-battery-cells> (accessed on 24 January 2022).

33. BU-304b: Making Lithiumion Safe. 2022. Available online: <https://batteryuniversity.com/article/bu-304b-making-lithium-ion-safe> (accessed on 24 January 2022).
34. Wagner, N.; Fichtner, M.; Bremes, H.G.; Wolter, C.; Zwanziger, I.; Remmlinger, J. Entwicklung und Herstellung von Wiederaufladbaren Magnesium-Schwefel Batterien ‘MagS’. 2019. Available online: <https://doi.org/10.2314/KXP:1680881833> (accessed on 28 January 2022). (In German) [CrossRef]
35. Montenegro, C.T.; Peters, J.F.; Zhao-Karger, Z.; Wolter, C.; Weil, M. Chapter 13—Life Cycle Analysis of a Magnesium–Sulfur Battery. In *Magnesium Batteries: Research and Applications*; Fichtner, M., Ed.; The Royal Society of Chemistry: London, UK, 2020; Energy and Environment Series. [CrossRef]
36. Bautista, S.P.; Weil, M.; Baumann, M. and Montenegro, C.T. Prospective Life Cycle Assessment of a Model Magnesium Battery. *Energy Technol.* **2021**, *9*, 2000964. [CrossRef]
37. Bieker, G.; Küpers, V.; Kolek, M.; Winter, M. Intrinsic differences and realistic perspectives of lithium-sulfur and magnesium-sulfur batteries. *Commun Mater* **2021**, *2*, 37. [CrossRef]
38. Chen, S.; Niu, C.; Lee, H.; Li, Q.; Yu, L.; Xu, W.; Zhang, J.-G.; Dufek, E.J.; Whittingham, M.S.; Meng, S.; et al. Critical parameters for evaluating coin cells and pouch cells of rechargeable Li-metal batteries. *Joule* **2019**, *3*, 1094–1105. [CrossRef]
39. Niu, C.; Lee, H.; Chen, S.; Li, Q.; Du, J.; Xu, W.; Zhang, J.G.; Whittingham, M.S.; Xiao, J.; Liu, J. High-energy lithium metal pouch cells with limited anode swelling and long stable cycles. *Nat. Energy* **2019**, *4*, 551–559. [CrossRef]
40. Walus, S.; Offer, G.; Hunt, I.; Patel, Y.; Stockley, T.; Williams, J.; Purkayastha, R. Volumetric expansion of lithium-sulfur cell during operation—Fundamental insight into applicable characteristics. *Energy Storage Mater.* **2018**, *10*, 233–245. [CrossRef]
41. Mueller, V.; Scurtu, R.G.; Richter, K.; Waldmann, T.; Memm, M.; Danzer, M.A.; Wohlfahrt-Mehrens, M. Effects of mechanical compression on the aging and the expansion behavior of si/C-composite NMC811 in different lithium-ion battery cell for-mats. *J. Electrochem. Soc.* **2019**, *166*, A3796–A3805. [CrossRef]
42. Li, X.; Banis, M.; Lushington, A.; Yang, X.; Sun, Q.; Zhao, Y.; Liu, C.; Li, Q.; Wang, B.; Xiao, W.; et al. A high-energy sulfur cathode in carbonate electrolyte by eliminating pol-ysulfides via solid-phase lithium-sulfur transformation. *Nat. Commun.* **2018**, *9*, 4509. [CrossRef]
43. Fan, Z.; Ding, B.; Guo, H.; Shi, M.; Zhang, Y.; Dong, S.; Zhang, T.; Dou, H.; Zhang, X. Dual dopamine derived polydopamine coated N-doped porous carbon spheres as a sulfur host for high-performance lithium-sulfur batteries. *Chemistry* **2019**, *25*, 10710–10717. [CrossRef]
44. Dai, F.; Shen, J.; Dailly, A.; Balogh, M.P.; Lu, P.; Yang, L.; Xiao, J.; Liu, J.; Cai, M. Hierarchical electrode architectures for high energy lithium-chalcogen rechargeable batteries. *Nano Energy* **2018**, *51*, 668–679. [CrossRef]
45. Jia, L.; Wang, J.; Chen, Z.; Su, Y.; Zhao, W.; Wang, D.; Wei, Y.; Jiang, K.; Wang, J.; Chun, O.; et al. High areal capacity flexible sulfur cathode based on multi-functionalized super aligned carbon nanotubes. *Nano Res.* **2019**, *12*, 1105–1113. [CrossRef]
46. Chung, S.H.; Manthiram, A. Designing lithium-sulfur batteries with high-loading cathodes at a lean electrolyte condition. *ACS Appl. Mater. Interfaces* **2018**, *10*, 43749–43759. [CrossRef]
47. Weller, C.; Thieme, S.; Härtel, P.; Althues, H.; Kaskel, S. Intrinsic shuttle sup-pression in lithium-sulfur batteries for pouch cell application. *J. Electrochem. Soc.* **2017**, *164*, A3766–A3771. [CrossRef]
48. Cheng, X.B.; Yan, C.; Huang, J.Q.; Li, P.; Zhu, L.; Zhao, L.; Zhang, Y.; Zhu, W.; Yang, S.T.; Zhang, Q. The gap between long lifespan Li-S coin and pouch cells: The im-portance of lithium metal anode protection. *Energy Storage Mater.* **2017**, *6*, 18–25. [CrossRef]
49. Salihoglu, O.; and Demir-Cakan, R. Factors affecting the proper functioning of a 3Ah Li-S pouch cell. *J. Electrochem. Soc.* **2017**, *164*, A2948–A2955. [CrossRef]
50. Doerfler, S.; Althues, H.; Haertel, P.; Abendroth, T.; Schumm, B.; Kaskel, S. Challenges and Key Parameters of Lithium-Sulfur Batteries on Pouch Cell Level. *Joule* **2020**, *4*, 539–554. [CrossRef]
51. Muldoon, J.; Bucur, C.B. Electrolyte for Magnesium Battery. U.S. Patent 8722242B2, 2011. Available online: <https://patents.google.com/patent/US8722242B2/en> (accessed on 24 January 2022).
52. Sheng, L.; Hao, Z.; Feng, J.; Du, W.; Gong, M.; Kang, L.; Shearing, P.R.; Brett, D.J.L.; Huang, Y.; Wang, F.R. Evaluation and realization of safer Mg-S battery: The decisive role of the electrolyte. *Nano Energy* **2021**, *83*, 105832. [CrossRef]
53. Saha, P.; Datta, M.K.; Velikokhatnyi, O.I.; Manivannan, A.; Alman, D.; Kumta, P.N. Rechargeable magnesium battery: Current status and key challenges for the future. *Prog. Mater. Sci.* **2014**, *66*, 1–86. [CrossRef]
54. Yoo, H.D.; Shterenberg, I.; Gofer, Y.; Gershinshy, G.; Pour, N.; Aurbach, D. Mg rechargeable batteries: An on-going challenge. *Energy Environ. Sci.* **2013**, *6*, 2265–2279. [CrossRef]
55. Aurbach, D.; Suresh, G.S.; Levi, E.; Mitelman, A.; Mizrahi, O.; Chusid, O.; Brunelli, M. Progress in Rechargeable Magnesium Battery Technology. *Adv. Mater.* **2007**, *19*, 4260–4266. [CrossRef]
56. Muldoon, J.; Bucur, C.B.; Oliver, A.G.; Sugimoto, T.; Matsui, M.; Kim, H.S.; Allred, G.D.; Zajicek, J.; Kotani, Y. Electrolyte roadblocks to a magnesium rechargeable battery. *Energy Environ. Sci.* **2012**, *5*, 5941–5950. [CrossRef]
57. Song, J.; Sahadeo, E.; Noked, M.; Lee, S.B. Mapping the Challenges of Magnesium Battery. *J. Phys. Chem. Lett.* **2016**, *7*, 1736–1749. [CrossRef] [PubMed]
58. Bucur, C.B. *Challenges of a Rechargeable Magnesium Battery. A Guide to the Viability of this Post Lithium-Ion Battery*; Springer: Cham, Switzerland, 2018.
59. Zhang, Y.; Chen, D.; Li, X.; Shen, J.; Chen, Z.; Cao, S.; Li, T.; Xu, F. a-MoS₃@CNT nanowire cathode for rechargeable Mg batteries: A pseudocapacitive approach for efficient Mg-storage. *Nanoscale* **2019**, *11*, 16043–16051. [CrossRef] [PubMed]

60. Aurbach, D.; Weissman, I.; Gofer, Y.; Levi, E. Nonaqueous magnesium electrochemistry and its application in secondary batteries. *Chem. Rec.* **2003**, *3*, 61–73. [CrossRef] [PubMed]
61. Lu, Z.; Schechter, A.; Moshkovich, M.; Aurbach, D. On the electrochemical behavior of magnesium electrodes in polar aprotic electrolyte solutions. *J. Electroanal. Chem.* **1999**, *466*, 203–217. [CrossRef]
62. Merrill, L.C.; Schaefer, J.L. The Influence of Interfacial Chemistry on Magnesium Electrodeposition in Non-nucleophilic Electrolytes Using Sulfone-Ether Mixtures. *Front. Chem.* **2019**, *7*, 194. [CrossRef]
63. Cheng, Y.; Shao, Y.; Zhang, J.G.; Sprenkle, V.L.; Liu, J.; Li, G. High performance batteries based on hybrid magnesium and lithium chemistry. *Chem. Commun.* **2014**, *50*, 9644–9646. [CrossRef]
64. Yang, Y.; Wang, W.; Nuli, Y.; Yang, J.; Wang, J. High Active Magnesium Trifluoromethanesulfonate-Based Electrolytes for Magnesium–Sulfur Batteries. *ACS Appl. Mater. Interfaces* **2019**, *11*, 9062–9072. [CrossRef]
65. Du, A.; Zhang, Z.; Qu, H.; Cui, Z.; Qiao, L.; Wang, L.; Chai, J.; Lu, T.; Dong, S.; Dong, T.; et al. An efficient organic magnesium borate-based electrolyte with non-nucleophilic characteristics for magnesium–sulfur battery. *Energy Environ. Sci.* **2017**, *10*, 2616–2625. [CrossRef]
66. Zhao-Karger, Z.; Liu, R.; Dai, W.; Li, Z.; Diemant, T.; Paranbath, V.B.; Bonatto Minella, C.; Yu, X.; Manthiram, A.; Behm, R.J.; et al. Toward Highly Reversible Magnesium–Sulfur Batteries with Efficient and Practical Mg[B(hfip)₄]₂ Electrolyte. *ACS Energy Lett.* **2018**, *3*, 2005–2013. [CrossRef]
67. Zhang, Z.; Cui, Z.; Qiao, L.; Guan, J.; Xu, H.; Wang, X.; Hu, P.; Du, H.; Li, S.; Zhou, X.; et al. Novel Design Concepts of Efficient Mg-Ion Electrolytes toward High-Performance Magnesium–Selenium and Magnesium–Sulfur Batteries. *Adv. Energy Mater.* **2017**, *7*, 1602055. [CrossRef]
68. Zhou, X.; Tian, J.; Hu, J.; Li, C. High Rate Magnesium–Sulfur Battery with Improved Cyclability Based on Metal–Organic Framework Derivative Carbon Host. *Adv. Mater.* **2018**, *30*, 1704166. [CrossRef] [PubMed]
69. Xu, H.; Zhang, Z.; Li, J.; Qiao, L.; Lu, C.; Tang, K.; Dong, S.; Ma, J.; Liu, Y.; Zhou, X.; et al. Multifunctional additives improve the electrolyte properties of magnesium borohydride toward magnesium–sulfur batteries. *ACS Appl. Mater. Interfaces* **2018**, *10*, 23757–23765. [CrossRef] [PubMed]
70. Li, X.; Gao, T.; Han, F.; Ma, Z.; Fan, X.; Hou, S.; Eidson, N.; Li, W.; Wang, C. Reducing Mg Anode Overpotential via Ion Conductive Surface Layer Formation by Iodine Additive. *Adv. Energy Mater.* **2018**, *8*, 1701728. [CrossRef]
71. Zhao-Karger, Z.; Bardaji, M.E.G.; Fuhr, O.; Fichtner, M. A new class of non-corrosive, highly efficient electrolytes for rechargeable magnesium batteries. *J. Mater. Chem. A* **2017**, *5*, 10815–10820. [CrossRef]
72. Bi, Y.; He, S.; Fan, C.; Luo, J.; Yuan, B.; Liu, T.L. A robust ionic liquid magnesium electrolyte enabling Mg/S batteries. *J. Mater. Chem. A* **2020**, *8*, 12301–12305. [CrossRef]
73. Du, H.; Zhang, Z.; He, J.; Cui, Z.; Chai, J.; Ma, J.; Yang, Z.; Huang, C.; Cui, G. A Delicately Designed Sulfide Graphdiyne Compatible Cathode for High-Performance Lithium/Magnesium–Sulfur Batteries. *Small* **2017**, *13*, 1702277. [CrossRef]
74. Gao, T.; Hou, S.; Wang, F.; Ma, Z.; Li, X.; Xu, K.; Wang, C. Reversible S⁰/MgS_x Redox Chemistry in a MgTfSI₂/MgCl₂/DME Electrolyte for Rechargeable Mg/S Batteries. *Angew. Chem.* **2017**, *129*, 13711–13715. [CrossRef]
75. (CarlRoth-SDS-Mg) CarlRoth Safety Data Sheet. Magnesium Ribbon ≥99,5 %, CAS number 7439-95-4. 2021. Available online: <https://www.carlroth.com/medias/SDB-4468-IE-EN.pdf?context=bWFzdGVyfhHNIY3VyaXR5RGF0YXNoZWV0c3wyNjk5OTF8YXBwbGljYXRpb24vcGRmfHNIY3VyaXR5RGF0YXNoZWV0cy9oN2IvaDg5LzkwMzc2MjQyNzkwNzAucGRmfDYzN2VmNWQyOTZjNDdhYjUxNGNmZWRjMDU4YTg0NTY5MDkyN2U5MjAzMmE3OTZIMWFjZjjiYzAzMGRIMmNhODI> (accessed on 8 January 2022).
76. (NWSCI-SDS-Mg) NWSCI Avantor Safety Data Sheet. Magnesium Metal, Turnings and Ribbon, CAS number: 7439-95-4. 2014. Available online: https://www.nwsci.com/content/customer/docs/skudocs/JTB/jtb_sds_2418.pdf (accessed on 8 January 2022).
77. (ThermoFisher-SDS-Mg) ThermoFisher Scientific Safety Data Sheet. Magnesium Turnings, CAS No.: 7439-95-4. 2021. Available online: <https://www.thermofisher.in/> (accessed on 8 January 2022).
78. Xu, K. Nonaqueous Liquid Electrolytes for Lithium-Based Rechargeable Batteries. *Chem. Rev.* **2004**, *104*, 4303–4418. [CrossRef]
79. Son, S.B.; Gao, T.; Harvey, S.P.; Steirer, K.X.; Stokes, A.; Norman, A.; Wang, C.; Cresce, A.; Xu, K.; Ban, C. An artificial interphase enables reversible magnesium chemistry in carbonate electrolytes. *Nat. Chem.* **2018**, *10*, 532–539. [CrossRef]
80. Wang, Y.; Sahadeo, E.; Rubloff, G.; Lin, C.-F.; Lee, S.B. High-capacity lithium sulfur battery and beyond: A review of metal anode protection layers and perspective of solid-state electrolytes. *J. Mater. Sci.* **2019**, *54*, 3671–3693. [CrossRef]
81. Canepa, P.; Bo, S.H.; Sai Gautam, G.; Key, B.; Richards, W.D.; Shi, T.; Tian, Y.; Wang, Y.; Li, J.; Ceder, G. High magnesium mobility in ternary spinel chalcogenides. *Nat. Commun.* **2017**, *8*, 1759. [CrossRef]
82. Canepa, P.; Sai Gautam, G.; Broberg, D.; Bo, S.-H.; Ceder, G. Role of Point Defects in Spinel Mg Chalcogenide Conductors. *Chem. Mater.* **2017**, *29*, 9657–9667. [CrossRef]
83. Pinson, M.B.; Bazant, M.Z. Theory of SEI Formation in Rechargeable Batteries: Capacity Fade, Accelerated Aging and Lifetime Prediction. *J. Electrochem. Soc.* **2013**, *160*, A243. [CrossRef]
84. Marin, E.; Lanzutti, A.; Andreatta, F.; Lekka, M.; Guzman, L.; Fedrizzi, L. Atomic layer deposition: State-of-the-art and research/industrial perspectives. *Corros. Rev.* **2011**, *29*, 191–208. [CrossRef]
85. Kozen, A.C.; Lin, C.F.; Pearse, A.J.; Schroeder, M.A.; Han, X.; Hu, L.; Lee, S.; Rubloff, G.W.; Noked, M. Next-Generation Lithium Metal Anode Engineering via Atomic Layer Deposition. *ACS Nano*. **2015**, *9*, 5884–5892. [CrossRef] [PubMed]

86. Wang, P.C.; Shih, Y.T.; Lin, M.C.; Lin, H.C.; Chen, M.J.; Lin, K.M. A study of atomic layer deposited LiAl_xO_y films on Mg-Li alloys. *Thin Solid Film.* **2010**, *518*, 7501–7504. [CrossRef]
87. (NCBI- Al_2O_3) National Center for Biotechnology Information. PubChem Database. Alumina, CID=14769. 2020. Available online: <https://pubchem.ncbi.nlm.nih.gov/compound/Alumina> (accessed on 8 January 2022).
88. Zhang, S.S. A review on the separators of liquid electrolyte Li-ion batteries. *J. Power Sources* **2007**, *164*, 351–364. [CrossRef]
89. Zhu, J.; Yanilmaz, M.; Fu, K.; Chen, C.; Lu, Y.; Ge, Y.; Kim, D.; Zhang, X. Understanding glass fiber membrane used as a novel separator for lithium–sulfur batteries. *J. Membr. Sci.* **2016**, *504*, 89–96. [CrossRef]
90. Zhao-Karger, Z.; Zhao, X.; Wang, D.; Diemant, T.; Behm, R.J.; Fichtner, M. Performance Improvement of Magnesium Sulfur Batteries with Modified Non-Nucleophilic Electrolytes. *Adv. Energy Mater.* **2015**, *5*, 1401155. [CrossRef]
91. Sievert, B.; Häcker, J.; Bienen, F.; Wagner, N.; Friedrich, K.A. Magnesium Sulfur Battery with a New Magnesium Powder Anode. *ECS Trans.* **2017**, *77*, 413–424. [CrossRef]
92. Gao, T.; Ji, X.; Hou, S.; Fan, X.; Li, X.; Yang, C.; Han, F.; Wang, F.; Jiang, J.; Xu, K.; et al. Thermodynamics and Kinetics of Sulfur Cathode during Discharge in MgTFSI_2 -DME Electrolyte. *Adv. Mater.* **2018**, *30*, 1704313. [CrossRef] [PubMed]
93. Paranbath, V.B.; Zhao-Karger, Z.; Diemant, T.; Chakravadhanula, V.S.; Schwarzbürger, N.I.; Cambaz, M.A.; Behm, R.J.; Kubel, C.; Fichtner, M. Performance study of magnesium–sulfur battery using a graphene based sulfur composite cathode electrode and a non-nucleophilic Mg electrolyte. *Nanoscale* **2016**, *8*, 3296–3306. [CrossRef]
94. Wang, W.Q.; Yuan, H.C.; Nuli, Y.; Zhou, J.J.; Yang, J.; Wang, J.L. Sulfur@microporous Carbon Cathode with a High Sulfur Content for Magnesium-Sulfur Batteries with Nucleophilic Electrolytes. *J. Phys. Chem. C* **2018**, *122*, 26764–26776. [CrossRef]
95. Zeng, L.; Wang, N.; Yang, J.; Wang, J.; NuLi, Y. Application of a Sulfur Cathode in Nucleophilic Electrolytes for Magnesium/Sulfur Batteries. *J. Electrochem. Soc.* **2017**, *164*, A2504–A2512. [CrossRef]
96. Itaoka, K.; Kim, I.; Yamabuki, K.; Yoshimoto, N.; Tsutsumi, H. Room temperature rechargeable magnesium batteries with sulfur-containing composite cathodes prepared from elemental sulfur and bis(alkenyl) compound having a cyclic or linear ether unit. *J. Power Sources* **2015**, *297*, 323–328. [CrossRef]
97. Zhao, X.; Yang, Y.; NuLi, Y.; Li, D.; Wang, Y.; Xiang, X. A new class of electrolytes based on magnesium bis(diisopropyl)amide for magnesium–sulfur batteries. *Chem. Commun.* **2019**, *55*, 6086–6089. [CrossRef]
98. Lee, B.; Choi, J.; Na, S.; Yoo, D.-J.; Kim, J.H.; Cho, B.W.; Kim, Y.-T.; Yim, T.; Choi, J.W.; Oh, S.H. Critical role of elemental copper for enhancing conversion kinetics of sulphur cathodes in rechargeable magnesium batteries. *Appl. Surf. Sci.* **2019**, *484*, 933–940. [CrossRef]
99. GPRDirect. DIY Composites Ltd. Safety Data Sheet. Glass Fibre CSM. 2020. Available online: <https://www.gprdirect.com/1/2/f/1/sds-glass-fibre.pdf> (accessed on 28 January 2022).
100. Stars Berkeley Safety Data Sheet. Woven Unidirectional Fiberglass Fabric, CAS No.: 65997-17-3. 1997. Available online: https://stars.berkeley.edu/assets/files/Fiberglass_MSDS.pdf (accessed on 8 January 2022).
101. (ACS-SDS-CNF) ACS Material LLC Safety Data Sheet. Carbon Nanofibers, CAS No.: 308063-67-4. 2017. Available online: https://www.acsmaterial.com/pub/media/catalog/product/s/d/sds-carbon_nanofibers.pdf (accessed on 8 January 2022).
102. (AE-SDS-CNF) American Elements Safety Data Sheet. Carbon (Graphite) Nanofibers, CAS No.: 7782-42-5. 2021. Available online: <https://www.americanelements.com/carbon-nanofibers-7782-42-5> (accessed on 8 January 2022).
103. (Metrohm-MSDS-CNF) Metrohm DropSens Material Safety Data Sheet. Carbon Nanofibers Solution. 2020. Available online: http://www.dropsens.com/en/pdfs_productos/new_brochures/msds/msds_drp_cnfsol_en.pdf (accessed on 8 January 2022).
104. Zhou, G.; Tian, H.; Jin, Y.; Tao, X.; Liu, B.; Zhang, R.; Seh, Z.W.; Zhuo, D.; Liu, Y.; Sun, J.; et al. Catalytic oxidation of Li_2S on the surface of metal sulfides for Li-S batteries. *Proc. Natl. Acad. Sci. USA* **2017**, *114*, 840–845. [CrossRef]
105. Sun, X.; Bonnick, P.; Duffort, V.; Liu, M.; Rong, Z.; Persson, K.A.; Ceder, G.; Nazar, L.F. A high capacity thiospinel cathode for Mg batteries. *Energy Environ. Sci.* **2016**, *9*, 2273–2277. [CrossRef]
106. Sun, X.; Bonnick, P.; Nazar, L.F. Layered TiS_2 Positive Electrode for Mg Batteries. *ACS Energy Lett.* **2016**, *1*, 297–301. [CrossRef]
107. (LTS-SDS- TiS_2) LTS Research Laboratories, Inc. Safety Data Sheet. Titanium Sulfide, CAS No.: 12039-13-3. 2016. Available online: <https://www.ltschem.com/msds/TiS2.pdf> (accessed on 8 January 2022).
108. Gregory, T.D.; Hoffman, R.J.; Winterton, R.C. Nonaqueous Electrochemistry of Magnesium: Applications to Energy Storage. *J. Electrochem. Soc.* **1990**, *137*, 775–780. [CrossRef]
109. Kaveevivitchai, W.; Jacobson, A.J. High Capacity Rechargeable Magnesium-Ion Batteries Based on a Microporous Molybdenum–Vanadium Oxide Cathode. *Chem. Mater.* **2016**, *28*, 4593–4601. [CrossRef]
110. Levi, M.; Lancri, E.; Levi, E.; Gizbar, H.; Gofer, Y.; Aurbach, D. The effect of the anionic framework of Mo_6X_8 Chevrel Phase ($X = \text{S}, \text{Se}$) on the thermodynamics and the kinetics of the electrochemical insertion of Mg^{2+} ions. *Solid State Ion.* **2005**, *176*, 1695–1699. [CrossRef]
111. Ma, Z.; MacFarlane, D.R.; Kar, M. Mg Cathode Materials and Electrolytes for Rechargeable Mg Batteries: A Review. *Batter. Supercaps* **2019**, *2*, 115–127. [CrossRef]
112. Aurbach, D.; Lu, Z.; Schechter, A.; Gofer, Y.; Gizbar, H.; Turgeman, R.; Cohen, Y.; Moshkovich, M.; Levi, E. Prototype systems for rechargeable magnesium batteries. *Nature* **2000**, *407*, 724–727. [CrossRef]
113. Doe, R.E.; Han, R.; Hwang, J.; Gmitter, A.J.; Shterenberg, I.; Yoo, H.D.; Pour, N.; Aurbach, D. Novel, electrolyte solutions comprising fully inorganic salts with high anodic stability for rechargeable magnesium batteries. *Chem. Commun.* **2014**, *50*, 243–245. [CrossRef]

114. Du, A.; Zhang, H.; Zhang, Z.; Zhao, J.; Cui, Z.; Zhao, Y.; Dong, S.; Wang, L.; Zhou, X.; Cui, G. A Crosslinked Polytetrahydrofuran-Borate-Based Polymer Electrolyte Enabling Wide-Working-Temperature-Range Rechargeable Magnesium Batteries. *Adv. Mater.* **2019**, *31*, 1805930. [[CrossRef](#)]
115. Yu, L.; Zhang, X. Electrochemical insertion of magnesium ions into V_2O_5 from aprotic electrolytes with varied water content. *J. Colloid Interface Sci.* **2004**, *278*, 160–165. [[CrossRef](#)]
116. Shterenberg, I.; Salama, M.; Gofer, Y.; Levi, E.; Aurbach, D. The challenge of developing rechargeable magnesium batteries. *MRS Bull.* **2014**, *39*, 453–460. [[CrossRef](#)]
117. Rasul, S.; Suzuki, S.; Yamaguchi, S.; Miyayama, M. High capacity positive electrodes for secondary Mg-ion batteries. *Electrochim. Acta* **2012**, *82*, 243–249. [[CrossRef](#)]
118. Zhang, R.; Yu, X.; Nam, K.-W.; Ling, C.; Arthur, T.S.; Song, W.; Knapp, A.M.; Ehrlich, S.N.; Yang, X.-Q.; Matsui, M. α - MnO_2 as a cathode material for rechargeable Mg batteries. *Electrochem. Commun.* **2012**, *23*, 110–113. [[CrossRef](#)]
119. Gershinsky, G.; Yoo, H.D.; Gofer, Y.; Aurbach, D. Electrochemical and spectroscopic analysis of Mg^{2+} intercalation into thin film electrodes of layered oxides: V_2O_5 and MoO_3 . *Langmuir* **2013**, *29*, 10964–10972. [[CrossRef](#)]
120. Mao, M.; Gao, T.; Hou, S.; Wang, C. A critical review of cathodes for rechargeable Mg batteries. *Chem. Soc. Rev.* **2018**, *47*, 8804–8841. [[CrossRef](#)] [[PubMed](#)]
121. Muldoon, J.; Bucur, C.B.; Gregory, T. Quest for nonaqueous multivalent secondary batteries: Magnesium and beyond. *Chem. Rev.* **2014**, *114*, 11683–11720. [[CrossRef](#)]
122. Sano, H.; Senoh, H.; Yao, M.; Sakaebe, H.; Kiyobayashi, T. Mg^{2+} Storage in Organic Positive-electrode Active Material Based on 2,5-Dimethoxy-1,4-benzoquinone. *Chem. Lett.* **2012**, *41*, 1594–1596. [[CrossRef](#)]
123. NuLi, Y.; Guo, Z.; Liu, H.; Yang, J. A new class of cathode materials for rechargeable magnesium batteries: Organosulfur compounds based on sulfur-sulfur bonds. *Electrochem. Commun.* **2007**, *9*, 1913–1917. [[CrossRef](#)]
124. Pan, B.; Huang, J.; Feng, Z.; Zeng, L.; He, M.; Zhang, L.; Vaughney, J.T.; Bedzyk, M.J.; Fenter, P.; Zhang, Z.; et al. Polyanthraquinone-Based Organic Cathode for High-Performance Rechargeable Magnesium-Ion Batteries. *Adv. Energy Mater.* **2016**, *6*, 1600140. [[CrossRef](#)]
125. Zhang, R.; Mizuno, F.; Ling, C. Fullerenes: Non-transition metal clusters as rechargeable magnesium battery cathodes. *Chem. Commun.* **2015**, *51*, 1108–1111. [[CrossRef](#)]
126. Zhao-Karger, Z.; Fichtner, M. Beyond Intercalation Chemistry for Rechargeable Mg Batteries: A Short Review and Perspective. *Front. Chem.* **2019**, *6*, 656. [[CrossRef](#)]
127. Levi, E.; Gofer, Y.; Vestfreed, Y.; Lancry, E.; Aurbach, D. $Cu_2Mo_6S_8$ chevrel phase, a promising cathode material for new rechargeable Mg batteries: A mechanically induced chemical reaction. *Chem. Mater.* **2002**, *14*, 2767–2773. [[CrossRef](#)]
128. Huie, M.M.; Bock, D.C.; Takeuchi, E.S.; Marschilok, A.C.; Takeuchi, K.J. Cathode materials for magnesium and magnesium-ion based batteries. *Coord. Chem. Rev.* **2015**, *287*, 15–27. [[CrossRef](#)]
129. Huang, M.; Li, M.; Niu, C.; Li, Q.; Mai, L. Recent Advances in Rational Electrode Designs for High-Performance Alkaline Rechargeable Batteries. *Adv. Funct. Mater.* **2019**, *29*, 1807847. [[CrossRef](#)]
130. Bucur, C.B.; Gregory, T.; Oliver, A.G.; Muldoon, J. Confession of a Magnesium Battery. *J. Phys. Chem. Lett.* **2015**, *6*, 3578–3591. [[CrossRef](#)] [[PubMed](#)]
131. Xu, Y.; Zhou, G.; Zhao, S.; Li, W.; Shi, F.; Li, J.; Feng, J.; Zhao, Y.; Wu, Y.; Guo, J.; et al. Improving a Mg/S battery with YCl_3 additive and magnesium polysulfide. *Adv. Sci.* **2019**, *6*, 1800981. [[CrossRef](#)] [[PubMed](#)]
132. Paskach, T.J.; Schrader, G.L.; McCarley, R.E. Synthesis of Methanethiol from Methanol over Reduced Molybdenum Sulfide Catalysts Based on the Mo_6S_8 Cluster. *J. Catal.* **2002**, *211*, 285–295. [[CrossRef](#)]
133. Rabiller-Baudry, M.; Sergent, M.; Chevrel, R. Convenient syntheses of chevrel phase compounds from soluble sulfide precursors under flowing hydrogen atmosphere. *Mat. Res. Bull.* **1991**, *26*, 519–526. [[CrossRef](#)]
134. Chevrel, R.; Sergent, M.; Prigent, J. Un nouveau sulfure de molybdene: Mo_3S_4 preparation, proprietes et structure cristalline. *Mater. Res. Bull.* **1974**, *9*, 1487–1498. [[CrossRef](#)]
135. Chen, W.; Qi, W.; Lu, W.; Chaudhury, N.R.; Yuan, J.; Qin, L.; Lou, J. Direct Assessment of the Toxicity of Molybdenum Disulfide Atomically Thin Film and Microparticles via Cytotoxicity and Patch Testing. *Small* **2018**, *14*, 1702600. [[CrossRef](#)]
136. (US-RN-SDS-MoS2) US Research Nanomaterials, Inc. Safety Data Sheet. Molybdenum Disulfide (MoS_2) Powder, CAS No.: 1317-33-5. 2016. Available online: <https://n.b5z.net/i/u/10091461/f/MSDS-NANOPOWDERS/US2180.pdf> (accessed on 8 January 2022).
137. Lee, H.Y.; Goodenough, J.B. Supercapacitor behavior with KCl electrolyte. *J. Solid State Chem.* **1999**, *144*, 220–223. [[CrossRef](#)]
138. Lee, H.Y.; Manivannan, V.; Goodenough, J. Electrochemical capacitors with KCl electrolyte. *Comptes Rendus Acad. Des. Sci. Ser. IIC Chem.* **1999**, *2*, 565–577. [[CrossRef](#)]
139. Lee, T.H.; Pham, D.T.; Sahoo, R.; Seok, J.; Luu, T.H.T.; Lee, Y.H. High energy density and enhanced stability of asymmetric supercapacitors with mesoporous $MnO_2@CNT$ and nanodot $MoO_3@CNT$ free-standing films. *Energy Storage Mater.* **2018**, *12*, 223–231. [[CrossRef](#)]
140. Ji, L.; Lin, Z.; Alcoutlabi, M.; Zhang, X. Recent developments in nanostructured anode materials for rechargeable lithium-ion batteries. *Energy Env. Sci.* **2011**, *4*, 2682–2699. [[CrossRef](#)]
141. (NCBI-MnO2) National Center for Biotechnology Information. PubChem Database. Manganese Dioxide, CID = 14801. 2020. Available online: <https://pubchem.ncbi.nlm.nih.gov/compound/Manganese-dioxide> (accessed on 8 January 2022).

142. (Evraz-SDS-V₂O₅) Evraz Stratcor Inc. Safety Data Sheet. Vanadium Pentoxide (V₂O₅). 2015. Available online: www.evrazstratcor.com (accessed on 8 January 2022).
143. Whittingham, M.S. Ultimate limits to intercalation reactions for lithium batteries. *Chem. Rev.* **2014**, *114*, 11414–11440. [CrossRef]
144. (Materion-SDS-MoO₃) Materion Safety Data Sheet. Molybdenum Trioxide (MoO₃), CAS No.: 1313-27-5. 2018. Available online: [https://www.materion.com/api/materion/Msds/Download?fileName=1XC_MOLYBDENUM%20OXIDE%20\(MOO3\)_SDS-EU_EU%20English.pdf](https://www.materion.com/api/materion/Msds/Download?fileName=1XC_MOLYBDENUM%20OXIDE%20(MOO3)_SDS-EU_EU%20English.pdf) (accessed on 8 January 2022).
145. (SA-SDS-C8H8O4) Sigma-Aldrich Safety Data Sheet. 2,5-Dimethoxy-(1,4)benzoquinone. 2021. Available online: <https://www.sigmaaldrich.com/PL/en/sds/aldrich/r164348> (accessed on 8 January 2022).
146. (TCI-MSDS-C8H8O4) TCI America Material Safety Data Sheet. 2,5-Dimethoxy-1,4-benzoquinone, CAS No.: 3117-03-1. 2005. Available online: https://www.zoro.com/static/cms/enhanced_pdf/ZQ_7n4jgko.PDF (accessed on 8 January 2022).
147. Strem Chemicals, Inc. Safety Data Sheet. Fullerenes—C₆₀ /C₇₀ Mixture, CAS No.: 131159-39-2. 2021. Available online: https://www.strem.com/uploads/sds/sd06-0500_US.pdf (accessed on 8 January 2022).
148. (ThermoFisher-SDS-Fullerene) ThermoFisher Scientific Safety Data Sheet. Fullerene C₆₀. 2018. Available online: <https://www.fishersci.com/store/msds?partNumber=AC295010010&productDescription=FULLERENE+C60%2C+99.90%25+1GR&vendorId=VN00032119&countryCode=US&language=en> (accessed on 8 January 2022).
149. (Cheap Tubes-MSDS-Fullerenes) Cheap Tubes Inc. Material Safety Data Sheet. Carbon Fullerenes. 2015. Available online: <https://www.ctimaterials.com/wp-content/uploads/2015/03/Fullerenes-MSDS.pdf> (accessed on 8 January 2022).
150. Muldoon, J.; Bucur, C.B.; Gregory, T. Magnesiumbatterien—Ein Aufruf an Synthesechemiker: Elektrolyte und Kathoden dringend gesucht. *Angew. Chem.* **2017**, *129*, 12232–12253. [CrossRef]
151. (Airgas-SDS-O₂) Airgas USA Safety Data Sheet. Oxygen, CAS No.: 7782-44-7. 2020. Available online: <https://www.airgas.com/msds/001043.pdf> (accessed on 8 January 2022).
152. (BOC-SDS-O₂) BOC Safety Data Sheet. Oxygen Compressed, CAS No.: 7782-44-7. 2016. Available online: https://www.boconline.co.uk/en/images/10021701_tcm410-84499.pdf (accessed on 8 January 2022).
153. (ThermoFisher-SDS-CuF₂) ThermoFisher Scientific Safety Data Sheet. Copper(II) Fluoride, CAS-No 7789-19-7. 2020. Available online: [https://ukpai-acrest-p1.acros.com/DirectWebViewer/private/document.aspx?prd=ACR20337~{}~{}PDF~{}~{}MTR~{}~{}CLP1~{}~{}EN~{}~{}2020-12-13%2005:35:40~{}~{}Copper\(II\)](https://ukpai-acrest-p1.acros.com/DirectWebViewer/private/document.aspx?prd=ACR20337~{}~{}PDF~{}~{}MTR~{}~{}CLP1~{}~{}EN~{}~{}2020-12-13%2005:35:40~{}~{}Copper(II)) (accessed on 8 January 2022).
154. (ThermoFisher-SDS-CuF₂) ThermoFisher Scientific Safety Data Sheet. Copper(II) Fluoride, CAS-No 7789-19-7. 2018. Available online: <https://www.fishersci.com/store/msds?partNumber=AC203370250&productDescription=COPPER%28II%29+FLUORIDE%2C+ANH+25GR&vendorId=VN00032119&countryCode=US&language=en> (accessed on 8 January 2022).
155. (CarlRoth-SDS-AgCl) CarlRoth Safety Data Sheet. Silver Chloride, CAS No.: 7783-90-6. 2017. Available online: <https://www.carlroth.com/medias/SDB-5302-GB-EN.pdf?context=bWFzdGVyfHNIY3VyaXR5RGF0YXNoZWV0c3wyMDI1ODN8YXBwbGljYXRpb24vcGRmFHNIY3VyaXR5RGF0YXNoZWV0cy9oODkvaGQzLzG5NTA3MTkzMTU5OTgucGRmDg0N2UxMTY3YzRjYTAyZTk0MWQ0MGUwN2ViZGM5NDY2MDZlMzZjMmU2MmQzODIwNDU0NTY4NzJmODYxZmRkOWY> (accessed on 8 January 2022).
156. (Fisher-MSDS-AgCl) Fisher Scientific Material Safety Data Sheet. Silver Chloride, CAS No.: 7783-90-6. 2008. Available online: <https://fscimage.fishersci.com/msds/20787.htm> (accessed on 8 January 2022).
157. (AquaPhoenix-SDS-AgCl) AquaPhoenix Scientific, Inc. Safety Data Sheet. Silver Chloride, CAS No.: 7783-90-6. 2015. Available online: https://beta-static.fishersci.com/content/dam/fishersci/en_US/documents/programs/education/regulatory-documents/sds/chemicals-s/S25524.pdf (accessed on 8 January 2022).
158. (Chem-Supply-SDS-S) Chem-Supply PTY Ltd. Safety Data Sheet. (ABN 19008264211). Sulfur. CAS No.: 7704-34-9. 2014. Available online: <https://www.chemsupply.com.au/documents/ST0061CH71.pdf> (accessed on 8 January 2022).
159. (SA-MSDS-S) Sigma-Aldrich Material Safety Data Sheet. Sulfur. CAS No.: 7704-34-9. 2012. Available online: www.sigma-aldrich.com (accessed on 8 January 2022).
160. Li, Y.; Zhang, Y.; Yu, M.; Pei, H.; Liu, W.; Guo, R.; Xie, J.; Wang, Y.; Yang, C. Lightweight flexible sulfur electrode and preparation method and application thereof. CN201811478988, 2019. Shanghai Space Dianyuan Institute. Available online: <https://www.jmrhip.com/static/patent/html/CN109713310A.html> (accessed on 8 January 2022).
161. Chaudhuri, I.; Fruijtjer-Pölloth, C.; Ngiewih, Y.; Levy, L. Evaluating the evidence on genotoxicity and reproductive toxicity of carbon black: A critical review. *Crit. Rev. Toxicol.* **2018**, *48*, 143–169. [CrossRef] [PubMed]
162. (TIMCAL-MSDS-Super P) TIMCAL Belgium, N.V. Material Safety Data Sheet. Ensaco 150/210/250/260/350 Granular, Ensaco 150/250P, Super P, Super P-Li, C-ENERGY Super C 45/65, CAS No.: 1333-86-4. 2011. Available online: <https://ehslegacy.unr.edu/msdsfiles/24831.pdf> (accessed on 8 January 2022).
163. Lenntech, B.V. Chemical Properties of Carbon—Health Effects of Carbon—Environmental Effects of Carbon. 2020. Available online: <https://www.lenntech.com/periodic/elements/c.htm> (accessed on 8 January 2022).
164. Tamames-Tabar, C.; Cunha, D.; Imbuluzqueta, E.; Ragon, F.; Serre, C.; Blanco-Prieto, M.; Horcajada, P. Cytotoxicity of nanoscaled metal-organic frameworks. *J. Mater. Chem. B* **2014**, *2*, 262–271. [CrossRef] [PubMed]
165. Ruyra, A.; Yazdi, A.; Espin, J.; Maspoch, D. Synthesis, culture medium stability, and in vitro and in vivo zebrafish embryo toxicity of metal-organic framework nanoparticles. *Chem.-Eur. J.* **2015**, *21*, 2508–2518. [CrossRef]
166. Ren, F.; Yang, B.C.; Cai, J.; Jiang, Y.D.; Xu, J.; Wang, S. Toxic effect of zinc nanoscale metal-organic frameworks on rat pheochromocytoma (PC12) cells in vitro. *J. Hazard. Mater.* **2014**, *271*, 283–291. [CrossRef]

167. Grall, R.; Hidalgo, T.; Delic, J.; Garcia-Marquez, A.; Chevillard, S.; Horcajada, P. In vitro biocompatibility of mesoporous metal (III.; Fe, Al, Cr) trimesate MOF nanocarriers. *J. Mater. Chem. B* **2015**, *3*, 8279–8292. [CrossRef]
168. Wagner, A.; Liu, Q.; Rose, O.L.; Eden, A.; Vijay, A.; Rojanasakul, Y.; Dinu, C.Z. Toxicity screening of two prevalent metal organic frameworks for therapeutic use in human lung epithelial cells. *Int. J. Nanomed.* **2019**, *14*, 7583–7591. [CrossRef] [PubMed]
169. (BakerCorp-SDS-AC) BakerCorp Safety Data Sheet. Activated Carbon, CAS No.: 7440-44-0. 2015. Available online: <https://newpig.scene7.com/is/content/NewPig/pdfs/MSD-V021.pdf> (accessed on 8 January 2022).
170. (CarlRoth-SDS-AC) Carl Roth Safety Data Sheet. Activated Carbon Powder, CAS No.: 7440-44-0. 2021. Available online: <https://www.carlroth.com/medias/SDB-5963-GB-EN.pdf?context=bWFzdGVyfHNIY3VyaXR5RGF0YXNoZWV0c3wyNTM2MTh8YXBwbGljYXRpb24vcGRmfHNIY3VyaXR5RGF0YXNoZWV0cy9oZjAvaGE1LzkwMjYyNTU3NTQyNzAucGRmfDMxNDI5OWI3OTgwNTdkYTdjZTRhMmM5ZmNiOTZlODEyN2Y1MjgyYjM1YTMzMmEwYjYmYmNmI2MwVmMDJmNDA> (accessed on 8 January 2022).
171. Chen, R.; Zhao, T.; Wu, F. From a historic review to horizons beyond: Lithium–sulphur batteries run on the wheels. *Chem. Commun.* **2015**, *51*, 18–33. [CrossRef] [PubMed]
172. Wu, H.B.; Wei, S.; Zhang, L.; Xu, R.; Huang, H.H.; Lou, X.W. Embedding Sulfur in MOF-Derived Microporous Carbon Polyhedrons for Lithium–Sulfur Batteries. *Chem. Eur. J.* **2013**, *19*, 10804. [CrossRef] [PubMed]
173. Oschatz, M.; Thieme, S.; Borchardt, L.; Lohe, M.R.; Biemelt, T.; Bruckner, J.; Althues, H.; Kaskel, S. A new route for the preparation of mesoporous carbon materials with high performance in lithium–sulphur battery cathodes. *Chem. Commun.* **2013**, *49*, 5832–5834. [CrossRef]
174. Chen, S.; Huang, X.; Liu, H.; Sun, B.; Yeoh, W.; Li, K.; Zhang, J.; Wang, G. 3D Hyperbranched Hollow Carbon Nanorod Architectures for High-Performance Lithium–Sulfur Batteries. *Adv. Energy Mater.* **2014**, *4*, 1301761. [CrossRef]
175. Jayaprakash, N.; Shen, J.; Moganty, S.S.; Corona, A.; Archer, L.A. Porous Hollow Carbon@Sulfur Composites for High-Power Lithium–Sulfur Batteries. *Angew. Chem.* **2011**, *123*, 6026–6030. [CrossRef]
176. He, G.; Evers, S.; Liang, X.; Cuisinier, M.; Garsuch, A.; Nazar, L.F. Tailoring Porosity in Carbon Nanospheres for Lithium–Sulfur Battery Cathodes. *ACS Nano.* **2013**, *7*, 10920–10930. [CrossRef]
177. Ji, X.; Lee, K.T.; Nazar, L.F. A highly ordered nanostructured carbon–sulphur cathode for lithium–sulphur batteries. *Nat. Mater.* **2009**, *8*, 500–506. [CrossRef]
178. Zuo, P.; Li, Y.; He, M.; Li, R.; Ma, Y.; Du, C.; Gao, Y.; Yin, G. Method for Carbon Fiber Reinforced High-Load Sulfur Electrode. CN107910535A, 2018. Harbin Institute of Technology. Available online: <https://patents.google.com/patent/CN107910535A/zh> (accessed on 8 January 2022).
179. (ACS-SDS-CMK-3) ACS Material LLC Safety Data Sheet. ACS Material Ordered Mesoporous Carbon CMK-3, CAS-No.: 7440-44-0. 2017. Available online: https://www.acsmaterial.com/pub/media/catalog/product/s/d/sds-ordered_mesoporous_carbon_cmk-3.pdf (accessed on 8 January 2022).
180. (SA-SDS-MeC) Sigma-Aldrich Safety Data Sheet. Carbon, Mesoporous, CAS No.: 1333-86-4. 2021. Available online: <https://www.sigmaaldrich.com/PL/en/sds/aldrich/702102> (accessed on 8 January 2022).
181. Wang, T.; Jiang, X. Toxicity Mechanism of Graphene Oxide and Nitrogen-doped Graphene Quantum Dots in RBCs Revealed by Surface-Enhanced Infrared Absorption Spectroscopy. *Toxicol. Res.* **2015**, *4*, 885–894. [CrossRef]
182. (CN-MSDS-GP) Cambridge Nanosystems Ltd. Material Safety Data Sheet. CamGraph Graphene Powder. 2019. Available online: https://cambridgenanosystems.com/wp-content/uploads/2015/05/CNS_CamGraph_MSDS_V1.0.pdf (accessed on 8 January 2022).
183. (GS-SDS-CGS) Graphene Supermarket Safety Data Sheet. Conductive Graphene Sheets. CAS-No.: 7782-42-5. 2016. Available online: www.graphene-supermarket.com (accessed on 8 January 2022).
184. Ou, L.; Song, B.; Liang, H.; Liu, J.; Feng, X.; Deng, B.; Sun, T.; Shao, L. Toxicity of graphene-family nanoparticles: A general review of the origins and mechanisms. *Part Fibre Toxicol.* **2016**, *13*, 57. [CrossRef]
185. (Raymor-SDS-CNT) Raymor Nanotech, Division of Raymor Industries Inc. Safety Data Sheet. Carbon Nanotube, Single-Walled. 2014. Available online: <https://raymor.com/wp-content/uploads/2014/10/MSDS-SWNT-RN-020.pdf> (accessed on 8 January 2022).
186. (Pyrograf-SDS-CNF) Pyrograf Products, Inc. Safety data Sheet. Pyrograf III Carbon Nanofiber, PS Grade. 2016. Available online: <https://apsci.com/wp-content/uploads/2021/05/UPDATED-SDS-Version-9-PS-grade.pdf> (accessed on 8 January 2022).
187. (GOLeafe-MSDS-rGO) GOLeafe Materials Safety Data Sheet. Reduced Graphene Oxide, rGO, CAS No.: 7782-4-5. 2019. Available online: <https://goleafe.com/wp-content/uploads/2017/09/GOLEafe-MSDS.pdf> (accessed on 8 January 2022).
188. (ACS-SDS-rGO) ACS Material LLC Safety Data Sheet. ACS Material Reduced Graphene Oxide (rGO), CAS-No.: 7782-42-5. 2017. Available online: https://www.acsmaterial.com/pub/media/catalog/product/file/SDS-Reduced_Graphene_Oxide_rGO_.pdf (accessed on 8 January 2022).
189. (CGT-MSDS-rGO) Ceylon Graphene Technologies Pvt Ltd. Material Safety Data Sheet, Reduced Graphene Oxide. 2021. Available online: <https://www.ceylongraphene.com/pdf/reduced-graphene-oxide-msds.pdf> (accessed on 8 January 2022).
190. (XiXisys-SDS-MgS) XiXisys Safety Data Sheet. Magnesium Sulfide (MgS), CAS No.: 12032-36-9. 2017. Available online: <https://www.guidedchem.com/msds/12032-36-9.html> (accessed on 28 January 2022).
191. Zheng, T.; Gao, Y.; Deng, X.; Liu, H.; Liu, J.; Liu, R.; Shao, J.; Li, Y.; Jia, L. Comparisons between Graphene Oxide and Graphdiyne Oxide in Physicochemistry Biology and Cytotoxicity. *ACS Appl. Mater. Interfaces* **2018**, *10*, 32946–32954. [CrossRef] [PubMed]

192. Cui, G.; Fu, L.; Huimin, X.; Zhonghua, Z.; Xu, H.; Wang, X. Sulfur/Sulfide/Copper Ternary Composite Positive Electrode and Its Preparation and Application in Magnesium-Sulfur Battery. CN106935796 A, 2017. Qingdao Institute of Bioenergy & Bioprocess Technology Chinese Academy of Science. Available online: <https://patents.google.com/patent/CN106935796A/en> (accessed on 8 January 2022).
193. (SA-SDS-MiC) Sigma-Aldrich Safety Data Sheet. Microporous Carbon Boiling Chips. 2021. Available online: <https://www.sigmaaldrich.com/PL/en/sds/aldrich/z265918> (accessed on 8 January 2022).
194. (LTS-SDS-FeS₂) LTS Research Laboratories, Inc. Safety Data Sheet. Iron Disulfide FeS₂, CAS No.: 12068-85-8. 2018. Available online: <https://www.ltschem.com/msds/FeS2.pdf> (accessed on 8 January 2022).
195. (LTS-SDS-SnS₂) LTS Research Laboratories, Inc. Safety Data Sheet. Tin Sulfide SnS₂, CAS No.: 1315-01-1. 2015. Available online: <https://www.ltschem.com/msds/SnS2.pdf> (accessed on 8 January 2022).
196. (LTS-SDS-MoS₂) LTS Research Laboratories, Inc. Safety Data Sheet. Molybdenum Sulfide, CAS No.: 1317-33-5. 2015. Available online: <https://www.ltschem.com/msds/MoS2.pdf> (accessed on 8 January 2022).
197. Lorad Chemical Corporation Safety Data Sheet. Cobalt Disulfide CoS₂, CAS No: 12013-10-4. 2017. Available online: <https://loradchemical.com/data/sds/SDS-Cobalt-Disulfide.pdf> (accessed on 8 January 2022).
198. (AE-SDS-Ni₂S₃) American Elements Safety Data Sheet Nickel(III) Sulfide, CAS No.: 12259-56-2. 2021. Available online: <https://www.americanelements.com/nickel-iii-sulfide-12259-56-2> (accessed on 8 January 2022).
199. Frey, M.; Zenn, R.K.; Warneke, S.; Müller, K.; Hintennach, A.; Dinnebier, R.E.; Buchmeiser, M.R. Easily Accessible, Textile Fiber-Based Sulfurized Poly(acrylonitrile) as Li/S Cathode Material: Correlating Electrochemical Performance with Morphology and Structure. *ACS Energy Lett.* **2017**, *2*, 595–604. [CrossRef]
200. Warneke, S.; Eusterholz, M.; Zenn, R.K.; Hintennach, A.; Dinnebier, R.; Buchmeiser, M.R. Differences in Electrochemistry between Fibrous SPAN and Fibrous S/C Cathodes Relevant to Cycle Stability and Capacity. *J. Electrochem. Soc.* **2018**, *165*, A6017–A6020. [CrossRef]
201. Warneke, S.; Zenn, R.K.; Leberherz, T.; Müller, K.; Hintennach, A.; Starke, U.; Dinnebier, R.E.; Buchmeiser, M.R. Hybrid Li/S Battery Based on Dimethyl Trisulfide and Sulfurized Poly(acrylonitrile). *Adv. Sustain. Syst.* **2018**, *2*, 1700144. [CrossRef]
202. Fanous, J.; Wegner, M.; Spera, M.B.M.; Buchmeiser, M.R. High Energy Density Poly(acrylonitrile)-Sulfur Composite-Based Lithium-Sulfur Batteries. *J. Electrochem. Soc.* **2013**, *160*, A1169–A1170. [CrossRef]
203. Fanous, J.; Wegner, M.; Grimminger, J.; Rolff, M.; Spera, M.B.M.; Tenzerb, M.; Buchmeiser, M.R. Correlation of the electrochemistry of poly(acrylonitrile)-sulfur composite cathodes with their molecular structure. *J. Mater. Chem.* **2012**, *22*, 23240–23245. [CrossRef]
204. Fanous, J.; Wegner, M.; Grimminger, J.; Andresen, Ä.; Buchmeiser, M.R. Structure-Related Electrochemistry of Sulfur-Poly(acrylonitrile) Composite Cathode Materials for Rechargeable Lithium Batteries. *Chem. Mater.* **2011**, *23*, 5024–5028. [CrossRef]
205. Mayer, A.; Buchmeiser, M.R. Communication—Influence of Temperature and Electrolyte Viscosity on the Electrochemical Performance of SPAN-Based Lithium-Sulfur Cells. *J. Electrochem. Soc.* **2018**, *165*, A3943–A3945. [CrossRef]
206. Hintennach, A. Verfahren zur Herstellung eines mit einer Schutzschicht versehenen aktiven Kathodenmaterials für eine Metall-Schwefel-Batterie sowie Kathode für eine Metall-Schwefel-Batterie mit einem derartigen Kathodenmaterial. DE102016014148A1. 2017. Available online: <https://www.freepatentonline.com/DE102016014148A1.html> (accessed on 8 January 2022).
207. Lv, D.P.; Xu, T.; Saha, P.; Datta, M.K.; Gordin, M.L.; Manivannan, A.; Kumta, P.N.; Wang, D.H. A Scientific Study of Current Collectors for Mg Batteries in Mg(AlCl₂EtBu)₂/THF Electrolyte. *J. Electrochem. Soc.* **2013**, *160*, A351–A355. [CrossRef]
208. (Alufoil-MSDS-Al) Alufoil Products Co., Inc. Material Safety Data Sheet, Uncoated Aluminum Metal, CAS No.: 7429-90-5. 2007. Available online: <http://aluminumfoil.alufoil.com/Asset/MSDS-1XXX-20070101-Alufoil.pdf> (accessed on 8 January 2022).
209. (ThermoFisher-SDS-Al) ThermoFisher Scientific Safety Data Sheet. Aluminium Foil, CAS No.: 7429-90-5. 2020. Available online: <https://www.fishersci.ca/store/msds?partNumber=AA00004KI&productDescription=aluminum-foil-0-13mm-0-005in-thick-50x125mm-2-0x4-9in-99-9995-metals-basis-alfa-aesar-2&language=en&countryCode=CA> (accessed on 8 January 2022).
210. (CDH-SDS-Al) Central Drug House Safety Data Sheet, Aluminium Foil, CAS-No.: 7429-90-5. 2021. Available online: [https://www.cdhfinechemical.com/images/product/msds/51_142322642_AluminiumFoil\(Roll\)-CASNO-7429-90-5-MSDS.pdf](https://www.cdhfinechemical.com/images/product/msds/51_142322642_AluminiumFoil(Roll)-CASNO-7429-90-5-MSDS.pdf) (accessed on 8 January 2022).
211. (Haydon-SDS-Al) Norandal Aluminum Inc. Safety Data Sheet. Aluminum Sheet and Foil. 2015. Available online: <https://www.haydoncorp.com/portals/0/documents/msds/Aluminum%20Sheet%20and%20Foil%20-%20Safety%20Data%20Sheet.pdf> (accessed on 8 January 2022).
212. (Oxford-MSDS-Al) Oxford Lab Fine Chem LLP Material Safety Data Sheet. Aluminium Metal Foil AR, CAS No.: 7429-90-5. 2021. Available online: [https://www.oxfordlabchem.com/msds/\(A-00455\)%20ALUMINIUM%20METAL%20FOIL%20AR.pdf](https://www.oxfordlabchem.com/msds/(A-00455)%20ALUMINIUM%20METAL%20FOIL%20AR.pdf) (accessed on 8 January 2022).
213. (Uddeholm-SDS-Steel) Uddeholm Safety Data Sheet. Stainless Steel Foil Supplied by Uddeholm. 2010. Available online: https://www.uddeholm.com/app/uploads/sites/41/2017/12/MSDS_Stainless_steel_foil_supplied_by_Uddeholm.pdf (accessed on 8 January 2022).
214. (NS-SDS-Steel) Nippon Steel Chemical & Material Co., Ltd. Safety Data Sheet. Stainless Steel Foil Product. 2018. Available online: [https://www.nscm.nipponsteel.com/stainless_steel_foil/pdf/20181001%20SDS%20\(SS112\)_E.pdf](https://www.nscm.nipponsteel.com/stainless_steel_foil/pdf/20181001%20SDS%20(SS112)_E.pdf) (accessed on 8 January 2022).

215. (ThyssenKrupp-SDS-Steel) ThyssenKrupp Materials NA, Inc., Safety Data Sheet. Stainless Steel and Alloys of Stainless Steel. 2018. Available online: https://ucpcdn.thyssenkrupp.com/_legacy/UCPthyssenkruppBAMXNA/assets.files/tkmna_com/resources/safety-data-sheets/metals/stainless_steel_and_alloys_of_stainless_steel_sds_2018.pdf (accessed on 8 January 2022).
216. (MTI-SDS-Al) MTI Corporation Safety Data Sheet. Aluminum, CAS No.: 7429-90-5. 2018. Available online: https://www.mtixtl.com/sds/Aluminum_SDS.pdf (accessed on 8 January 2022).
217. (MTI-SDS-Graphite) MTI Corporation Safety Data Sheet. Graphite, CAS No.: 7782-42-5. 2018. Available online: https://www.mtixtl.com/sds/Conductive_Graphite_Powder_SDS.pdf (accessed on 8 January 2022).
218. (Breckland-SDS-Cu) Breckland Scientific Supplies Ltd. Safety Data Sheet. Copper Metal—Foil 0.1Mm, CAS No.: 7440-50-8. 2018. Available online: <https://www.brecklandscientific.co.uk/v/vspfiles/MSDS/S0002033.pdf> (accessed on 8 January 2022).
219. (AA-SDS-Cu) Alfa Aesar, Johnson Matthey Company; Johnson Matthey Catalog Company, Inc. Safety Data Sheet. Copper foil, CAS No. 7440-50-8. 2011. Available online: https://rsc.aux.eng.ufl.edu/_files/msds/2/Copper%20Foil.pdf (accessed on 8 January 2022).
220. (Denkai-SDS-Cu) Denkai America, Inc. Safety Data Sheet. Copper Foil. 2020. Available online: <http://denkaiamerica.com/wp-content/uploads/2021/01/Safety-Data-Sheets.pdf> (accessed on 8 January 2022).
221. (AquaPhoenix-SDS-Cu) AquaPhoenix Scientific, Inc. Safety Data Sheet. Copper, Metal Foil, CAS NO.: 7440-50-8. 2015. Available online: <https://preview.fishersci.com/store/msds?partNumber=S25267&productDescription=COPPER+METAL+FOIL+100G+.005&vendorId=VN00115888&countryCode=US&language=en> (accessed on 8 January 2022).
222. (ESPI-MSDS-Incontel) Electronic Space Products International Material Safety Data Sheet. Incontel. 2002. Available online: <http://www.ifa.hawaii.edu/instr-shop/SDS/Inconel.pdf> (accessed on 8 January 2022).
223. (Renishaw-SDS-Incontel) Renishaw Plc Safety Data Sheet. Inconel 625 Powder. 2016. Available online: <http://resources.renishaw.com> (accessed on 8 January 2022).
224. (GPT-MSDS-Incontel) GPT Industries Material Safety Data Sheet. Inconel 625. 2016. Available online: https://www.gptindustries.com/sites/default/files/documents/en/Inconel%20625%20Material%20Safety%20Data%20Sheet_0.pdf (accessed on 8 January 2022).
225. Muldoon, J.; Bucur, C.B.; Oliver, A.G.; Zajicek, J.; Allred, G.D.; Boggess, W.C. Corrosion of magnesium electrolytes: Chlorides—The culprit. *Energy Environ. Sci.* **2013**, *6*, 482–487. [CrossRef]
226. Muthuraj, D.; Ghosh, A.; Kumar, A.; Mitra, S. Nitrogen and Sulfur Doped Carbon Cloth as Current Collector and Polysulfide Immobilizer for Magnesium-Sulfur Batteries. *ChemElectroChem* **2019**, *6*, 684–689. [CrossRef]
227. (ACS-SDS-NdGPC) ACS Material LLC, Safety Data Sheet. ACS Material Nitrogen-Doped Graphitic Porous Carbon, CAS-No.: 7440-44-0. 2017. Available online: https://www.acsmaterial.com/pub/media/catalog/product/s/d/sds-nitrogen-doped_graphitic_porous_carbon_.pdf (accessed on 8 January 2022).
228. (AE-SDS-N/ScdGO) American Elements, Safety Data Sheets. Nitrogen/Sulfur Co-Doped Graphene, CAS No.: 1034343-98-0. 2021. Available online: <https://www.americanelements.com/nitrogen-sulfur-co-doped-graphene-1034343-98-0> (accessed on 8 January 2022).
229. Ji, Z.; Arvapalli, D.M.; Zhang, W.; Yin, Z.; Wei, J. Nitrogen and sulfur co-doped carbon nanodots in living EA.hy926 and A549 cells: Oxidative stress effect and mitochondria targeting. *J. Mater. Sci.* **2020**, *55*, 6093–6104. [CrossRef]
230. Fluorochem Ltd. Safety Data Sheet. Poly(Vinylidene Fluoride), CAS No.: 24937-79-9. 2011. Available online: <http://www.fluorochem.co.uk> (accessed on 8 January 2022).
231. Sajid, M.; Ilyas, M. PTFE-coated non-stick cookware and toxicity concerns: A perspective. *Env. Sci. Pollut. Res. Int.* **2017**, *24*, 23436–23440. [CrossRef] [PubMed]
232. Shimizu, T.; Hamada, O.; Sasaki, A.; Ikeda, M. Polymer fume fever. *BMJ Case Rep.* **2012**, *2012*, bcr2012007790. [CrossRef] [PubMed]
233. HaloPolymer Kirovo-Chepetsk, LLC Safety Data Sheet. Polytetrafluoroethylene, CAS No.: 9002-84-0. 2017. Available online: www.halopolymer.com (accessed on 8 January 2022).
234. (MTI-SDS-CMCS) MTI Corporation Safety Data Sheet. Carboxymethylcellulose Sodium, CAS No.: 9004-32-4. 2018. Available online: https://www.mtixtl.com/sds/EQ-Lib-CMC_SDS.pdf (accessed on 8 January 2022).
235. (MTI-SDS-SBR) MTI Corporation Safety Data Sheet. SBR Binder for Li-Ion Anode. 2013. Available online: http://mtikorea.co.kr/web/smh/pdf/MSDS_SBR_Binder.pdf (accessed on 8 January 2022).
236. (CarlRoth-SDS-AlCl3) CarlRoth Safety Data Sheet. Aluminium Chloride $\geq 98\%$, Anhydrous, Resublimated, CAS Number 7446-70-0. 2021. Available online: <https://www.carlroth.com/medias/SDB-CN86-MT-EN.pdf?context=bWVzdGVyfhNlY3VyaXR5RGF0YXNoZWV0c3wzMDMyOTR8YXBwbGljYXRpb24vcGRmfHNIY3VyaXR5RGF0YXNoZWV0cy9oZjgvaGYwLzkwMzY0MDY1MjE4ODYucGRmfGEyY2Q2ZjAxODQxNGRjMjFhNDU3YTZiZWQ0MzE5MmMzYjY2MjliMDJiMwIyNTdjMDNlYjQxMmE3MTczYmVkZmM> (accessed on 8 January 2022).
237. (ThermoFisher-SDS-AlCl3) ThermoFisher Scientific Safety Data Sheet. Aluminium Chloride, CAS Number 7446-70-0. 2019. Available online: <https://www.fishersci.com/msds?productName=AC217460050&product> (accessed on 8 January 2022).
238. (SA-SDS-PhMgCl) Sigma-Aldrich Safety Data Sheet. Phenylmagnesium Chloride Solution. 2021. Available online: <https://www.sigmaaldrich.com/PL/en/sds/aldrich/224448> (accessed on 8 January 2022).
239. (CarlRoth-SDS-LiCl) CarlRoth Safety Data Sheet. Lithium Chloride, CAS No.: 7447-41-8. 2018. Available online: <https://www.carlroth.de/medias/SDB-P007-AU-EN.pdf?context=bWVzdGVyfhNlY3VyaXR5RGF0YXNoZWV0c3wyMjE2MDh8YXBwbGljYXRpb2>

- 4vcGRmfHNIY3VyaXR5RGF0YXNoZWV0cy9oNmMvaDg1Lzg5Njk3Mzk3OTY1MTAucGRmfDFmMWRIODdmOGQ0MWJmODk4ZGRINTQ2ZDRiNjQ4MzViZTNjZDI4ZjhhZWVjNDc0YzNiNWZDQ1ZDBmOTY2NTk (accessed on 8 January 2022).
240. Wall, C.; Zhao-Karger, Z.; Fichtner, M. Corrosion Resistance of Current Collector Materials in Bisamide Based Electrolyte for Magnesium Batteries. *ECS Electrochem. Lett.* **2014**, *4*, C8–C10. [CrossRef]
241. Liebenow, C.; Yang, Z.; Lobitz, P. The electrodeposition of magnesium using solutions of organomagnesium halides, amidomagnesium halides and magnesium organoborates. *Electrochem. Commun.* **2000**, *2*, 641645. [CrossRef]
242. (Linde-SDS-BF3) Linde Inc. Safety Data Sheet. Boron Trifluoride. CAS-No.: 7637-07-2. 2016. Available online: <https://www.lindeus.com/-/media/corporate/praxairus/documents/sds/boron-trifluoride-bf3-safety-data-sheet-sds-p4567.pdf?la=en> (accessed on 8 January 2022).
243. (SA-SDS-Hexamethyldisilazane) Sigma-Aldrich Safety Data Sheet. Hexamethyldisilazane, CAS No.: 999-97-3. 2016. Available online: <https://www.tnstate.edu/nanobio/documents/Hexamethyldisilazane%20HMDS.pdf> (accessed on 8 January 2022).
244. (AE-SDS-Magnesium Bis(hexamethyldisilazide) American Element Safety Data Sheet. Magnesium Bis(hexamethyldisilazide), CAS No.: 857367-60-3. 2021. Available online: <https://www.americanelements.com/magnesium-bis-hexamethyldisilazide-857367-60-3> (accessed on 8 January 2022).
245. (AE-SDS-Magnesium bis(diisopropyl)amide) American Elements Safety Data Sheet. Magnesium Bis(diisopropyl)amide Solution 0.70 M in THF, CAS No.: 23293-23-4. 2021. Available online: <https://www.americanelements.com/magnesium-bis-diisopropylamide-23293-23-4> (accessed on 8 January 2022).
246. (CarlRoth-SDS-Tetrahydrofuran) CarlRoth Safety Data Sheet. Tetrahydrofuran $\geq 99.5\%$, Stabilized, for Synthesis, CAS No.: 109-99-9. 2021. Available online: <https://www.carlroth.com/medias/SDB-4745-IE-EN.pdf?context=bWFzdGVyfHNIY3VyaXR5RGF0YXNoZWV0cy9oOWEvaDk3LzkwMjcwMDIyMDQxOTAucGRmfGY4MmJkODc3OGNkOGJmNjJmYWw4NTc0YjIjODUxODRhOTM3MGMyZTBjYWY3M2RiZjNmZWJmMjRjYmE2YjZlMGI> (accessed on 8 January 2022).
247. (ThermoFisher-SDS-2-Methoxyethyl ether) ThermoFisher Scientific Safety Data Sheet. 2-Methoxyethyl Ether, CAS No.: 111-96-6. 2021. Available online: https://www.fishersci.co.uk/chemicalProductData_uk/wercs?itemCode=10020110&lang=EN (accessed on 8 January 2022).
248. (SA-SDS-Tetraethylene glycol dimethyl ether) Sigma-Aldrich Safety Data Sheet. Tetraethylene Glycol Dimethyl Ether for Synthesis, CAS No.: 143-24-8. 2019. Available online: https://www.merckmillipore.com/PL/pl/product/msds/MDA_CHEM-820959?Origin=PDP (accessed on 8 January 2022).
249. (NCBI-TEGDME) National Center for Biotechnology Information. PubChem Compound Summary for CID 8925, Tetraglyme. 2021. Available online: <https://pubchem.ncbi.nlm.nih.gov/compound/Tetraglyme> (accessed on 8 January 2022).
250. (Acros-SDS-TEGDME) Acros Organics, N.V. Safety Data Sheet. Tetraethylene Glycol Dimethyl Ether, 99%, CAS No.: 143-24-8. 2008. Available online: <https://fscimage.fishersci.com/msds/34316.htm> (accessed on 8 January 2022).
251. Zuo, P.; Li, Y.; Yin, G.; Li, R.; Ma, Y.; Du, C.; Gao, Y. Preparation Method and Application of Magnesium-Sulfur Battery Electrolyte Containing Lithium Ion Additive, CN109244544B, 2020. Harbin Institute of Technology. Available online: <https://patents.google.com/patent/CN109244544B/en> (accessed on 8 January 2022).
252. (GB-SDS-C2F6LiNO4S) Gold Biotechnology, Inc. Safety Data Sheet. Bis(trifluoromethane)sulfonimide Lithium Salt, CAS No.: 90076-65-6. 2018. Available online: [https://www.goldbio.com/documents/3819/B-340-SDS_\(MSDS\).pdf](https://www.goldbio.com/documents/3819/B-340-SDS_(MSDS).pdf) (accessed on 8 January 2022).
253. (SA-MSDS-Li) Sigma-Aldrich Material Safety Data Sheet. Lithium, CAS No.: 7439-93-2. 2014. Available online: <https://www.nwmissouri.edu/naturalsciences/sds/1/Lithium.pdf> (accessed on 8 January 2022).
254. NuLi, Y.; Zhao, X.; Yang, Y.; Yang, J.; Wang, J. CN109687072A, 2019. Shanghai Jiao Tong University.
255. (AS-SDS-THFPB) Apollo Scientific Ltd. Safety Data Sheet. Tris(2H-hexafluoroisopropyl) Borate, CAS: 6919-80-8. 2007. Available online: <https://cymitquimica.com/products/54-PC3486/6919-80-8/tris2h-hexafluoroisopropyl-borate/> (accessed on 8 January 2022).
256. Ding, M.S.; Diemant, T.; Behm, R.J.; Passerini, S.; Giffin, G.A. Dendrite Growth in Mg Metal Cells Containing Mg(TFSI)₂/Glyme Electrolytes. *J. Electrochem. Soc.* **2018**, *165*, A1983–A1990. [CrossRef]
257. Hu, X.-C.; Shi, Y.; Lang, S.-Y.; Zhang, X.; Gu, L.; Guo, Y.-G.; Wen, R.; Wan, L.-J. Direct insights into the electrochemical processes at anode/electrolyte interfaces in magnesium-sulfur batteries. *Nano Energy* **2018**, *49*, 453–459. [CrossRef]
258. Yu, Y.; Baskin, A.; Valero-Vidal, C.; Hahn, N.T.; Liu, Q.; Zavadil, K.R.; Eichhorn, B.W.; Prendergast, D.; Crumlin, E.J. Instability at the electrode/electrolyte interface induced by hard cation chelation and nucleophilic attack. *Chem. Mater.* **2017**, *29*, 8504–8512. [CrossRef]
259. (CarlRoth-SDS-I₂) CarlRoth SafetyData Sheet. Iodine $\geq 99.5\%$, Ph.Eur. Resublimated, CAS No.: 7553-56-2. 2021. Available online: <https://www.carlroth.com/medias/SDB-7935-GB-EN.pdf?context=bWFzdGVyfHNIY3VyaXR5RGF0YXNoZWV0cy9oMTkvaGY2LzkwMTY4NDg4NzU1NTAucGRmfGQyM2IyNjlmZWw0OGZkMzBkNDYyMGE5ZTM0ODVmN2IzMTFiZDk5ZWVhNjI4ODhkMDg0ZDE1OWE3YjY2MDc4ZGQ> (accessed on 8 January 2022).
260. (SA-SDS-Mg(TFSI)₂) Sigma-Aldrich Safety Data Sheet. Magnesium bis(trifluoromethanesulfonimide), CAS-No.: 133395-16-1. 2021. Available online: <https://www.sigmaaldrich.com/PL/en/sds/aldrich/753424> (accessed on 8 January 2022).

261. (NCBI-C8H18Mg, 2021) National Center for Biotechnology Information. PubChem Compound Summary for CID 70929, Dibutylmagnesium. 2021. Available online: <https://pubchem.ncbi.nlm.nih.gov/compound/Dibutylmagnesium> (accessed on 8 January 2022).
262. (GuideChem-SDS-Trifluoromethanesulfonic acid) GuideChem Safety Data Sheet. Trifluoromethanesulfonic Acid, CAS No.: 1493-13-6. 2017. Available online: <https://www.guidechem.com/msds/1493-13-6.html> (accessed on 8 January 2022).
263. (BP-SDS-Butane) BP Australia Pty Ltd. Safety Data Sheet. BP Butane. 2021. Available online: https://www.bp.com/content/dam/bp/country-sites/en_au/australia/home/products-services/data-sheets/bp-butane.pdf (accessed on 8 January 2022).
264. (SA-MSDS-MgO) Sigma-Aldrich Material Safety Data Sheet. Magnesium oxide, CAS No.: 1309-48-4. 2014. Available online: <https://www.nwmissouri.edu/naturalsciences/sds/m/Magnesium%20oxide.pdf> (accessed on 8 January 2022).
265. (BS-SDS-Mg(OH)₂) Breckland Scientific Supplies Ltd Safety Data Sheet. Magnesium Hydroxide, CAS No.: 1309-42-8. 2018. Available online: <https://www.brecklandscientific.co.uk/v/vspfiles/MSDS/S0001197.pdf> (accessed on 8 January 2022).
266. (TCI-SDS-Crown Ether) TCI Europe N.V. Safety Data Sheet. 18-Crown 6-Ether, CAS-No.: 17455-13-9. 2018. Available online: <https://www.tcichemicals.com/HU/en/p/C0860#documentsSectionPDP> (accessed on 8 January 2022).
267. (ATI-SDS-MgCl₂) ATI Safety Data Sheet. Magnesium Chloride (from Titanium Production), CAS No.: 7786-30-3. 2020. Available online: [https://www.atimetals.com/safety-data-sheets/Documents/EuropeanUnion/EU-EN/SAC/SAC026%20Magnesium%20Chloride%20\(Ti\)%20EU-EN%20Rev3.pdf](https://www.atimetals.com/safety-data-sheets/Documents/EuropeanUnion/EU-EN/SAC/SAC026%20Magnesium%20Chloride%20(Ti)%20EU-EN%20Rev3.pdf) (accessed on 8 January 2022).
268. (AquaPhoenix-SDS-C₁₂H₁₂MgO₆) AquaPhoenix Scientific Safety Data Sheet. (2015) Magnesium Chloride, Hexahydrate, CAS 7791-18-6. Available online: https://beta-static.fishersci.com/content/dam/fishersci/en_US/documents/programs/education/regulatory-documents/sds/chemicals/chemicals-m/S25401.pdf (accessed on 8 January 2022).
269. (Fisher-MSDS-MgCl₂) Fisher Scientific Material Safety Data Sheet. Magnesium Chloride, CAS No.: 7786-30-3. 2007. Available online: <https://fscimage.fishersci.com/msds/91830.htm> (accessed on 8 January 2022).
270. (SA-SDS-Mg(CF₃SO₃)₂) Sigma-Aldrich Safety Data Sheet. Magnesium Trifluoromethanesulfonate, CAS-No. 60871-83-2. 2021. Available online: <https://www.sigmaaldrich.com/PL/en/sds/aldrich/337986> (accessed on 8 January 2022).
271. (Oxford-MSDS-Anthracene) Oxford Lab Fine Chem LLP Material Safety Data Sheet. Anthracene (For Scintillation), CAS No.: 120-12-7. 2021. Available online: [https://www.oxfordlabchem.com/msds/ANTHRACENE\(For%20Scintillation\).pdf](https://www.oxfordlabchem.com/msds/ANTHRACENE(For%20Scintillation).pdf) (accessed on 8 January 2022).
272. (SA-SDS-LiCF₃SO₃) Sigma-Aldrich Safety Data Sheet. Lithium Trifluoromethanesulfonate, CAS-No.: 33454-82-9. 2021. Available online: <https://www.sigmaaldrich.com/PL/en/sds/aldrich/481548> (accessed on 8 January 2022).
273. (Acros-SDS-PS) Acros Organics N.V. Safety data Sheet. Propyl Sulfone, CAS No.: 598-03-8. 2008. Available online: <https://fscimage.fishersci.com/msds/18978.htm> (accessed on 8 January 2022).
274. (TCI-SDS-DPS) TCI America Safety Data Sheet. Dipropyl Sulfone, CAS No.: 598-03-8. 2018. Available online: <https://www.tcichemicals.com/US/en/p/D1171#documentsSectionPDP> (accessed on 8 January 2022).
275. (SA-SDS-C₁₁H₂₀F₆N₂O₄S₂) Sigma-Aldrich Safety Data Sheet. 1-Butyl-1-methylpyrrolidinium bis(trifluoromethylsulfonyl)imide, CAS-No.: 223437-11-4. 2021. Available online: <https://www.sigmaaldrich.com/PL/en/sds/sial/40963> (accessed on 8 January 2022).
276. (ILT-SDS- C₁₁H₂₀F₆N₂O₄S₂) Ionic Liquids Technologies GmbH Safety Data Sheet. 1-Butyl-1-methylpyrrolidinium bis(trifluoromethylsulfonyl)imide, CAS-No.: 223437-11-4. 2017. Available online: https://iolitec.de/sites/iolitec.de/files/sds/SDS%20IL-0035%20BMPyrr%20BTA%2C%201-Butyl-1-methylpyrrolidinium%20bis%28trifluoromethylsulfonyl%29imide_Label_0.pdf (accessed on 8 January 2022).
277. (AA-SDS-YCl₃) Alfa Aesar Safety Data Sheet. Yttrium Trichloride, CAS-No 10361-92-9. 2016. Available online: https://www.chemblink.com/MSDS/MSDSFiles/10361-92-9_Alfa-Aesar.pdf (accessed on 8 January 2022).
278. Zuo, P.; Li, Y.; Yin, G.; Li, R.; Ma, Y.; Du, C.; Gao, Y. Preparation and Application of Electrolysis Liquid for Magnesium-Sulfur Battery. CN109473714A, 2019. Harbin Institute of Technology. Available online: <https://www.patentguru.com/inventor/%E6%9D%8E%E7%9D%BF%E6%A5%A0>. (accessed on 8 January 2022).
279. (Gelest-SDS-TiCl₄) Gelest, Inc. Safety Data Sheet. Titanium Tetrachloride, 99%, CAS No.: 7550-45-0. 2015. Available online: https://www.gelest.com/wp-content/uploads/product_msds/INTI065-msds.pdf (accessed on 8 January 2022).
280. Krossing, I.; Raabe, I. Noncoordinating Anions—Fact or Fiction? A Survey of Likely Candidates. *Angew. Chem.* **2004**, *43*, 2066–2090. [CrossRef]
281. Barriere, F.; Geiger, W.E. Use of Weakly Coordinating Anions to Develop an Integrated Approach to the Tuning of $\Delta E_{1/2}$ Values by Medium Effects. *J. Am. Chem. Soc.* **2006**, *128*, 3980–3989. [CrossRef] [PubMed]
282. Lau, K.C.; Seguin, T.J.; Carino, E.V.; Hahn, N.T.; Connell, J.G.; Ingram, B.J.; Persson, K.A.; Zavadil, K.R.; Liao, C. Widening Electrochemical Window of Mg Salt by Weakly Coordinating Perfluoroalkoxyaluminate Anion for Mg Battery Electrolyte. *J. Electrochem. Soc.* **2019**, *166*, A1510–A1519. [CrossRef]
283. (SA-SDS-(CF₃)₂CHOH) Sigma-Aldrich Safety Data Sheet. 1,1,1,3,3,3-Hexafluoro-2-propanol, CAS No.: 920-66-1. 2021. Available online: https://www.merckmillipore.com/PL/pl/product/msds/MDA_CHEM-804515?Origin=PDP (accessed on 8 January 2022).
284. Xiu, Y.; Li, Z.; Bhaghavathi Parambath, V.; Ding, Z.; Wang, L.; Reupert, A.; Fichtner, M.; Zhao-Karger, Z. Combining Quinone-Based Cathode with an Efficient Borate Electrolyte for High-Performance Magnesium Batteries. *Batter. Supercaps.* **2021**. [CrossRef]

285. Ji, Y.; Liu-Théato, X.; Xiu, Y.; Indris, S.; Njel, C.; Maibach, J.; Ehrenberg, H.; Fichtner, M.; Zhao-Karger, Z. Polyoxometalate Modified Separator for Performance Enhancement of Magnesium-Sulfur Batteries. *Adv. Funct. Mater.* **2021**, *31*, 2100868. [CrossRef]
286. (AE-SDS-Mg(BH₄)₂) American Elements Safety Data Sheet. Sodium Borohydride, CAS No.: 16903-37-0. 2021. Available online: <https://www.americanelements.com/magnesium-borohydride-16903-37-0> (accessed on 8 January 2022).
287. (LTS-SDS-MgF₂, 2014) LTS Research Laboratories, Inc. Safety Data Sheet. Magnesium Fluoride, CAS No.: 7783-40-6. 2014. Available online: <https://www.ltschem.com/msds/MgF2.pdf> (accessed on 8 January 2022).
288. (SA-MSDS-1,2-Dimethoxyethane) Sigma-Aldrich Material Safety Data Sheet. 1,2-Dimethoxyethane, CAS No.: 110-71-4. 2013. Available online: <https://www.nwmissouri.edu/naturalsciences/sds/0-9/1%202-Dimethoxyethane.pdf> (accessed on 8 January 2022).
289. Hintennach, A. Elektrolyt Für Wiederaufladbare Magnesium-Lonen- und Magnesium-Batterien Sowie Wiederaufladbare Magnesium-Lonen- und Magnesium-Batterien mit Dem Elektrolyt. DE102017007426A1, 2018. Daimler AG. Available online: <https://www.freepatentonline.com/DE102017007426A1.html> (accessed on 8 January 2022).
290. (CC-SDS-Thiobarbituric Acid) Cayman Chemical Company Safety Data Sheet. Thiobarbituric Acid, CAS No.: 504-17-6. 2014. Available online: <https://www.bioscience.co.uk/userfiles/pdf/10009055m.pdf> (accessed on 8 January 2022).
291. (SA-SDS-2-Thiobarbituric acid) Sigma-Aldrich Safety Data Sheet. 2-Thiobarbituric Acid, CAS No.: 504-17-6. 2021. Available online: <https://www.sigmaaldrich.com/PL/en/sds/sial/t5500> (accessed on 8 January 2022).
292. Sobianowska-Turek, A.; Urbanska, W.; Janicka, A.; Zawislak, M.; Matla, J. The Necessity of Recycling of Waste Li-Ion Batteries Used in Electric Vehicles as Objects Posing a Threat to Human Health and the Environment. *Recycling* **2021**, *6*, 35. [CrossRef]
293. The Merck Index. 2022. Available online: <https://www.rsc.org/merck-index> (accessed on 24 January 2022).
294. Fire Protection Guide to Hazardous Materials. 2010. Available online: <https://catalog.nfpa.org/Fire-Protection-Guide-to-Hazardous-Materials-2010-Edition-P14118.aspx> (accessed on 24 January 2022).
295. USA Department of Transportation. Emergency Response Guidebook. 2020. Available online: <https://www.phmsa.dot.gov/hazmat/erg/emergency-response-guidebook-erg> (accessed on 24 January 2022).
296. OSHA Occupational Chemical Database. 2022. Available online: www.osha.gov/chemicaldata (accessed on 24 January 2022).
297. Hazardous Substances Data Bank (HSDB). 2022. Available online: [Toxnet.nlm.nih.gov](http://toxnet.nlm.nih.gov) (accessed on 24 January 2022).
298. National Institute for Occupational Safety and Health (NIOSH). 2022. Available online: www.cdc.gov/niosh/topics/chemical.html (accessed on 24 January 2022).
299. NIOSH Pocket Guide to Chemical Hazards. 2022. Available online: www.cdc.gov/niosh/npg (accessed on 24 January 2022).
300. International Chemical Safety Cards. 2022. Available online: www.cdc.gov/niosh/ipcs (accessed on 24 January 2022).
301. OECD eChemPortal. 2022. Available online: <https://www.oecd.org/chemicalsafety/echemportalglobalportaltoinformationonchemicalsubstances.htm> (accessed on 24 January 2022).
302. Rumle, J.R. (Ed.) *CRC Handbook of Chemistry and Physics*, 102nd ed.; Taylor & Francis: Abingdon, UK, 2021.
303. *Sax's Dangerous Properties of Industrial Materials*; John Wiley & Sons, Inc: Hoboken, NJ, USA, 2004. [CrossRef]
304. Urben, P.G. (Ed.) *Bretherick's Handbook of Reactive Chemicals Hazards*, 8th ed.; Elsevier Ltd.: Amsterdam, The Netherlands, 2017.
305. Frank, R. Lautenberg Chemical Safety for the 21st Century Act. Public Law 114-182—June 22. 2016. Available online: <https://www.congress.gov/114/plaws/publ182/PLAW-114publ182.pdf> (accessed on 24 January 2022).
306. Centers for Disease Control and Prevention (CDC). 2022. Available online: <https://www.usa.gov/federal-agencies/centers-for-disease-control-and-prevention> (accessed on 24 January 2022).
307. Agency for Toxic Substances and Disease Registry (ATSDR). 2022. Available online: <https://www.atsdr.cdc.gov/> (accessed on 24 January 2022).
308. NIOSH Registry of Toxic Effects of Chemical Substances (RTECS®). 2022. Available online: www.cdc.gov/niosh/rtecs/RTECSAccess.html (accessed on 24 January 2022).
309. IARC Monographs on the Identification of Carcinogenic Hazards to Humans. Lyon (FR): International Agency for Research on Cancer. 1987. Available online: <https://www.ncbi.nlm.nih.gov/books/NBK294452/> (accessed on 24 January 2022).
310. NTP 15-th Annual Report on Carcinogens. 2021. Available online: <https://ntp.niehs.nih.gov/whatwestudy/assessments/cancer/roc/index.html> (accessed on 24 January 2022).
311. TLVs and BEIs (ACGIH). 2022. Available online: <https://www.acgih.org/science/tlv-bei-guidelines/policies-procedures-presentations/> (accessed on 24 January 2022).
312. Larrañaga, M.D.; Lewis Sr., R.J.; Lewis, R.A. *Hawley's Condensed Chemical Dictionary*, 16th ed. John Wiley & Sons, Inc.: Hoboken, NJ, USA, 2016. [CrossRef]
313. Hazard Communication. Hazard Classification Guidance for Manufacturers, Importers, and Employers. Occupational Safety and Health Administration U.S. Department of Labor. OSHA 3844-02 2016. Available online: <https://www.osha.gov/sites/default/files/publications/OSHA3844.pdf> (accessed on 24 January 2022).
314. Egbuna, C.; Parmar, V.K.; Jeevanandam, J.; Ezzat, S.M.; Patrick-Iwuanyanwu, K.C.; Adetunji, C.O.; Khan, J.; Onyeike, E.N.; Uche, C.Z.; Akram, M.; et al. Toxicity of Nanoparticles in Biomedical Application: Nanotoxicology. *J. Toxicol.* **2021**, *9954443*. [CrossRef]
315. Arning, J.; Matzke, M. Toxicity of Ionic Liquids Towards Mammalian Cell Lines. *Curr. Org. Chem.* **2011**, *15*, 1905–1917. [CrossRef]
316. Bailey, J.; Thew, M.; Balls, M. An analysis of the use of animal models in predicting human toxicology and drug safety. *Altern Lab Anim.* **2014**, *42*, 181–199. [CrossRef]

317. Hebert, C.D. Basic Overview of Preclinical Toxicology Animal Models. Southern Research Institute. 5 December 2013. Available online: <https://www.uab.edu/medicine/adda/images/131205%20Tox%20Animal%20Models.pdf>. (accessed on 24 January 2022).
318. Fuat Gatnik, M.; Worth, A. *Review of Software Tools for Toxicity Prediction*. EUR 24489 EN; Publications Office of the European Union: Luxembourg, 2010; JRC59685. [[CrossRef](#)]
319. Siczek, K. The Toxicity of Secondary Lithium-Sulfur Batteries Components. *Batteries* **2020**, *6*, 45. [[CrossRef](#)]
320. Liang, Z.; Zhao, Y.; Li, Y. Electrospun Core-Shell Nanofiber as Separator for Lithium-Ion Batteries with High Performance and Improved Safety. *Energies* **2019**, *12*, 3391. [[CrossRef](#)]
321. Kang, D.H.; Chen, M.; Ogunseitan, O.A. Potential environmental and human health impacts of rechargeable lithium batteries in electronic waste. *Env. Sci Technol.* **2013**, *47*, 5495–5503. [[CrossRef](#)] [[PubMed](#)]